

Part I - Spectroscopic Studies of Coal.

Part II - Mono and Dicarbonyl Radical Cations.

A thesis submitted by
Lynn Portwood for the degree
of Doctor of Philosophy in
the Faculty of Science of the
University of Leicester.

Department of Chemistry
The University
Leicester.

April 1987

Spectroscopic Studies of Coal and an Esr Study of Mono and Dicarbonyl Radical Cations:
by Miss L. Portwood.

Part I

Esr spectra of pure coals, oils and tars are presented; their g values and linewidths are calculated. Almost all the spectra are single, broad resonances; but one coal, Hucknall Coal, exhibits a two line spectrum, a narrow line superimposed on a broad line. On admission of oxygen the narrow line is reversibly lost. On the addition of various solvents to the samples, in most cases, an irreversible loss in esr signal intensity was observed. There seems to be no direct correlation between which solvent is added to which coal and the effect on the esr signal intensity. Infra-red spectra of pure coals are studied, both as pressed discs and thin films, and a method for the preparation of these discs and films is given. Solvent addition experiments were undertaken and the results show the breaking of weak coal/water hydrogen bonds and the formation of stronger coal/solvent hydrogen bonds.

Part II

Esr spectra of the radical cations of several mono and dicarbonyl compounds are presented and interpretation of these spectra are given. For most compounds the parent radical cation is seen, with the spin on oxygen. The cyclic dicarbonyls show the σ -bonded structure for the cation with coupling to the protons δ to the spin. Some non-aldehydic dicarbonyls show a rearranged structure with the spin on carbon. The aldehydic dicarbonyls all show, in addition to the parent radical cation, lines due to an acetal type species, as yet unidentified. Some compounds containing nitrogen or sulphur in addition to oxygen have the spin localised onto these alternative heteroatoms.

Statement

The experimental work described in this thesis was carried out solely by the author, except the work presented in chapter 8, which was carried out in conjunction with Dr. C.J. Rhodes, in the Department of Chemistry of the University of Leicester during the period September 1985 to September 1986.

The work in this thesis is not being concurrently presented for any other degree.

All work recorded herein is original unless otherwise stated in the text or by reference.

April 1987

signed by 

Dedicated to

Aunt Edie;

she was right in the end!

Acknowledgements

My sincere thanks go to Martyn Symons for all his help and assistance during the last three years, and to the S.E.R.C. and the British Gas Corporation for their financial support. I wish to express my appreciation to my parents for all their moral and financial support over the past seven years, and to Phil for his friendship and the loan of his word-processor. I also wish to acknowledge the comradeship of the "Friday" crowd, especially Graham and Chris; for listening to my problems and still buying me a drink afterwards. Finally I would like to thank some friends of mine; the sort of people that make life worth living, the members of the Ratae Road Club. And lastly Dave, thanks for everything!

It is only about things that do not interest one that one can give a really unbiased opinion, which is no doubt the reason why an unbiased opinion is always absolutely valueless.

Oscar Wilde (1854-1900)

It is one of the blessings of old friends that you can afford to be stupid with them.

Ralph Waldo Emerson (1803-1882)

I say to you that when you have eliminated the impossible, whatever remains, however improbable, must be the truth!

Sir Arthur Conan Doyle (1859-1930)

CONTENTS

| | <u>Page</u> | |
|----------------|-----------------------------------|----|
| <u>Part I</u> | | |
| 1 | <u>Introduction</u> | |
| 1.1 | Background | 1 |
| 1.2 | Experimental | 16 |
| 2 | <u>Esr Study of Tars and Oils</u> | |
| 2.1 | Introduction | 20 |
| 2.2 | Pure Tars and Oils | 20 |
| 2.3 | Solvent Addition to Tars | 24 |
| 3 | <u>Esr Study of Coals</u> | |
| 3.1 | Introduction | 28 |
| 3.2 | Pure Coals | 28 |
| 3.3 | Solvent Addition | 36 |
| 4 | <u>Ir Study of Coals</u> | |
| 4.1 | Pure Coals | 53 |
| 4.2 | Solvent Addition | 59 |
| | <u>References to Part I</u> | 69 |
| <u>Part II</u> | | |
| 5 | <u>Introduction</u> | |
| 5.1 | Background | 73 |
| 5.2 | Experimental | 75 |

cont...

| | <u>Page</u> |
|---|-------------|
| <u>6</u> <u>Acyclic Carbonyls (non-aldehydic)</u> | |
| 6.1 Introduction | 78 |
| 6.2 Acyclic Monocarbonyls | 79 |
| 6.3 Acyclic Dicarboxyls | 81 |
| | |
| <u>7</u> <u>Cyclic Carbonyls</u> | |
| 7.1 Introduction | 90 |
| 7.2 Saturated Cyclic Monocarbonyl | 91 |
| 7.3 Saturated Cyclic Dicarboxyls | 91 |
| 7.4 Unsaturated Cyclic Carbonyls | 102 |
| | |
| <u>8</u> <u>Aldehydic Carbonyls</u> | |
| 8.1 Introduction | 114 |
| 8.2 Aldehydic Monocarbonyl | 114 |
| 8.3 Aldehydic Dicarboxyls | 118 |
| | |
| <u>9</u> <u>Derivatives of Carbonyl Compounds</u> | |
| 9.1 Introduction | 127 |
| 9.2 Hydroxyl Derivatives | 128 |
| 9.3 Halogenated Derivatives | 130 |
| 9.4 Nitrogen and Sulphur Derivatives | 135 |
| | |
| <u>References to Part II</u> | 142 |

Part I

Spectroscopic Studies

Of Coal

Chapter 1

1 INTRODUCTION

1.1 Background

In the past several years there has been a renewed interest in the fundamental studies of coals and coal conversions. This interest is due to the expectation that an understanding of the structure of coal and of the fundamental processes during coal conversion would aid the development of technology for the utilisation of coal on cost-effective and environmentally acceptable terms.

Coal is a very complex, heterogenous mixture of organic compounds and minerals. A very simple but useful analogy is to think of coal as being like a fruitcake.^(1,2) The various components in the plant material such as wood, bark, sap, leaves etc., which make up coal are analogous to the fruits, nuts and batter which are used to make a fruitcake. Considerable mixing before "baking" occurs in both cases. How well "done" a cake is has a parallel in coal science, called the rank of the coal, or the extent of metamorphism.

The rank of a coal may be defined as the extent to which the organic material has matured during geologic time; ongoing from peat to anthracite. The change in rank of coal is largely affected by the duration of burial, pressure and temperature. For research purposes, chemists commonly use the carbon content (percentage carbon %C) as a measure of the degree of metamorphism. The carbon content

of coals increases from 70% in lignites to the upper 90% for anthracites.

Clearly, because of its heterogeneous nature, it is not possible to define the structure of coal in the same precise way as for a pure crystalline compound. A schematic representation of a possible structure of coal is illustrated in *fig. 1(i)*. Coal components are named as the types of materials which can be identified with the unaided eye. Vitrain is the most common component of coal and originates from wood or bark. This material forms the uniform, shiny black bands commonly found in coal. Durain is dull and of variable composition and origin. It is the hardest component of coal. Fusain, the softest component of coal, is mineral charcoal and is believed to originate from the same material as vitrain.

The term macerals was proposed for the components of the organic rock, coal, in direct analogy to minerals comprising inorganic rocks. ⁽¹⁾ Macerals are the smallest subdivision commonly used and are often referred to by their group and they can be recognised by their -inite endings. The vitrinite group originates from wood or bark and is the most abundant maceral group. The exinite group was formed from the remains of spores, resins, algae and cuticles. The inertinite group comes from the same type of plant components as vitrinite, although this material was strongly affected by oxygen during the early stages of coalification.

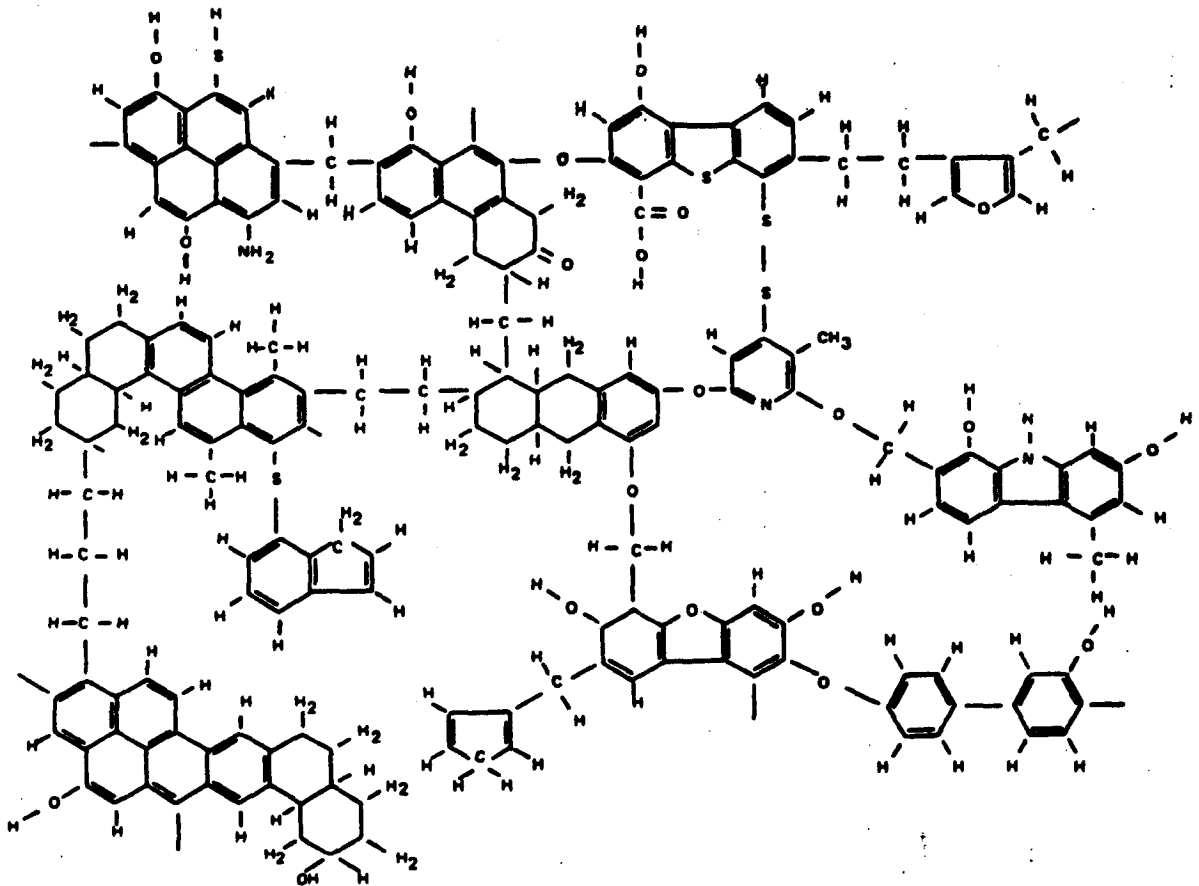


Figure 1(1): Schematic representation of structural groups and connecting bridges in bituminous coal.

The chemical and physical characteristics of coals change in a more or less systematic, though often nonlinear, fashion with rank.^{'3'} Investigations^{'4'} of a series of coals using X-ray diffraction methods has resulted in the proposal of three main types of structure for coals:-

- [1] low rank - an open structure of randomly oriented and cross-linked condensed aromatic layers,
- [2] medium rank - a structure with fewer cross-links, reduced porosity and a moderate degree of ring orientation,
- [3] high rank - larger layers with a greater degree of orientation and an oriented pore system.

Models of these structures are illustrated in *fig. 1(ii)*. These models are mainly guides to possible structures that represent a statistical average of composition data. They should be used with care, bearing in mind the inhomogeneity of coal.

Considerable evidence has been presented^{'5'} to support the view that bituminous coals consist of a three-dimensional cross-linked macromolecular structure together with appreciable amounts of low molecular weight (≈ 1000 a.m.u.) material. The main evidence is provided by the fact that these coals swell to equilibrium without dissolution in the presence of specific solvents and by the ability of

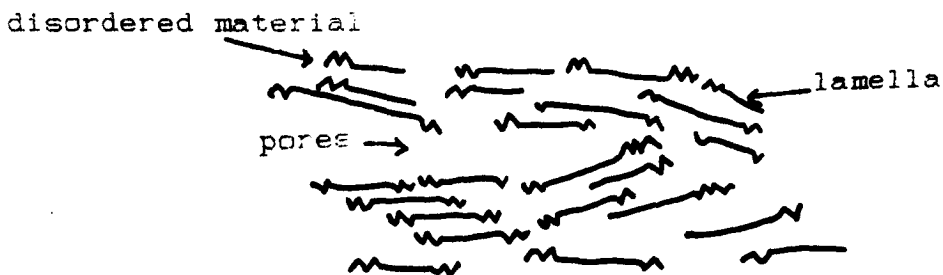
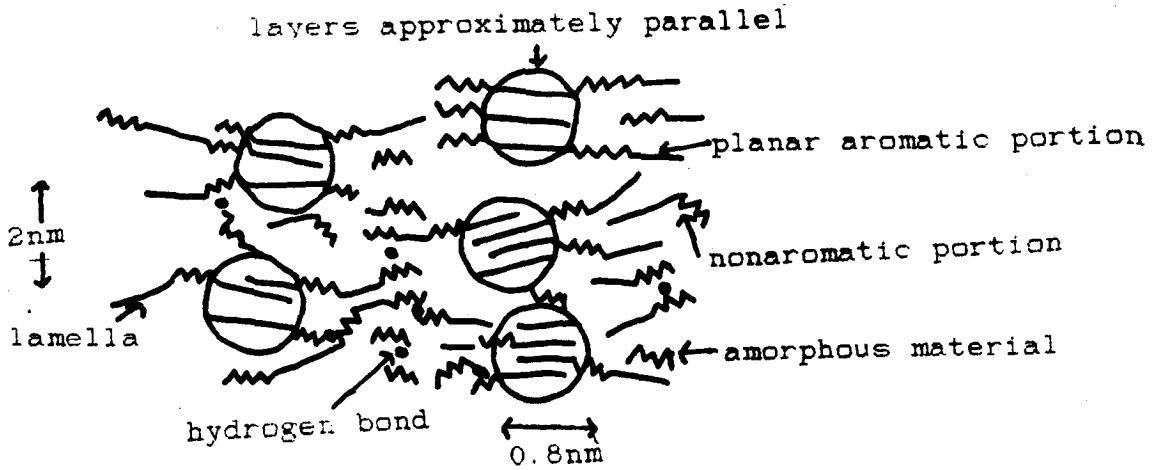
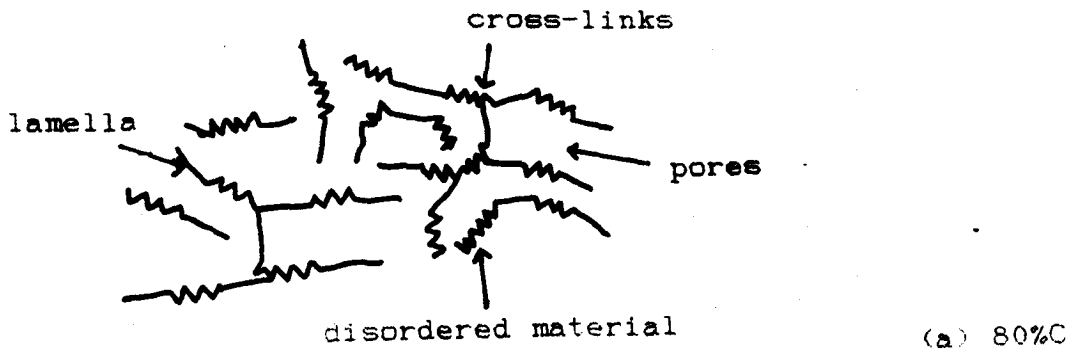


Figure 1(ii): Structural models of coal; (a) open structure, (b) "liquid" structure, (c) anthracitic structure. (4)

such solvents to extract up to $\approx 25\text{wt}\%$ of the coals under ambient conditions. The most effective agents for bituminous coals are nucleophilic (electron-donor) solvents such as pyridine and ethylenediamine.^(6,7)

The high concentration of organic components in coal results in an optically dense material and the presence of large amounts of mineral matter and void spaces results in a material which easily scatters light.⁽⁸⁾ Viewed in white light, most coals appear black or dark brown. Transmitted light does not pass through pieces of coal which are thicker than a few nanometres. As a result, many spectroscopically based techniques applicable to non-carbonaceous microporous solids cannot be applied to composition or reaction studies of coal.⁽⁹⁾

Under the microscope, coal is seen to contain holes, cracks and macropores which represent gaps between particles. At the atomic scale, coals may have an ultra-fine structure with pore sizes down to a few nanometres in size. The pores represent holes in or between macromolecules. Some of the pores may be open giving gases access to the internal surface area of the coal whilst others are closed, but may open during reaction.⁽¹⁰⁾

A number of workers have studied the interaction of solvent vapours with coal,⁽¹¹⁻⁶⁾ but for present purposes some findings of Hsieh and Duda are particularly interesting. Duda and Hsieh⁽³⁾ proposed a model *fig. 1(iii)* to illustrate phenomena involved in

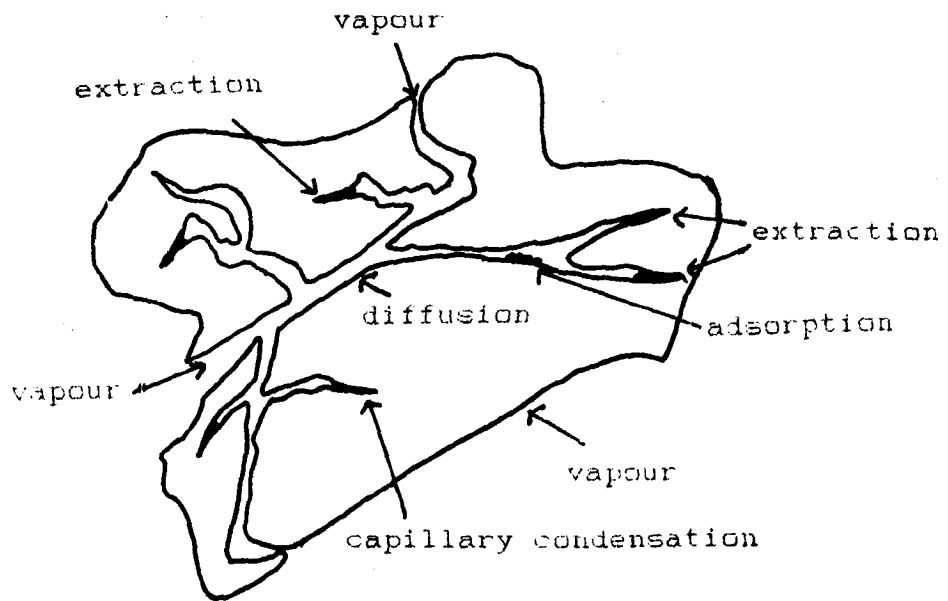


Figure 1(iii): Diagrammatic model of the uptake of solvent vapour by a coal particle. (3)

interactions of coal with a solvent. When a coal is exposed to the vapour of, for example, benzene, uptake still continues after 60 days with no sign of equilibrium being reached, as has been known for some time. Benzene vapour diffuses in through the pores, and undergoes capillary condensation. The liquid benzene extracts material from the walls of the pores, and the resulting solution has a lower vapour pressure than the pure benzene outside the coal particle. Therefore there is a driving force constantly pushing more benzene in, to dilute the solution.

Accordingly, Duda and Hsieh extracted the coal with pyridine before starting to measure benzene uptake. In this case, the rate of uptake does become quite slow after about 2 days. Toluene at 110°C shows similar behaviour. It is thought that only about one-third of the uptake is due to adsorption on the walls of the pores and that the remainder dissolves in the "solid" coal matrix. Confirmation of the idea of dissolution in the matrix comes from the fact that once the hydrocarbon has entered the coal only about one-half can be removed by prolonged exposure of the coal to a high vacuum. The swelling of a cross-linked polymer sets up mechanical stresses; such stresses are relieved by a relaxation process in which the structure readjusts itself. It is probably this relaxation that traps solvent inside coals (however, coals are unusual in showing this degree of trapping). The most abundant heteroatom in coals, oxygen, occurs in three basic forms: phenols, ethers and

heteroaromatics. Sulphur, though less abundant than oxygen, is just as important because it is a major source of pollution in coal utilisation, but with both sulphur and nitrogen only heteroaromatics have been isolated.^{'17'}

Free radicals have lifetimes varying over many orders of magnitude, from milliseconds to eons. Extremely long-lived free radicals, formed during geologic time, have been observed in fossil energy materials, including petroleum crudes, oil shales and coals.^{'18'} Austin *et al.*^{'19'} suggested three possibilities as to the genesis of the free radicals in coal and the changes in quantity, as well as the nature of free radicals during subsequent coalification:-

- [1] stable free radicals were formed during diagenesis of the organic sediment and these have persisted,
- [2] radicals were formed in pyrolytic reactions during metamorphosis as a result of homolytic splitting of certain functional groups,
- [3] radicals were produced by radiolysis.

Electron spin resonance (esr) is particularly suited to the study of the structure and behaviour of free radicals. Esr spectra of coals were first obtained in 1954 by three independent groups of workers; Uebersfeld *et al.*,^{'19'} Ingram *et al.*^{'20'} and Commoner *et al.*^{'21'} It was concluded by all these workers that the esr signals were derived from free radicals within the coals.

Free radicals can be formed as a result of homolytic

fission, or by unsatisfied valencies produced during ring formation, but these will be short-lived unless they are stabilised in some way. The high delocalisation energy associated with the aromatic ring clusters in coal can provide the necessary stabilisation. During coalification non-aromatic structures are progressively lost; a corresponding increase in the number and size of aromatic ring clusters occurs, and consequently the capacity of the coal to accommodate stable unpaired electrons increases.

The *esr* spectra of coal usually consist of a single broad symmetrical resonance near to $g = 2$. No hyperfine structure is anticipated because free radicals in coal are undoubtedly extremely complex in structure and spectral fine structure, resulting from electron coupling with neighbouring magnetic nuclei, has never been observed. ⁽²²⁾

The variation of parameters of *esr* of coals with rank or with carbon content is well documented. ⁽²³⁻⁹⁾ Of the *esr* parameters usually considered, spectral linewidths are the most frequently reported, presumably because of the relative ease with which reliable measurements can be made. For coals having between 55 and 90%C, peak to peak linewidths, as measured using the derivative of the absorption curve, range from $\approx 5.2G$ to $\approx 8.6G$. A gradual increase in linewidth with increasing carbon content is first observed; this trend is reversed at a carbon content of $\approx 80\%$. The rate of decrease becomes very rapid for coals having between 90 and 95%C; linewidths of only a few tenths

of a gauss have been measured for several such coals. ⁽²²⁾

The esr spectra of some coals show a narrow peak in addition to the usual broad resonance. ⁽³⁰⁻³⁾ The width of each component decreases as the rank of the coal increases. ⁽³⁵⁾ The narrow signal can be attributed to the presence of fusain. ⁽³⁶⁾ It is difficult to suggest a reason why fusain gives a sharp line, however it may be considered that the spin centre is closely related to the condensed aromatic ring system. ⁽⁴⁰⁾ This narrow fusain line broadens and merges with the broad vitrain signal when air is admitted to the sample. ^(33,36-8) Presumably the presence of paramagnetic oxygen leads to a decrease in the electron relaxation times and this gives rise to the broadening of spectral lines. ⁽³⁰⁾ Nearly all coals seem to be sensitive to the presence or absence of air (oxygen) in the sample, ⁽⁴¹⁾ and it is well known that the prolonged outdoor storage results in a deterioration of the fuel by means of a slow process of atmospheric oxidation. ⁽⁴²⁻³⁾

The g-value is a very important esr spectral parameter that is sensitive to the molecular environment of an unpaired electron, was unfortunately treated only casually in early coal studies. The utility of the parameter in coal research is becoming more apparent as more precise values become available. A plot of the esr g-values of coals as a function of their carbon content is reproduced in *fig. 1(iv)*. ⁽³⁶⁾

A variation in the g-tensors of coals has been noted

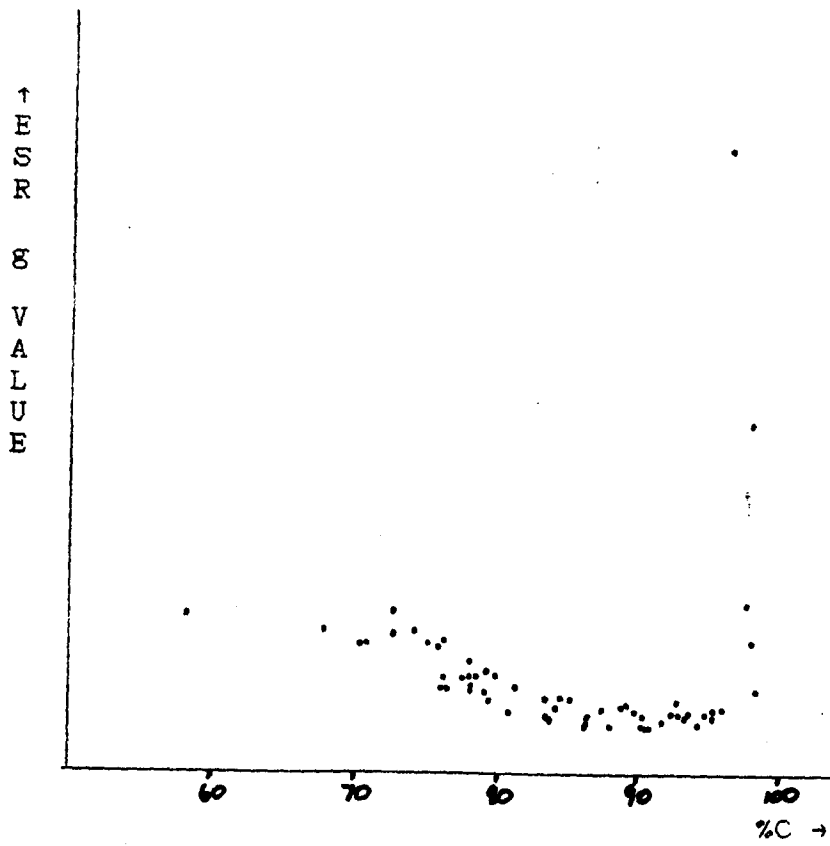


Figure 1(iv): A plot of the esr g-values as a function of %C.

by several workers. ^(18,23,24,44-5) The value of the g-tensor depends on if the free radical is on a heteroatom, e.g. oxygen, nitrogen or sulphur in the coal. Oxygen is believed to be the atom responsible for changes in the g-tensor with rank for various reasons. Among the heteroatoms found in the hydrocarbon framework of coal, only the oxygen content varies in a regular fashion with rank; the nitrogen and sulphur content is more or less constant. ⁽²³⁾ The variation of the g-tensor with coal rank can be best rationalised as follows. For very low rank coals, the values of the g-tensor indicate that the unpaired electrons are partially localised onto the oxygen atoms, as rank increases the g-tensor decreases because the radicals become more hydrocarbon-like. ⁽⁴⁵⁾ For high rank bituminous coals the g-tensor is approximately equal to the free spin value, i.e. the free radicals are associated with aromatic hydrocarbon centres. It must be remembered, however, that the g-tensor found for a particular coal sample reflects the nature of all of the radicals present and is not the isotropic value of the g-tensor of a pure compound.

The concentration of the unpaired electrons in coal rises exponentially with increasing rank up to 94%C. However, for coals with a carbon content of greater than 94%, the free radical concentration decreases rapidly with rank increase. It is feasible that the increasing size of aromatic ring clusters, which occurs with increasing rank, eventually makes it possible for the unpaired electrons to

move freely between the molecules, so losing their identity with any particular one. It is not clear whether these unpaired electrons then pair to form chemical bonds or become part of a conduction band; in neither case will an esr signal be obtained. In coal of 70%C there is one radical for every 50,000 carbon atoms, whereas for an anthracite, with 94%C, there is one radical for every 1000 carbon atoms.

Data on the influence of organic and inorganic solvents on the esr spectrum of coal are still scarce and no uniform picture of the mechanism underlying the changes in its unpaired electron concentration caused by solvents is available. The majority of current papers report esr studies of coal-solvent interactions at high temperatures. (37,40-1,46-9) Only Yokokawa (46) has used esr to study this interaction at room temperature. Using a wide variety of both organic and inorganic solvents, he found that the variation in paramagnetic centre concentration depends on the rank of the coal sample. Yokokawa obtained the greatest decrease in unpaired electron concentration for coals of 82-84%C saturated with organic solvents whereas coals with < 78%C exhibited an increase in unpaired electron concentration.

Optical spectra are available for coal in both the visible/near ultraviolet and the infrared (ir) regions of the spectrum. The molecular information available from these two spectral regions is different. The visible/near

ultraviolet spectra are discussed fully elsewhere. (8,24,50-3)

Ir spectroscopy has played an important part in structural studies of carbonaceous materials; major contributions were made towards the spectral analysis of coal structure when in 1945 Cannon and Sutherland⁽⁵⁴⁻⁵⁾ produced successful *ir* spectra of coal.

In *ir* spectroscopy there is a choice between several different sample preparation techniques, including the use of mulls, solutions, alkali halide pellets and thin sections. The problem with the use of mulls such as Nujol (a mixture of liquid paraffins) is the superimposition of the *ir* spectrum of the mulling agent on that of the coal; to record the full spectrum, several mulling agents may be required, so the compilation of the complete spectrum can be a lengthy process. The intractable nature of coal precludes the use of solution techniques, although they can be useful with regard to coal extracts, and the use of thin sections of coal has been strictly limited owing to the practical problems of producing suitable thin sections. The most common technique is to use alkali halide pellets, and most of the work on coal and other carbonaceous materials has been carried out with this method. However, the absorption of moisture by the alkali halide can create problems.

Major absorption bands are seen which can be attributed to the major classes of functional groups expected to be found in coal. Tables have been compiled

which assign these various *ir* bands, ^(24.50) see table 1.

The *ir* spectra of coals show distinct effects due to rank. ⁽⁵⁶⁾ With increase in rank there is:-

- [1] a general decrease in the number of hydroxyl groups present, particularly in the associated -OH/phenol region around 3300cm^{-1} ,
- [2] an increase in the number of aromatic C-H groups present (3050cm^{-1}),
- [3] a decrease in the number of aliphatic C-H groups present (2925cm^{-1}).

Transmission *ir* difference spectroscopy studies of the binding of nitrogen containing bases to the pore surface of coal indicated that the treatment of coal by a swelling solvent (e.g. pyridine) might be causing a change in the amount of light scattered by the coal sample. The trend exhibited by the *ir* transmission data towards increasing transmission at all wavelengths when solvent is added to the coal. ⁽³⁾

1.2 Experimental

The coal samples were stored in sealed jars under deoxygenated, deionised water, as advised by the British Gas Corporation and other authors. ⁽⁴²⁻³⁾ The tar and oil samples were stored in glass jars, as received.

Table 1

| Band Position (cm ⁻¹) | Assignment |
|--------------------------------------|---|
| 3300 | -OH str. { phenolic OH...O -OH (Hydroperoxide) -NH str. { >NH...N |
| 3030 | ar. CH str. |
| 2978 sh. | CH ₃ str. |
| 2925 } 2860 } | CH ₃ str., CH ₂ str., al. CH str. |
| 1700 | C=O str. |
| 1600 | { ar. C=C str. C=O...HO- |
| 1500 | ar. C=C str. |
| 1450 | { CH ₃ assym. def. CH ₂ scissor ar. C=C str. |
| 1380 | CH ₃ sym. def. |
| 1300 to 1000 | { C-O str. (phenols) OH def. C _{ar} -O-C _{ar} str. C-O str. (alcohols) C _{ar} -O-C _{al} str. C _{al} -O-C _{al} str. |
| 900 } to } 700 } | "aromatic bands" |
| 860 } 820 } 750 } | ar. HCC rocking (single and condensed rings) |
| 873 } 816 } 751 } | subst. benzene ring with isolated H subst. benzene ring with 2 neigh. H o-subst. benzene ring |

ar. = aromatic; al. = aliphatic; str. = stretching;
def. = deformation; sh. = shoulder; subst. = substituted.

Samples for esr spectroscopy

The coals were dried, and ground to a fine powder with a pestle and mortar. This powder was placed into 4mm quartz esr tubes. For the esr study of tars and oils, small samples were placed into 8mm quartz esr tubes, since the viscous tars could not successfully be placed into the 4mm quartz tubes used for the coal study. The tar was placed into the esr tubes via an ungraduated pipette. It was found to be very difficult to place a reproducible volume of tar into the esr tubes, because the tars adhered by differing amounts to the sides of the pipette and full draining was never attained. So the amount of tar present in each esr tube was assessed by weighing, and thus comparisons could be made between different samples.

Solvent addition for the tars and oils was via a graduated pipette, so that sample/solvent ratios could be calculated. For the coal study, the solvent was added via an ungraduated pipette and allowed to saturate the sample. The excess solvent was then decanted off. All the solvents used were dry, and deoxygenated samples were attained via the freeze-thaw method. The esr spectra were recorded on Varian E3 and E109 esr spectrometers with 100kHz modulation.

Samples for ir spectroscopy

Because of the problems experienced by other coal workers using alkali halide pellets, mulls and thin

sections, ⁵⁶ a relatively little used technique for the ir study of coal was used i.e. the use of thin films and/or pressed discs. This technique, described below, avoids the superimposition of substrate bands onto the coal spectrum.

Approximately 1g of the bulk sample was added to 10ml of de-oxygenated distilled water and crushed for 1 hour in a McCrone Micronising mill fitted with agate elements; fine grinding was critical to the successful production of suitable coal films and discs. Two drops of the resultant slurry were then spread on to the face of a ½" diameter polished stainless steel die and the water allowed to slowly evaporate away; too rapid a rate of evaporation results in the cracking of the coal film. To form a disc the coal remaining on the die was then compressed to approximately 130tons/in², giving a compacted disc which could be floated away from the die using a few drops of distilled water. The discs were about 10-30µm thick and weighed about 0.01g.

The addition of solvent was attained via a humidifying system. The coal film/disc was placed into a desiccator which contained dry solvent and allowed to absorb solvent vapour for a timed period. The sample was then removed and its spectrum recorded. The same sample was then replaced into the desiccator and further solvent addition allowed. The ir spectra were recorded on a Perkin Elmer 681 spectrometer.

Chapter 2

2 ESR Study of Tars and Oils

2.1 Introduction

The tars and oils studied here are the by-products of the gasification process. This process can be represented by the equation: $Coal \xrightarrow{\Delta} gas + tar + oil + ash$.

Elemental analyses for most of these tar and oil samples were supplied by British Gas and are given in *table 2(i)*. The Markham Main Tars and Oils labelled WSP 028 etc. are obtained from several different gasifier runs (026-032).

2.2 Pure Tars and Oils

Initial studies of the pure tars and oils showed that their esr spectra were broad singlets with g-values between 2.0026 and 2.0036, see *table 2(ii)*. It is noteworthy that the linewidths of the oils were approximately half that of the tars, as shown in *fig. 2(i)*. Also the esr signal from the oils was a factor of 10 less intense than that from the tars.

Little further work could be carried out on pure tars and oils at room temperature because of their high viscosity. So attention was switched to try to find a suitable solvent or solvents so that the tars and oils could be studied as solutions. Thus removing the viscosity problem.

Table 2(1)

| <u>Sample</u> | <u>%C</u> | <u>%H</u> |
|--------------------------|-----------|-----------|
| Markham Main Sales Tar | 85.8 | 6.6 |
| Markham Main Recycle Tar | 85.2 | 7.3 |
| Pittsburgh Recycle Tar | 84.5 | 6.7 |
| Manton Recycle Tar | 83.9 | 6.5 |
| Lynemouth Recycle Tar | 73.6 | 7.0 |
| Lynemouth Sales Tar | - | - |
| Markham Main Tars | | |
| WSP 026 Sales Tar | 84.8 | 6.4 |
| WSP 027 Recycle Tar | 85.8 | 6.3 |
| WSP 029 Recycle Tar | 86.2 | 6.5 |
| WSP 030 Sales Tar | 85.6 | 6.4 |
| WSP 031 Recycle Tar | 87.5 | 6.5 |
| WSP 032 Recycle Tar | 87.4 | 6.4 |
| Markham Main Oils | | |
| WSP 026 Sales Oil | 86.3 | 8.1 |
| WSP 027 Sales Oil | 86.2 | 8.0 |
| WSP 028 Wash Oil | 86.8 | 8.0 |
| WSP 029 Sales Oil | 87.0 | 8.1 |
| WSP 030 Sales Oil | 85.7 | 8.0 |
| WSP 031 Sales Oil | 86.5 | 8.1 |
| WSP 032 Wash Oil | 86.5 | 8.2 |

Table 2(ii)

| <u>Sample</u> | <u>g-value</u> | <u>Line-width (G)</u> |
|--------------------------|----------------|-----------------------|
| Markham Main Sales Tar | 2.0036 | 6.9 |
| Markham Main Recycle Tar | 2.0034 | 8.2 |
| Pittsburgh Recycle Tar | 2.0035 | 7.6 |
| Manton Recycle Tar | 2.0035 | 7.8 |
| Lynemouth Recycle Tar | 2.0034 | 7.6 |
| Lynemouth Sales Tar | 2.0034 | 8.0 |
| Markham Main Tars | | |
| WSP 026 Sales Tar | 2.0027 | 9.0 |
| WSP 027 Recycle Tar | 2.0028 | 9.0 |
| WSP 029 Recycle Tar | 2.0027 | 9.0 |
| WSP 030 Sales Tar | 2.0027 | 9.0 |
| WSP 031 Recycle Tar | 2.0028 | 8.0 |
| WSP 032 Recycle Tar | 2.0030 | 8.0 |
| Markham Main Oils | | |
| WSP 026 Sales Oil | 2.0031 | 4.5 |
| WSP 027 Sales Oil | 2.0026 | 4.4 |
| WSP 028 Wash Oil | 2.0032 | 4.5 |
| WSP 029 Sales Oil | 2.0034 | 4.4 |
| WSP 030 Sales Oil | 2.0033 | 3.8 |
| WSP 031 Sales Oil | 2.0032 | 4.4 |
| WSP 032 Wash Oil | 2.0030 | 4.8 |

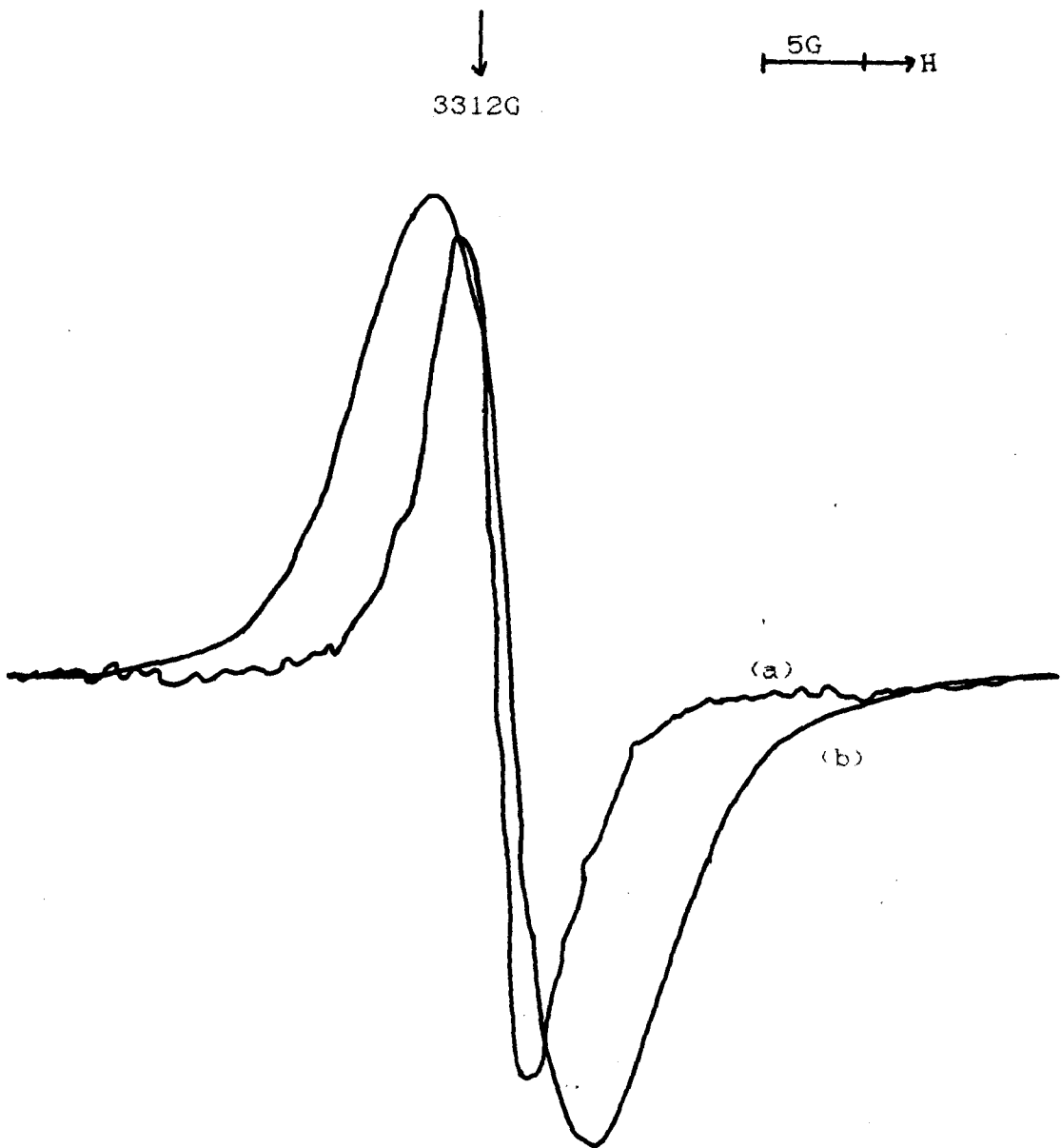


Figure 2(i): Typical esr spectra of pure tars and oils; (a) WSP 026 Sales Oil (gain $\times 10$), (b) WSP 026 Sales Tar.

2.3 Solvent Addition to Tars

It was hoped that a solvent would be found that dissolved the tar but did not affect its esr signal. The two solvents chosen were tetrahydrofuran (THF) and chloroform (CHCl_3), as suggested by British Gas. Both solvents dissolved the tars and it was found that both solvents had a similar effect on the tar esr signal.

Firstly the effect of varying the volume of solvent added to the tar was studied. The pure tar was placed into the esr tube, weighed and its spectrum recorded. This provides a blank against which all other spectra can be compared. Measured volumes of solvent were then added to the tar sample and the tar/solvent mixture reweighed. Thus the relative amounts of tar and solvent could be calculated, giving the axis [weight(solvent) + weight(tar)]. The esr spectrum of this mixture was then recorded. Further solvent was then added to this mixture and this weighing/recording process repeated several times.

An example of the obtained results is shown in *fig. 2(ii)*. It was observed that the esr signal drops as more solvent is added to the tar; this eventually seems to reach a bottom limit after which no further addition of solvent affects the signal. It was also noted, however, that if the tar/solvent mixture was left to stand, for a few hours, before it had reached this bottom limit, that the intensity of its esr signal had decreased, even though

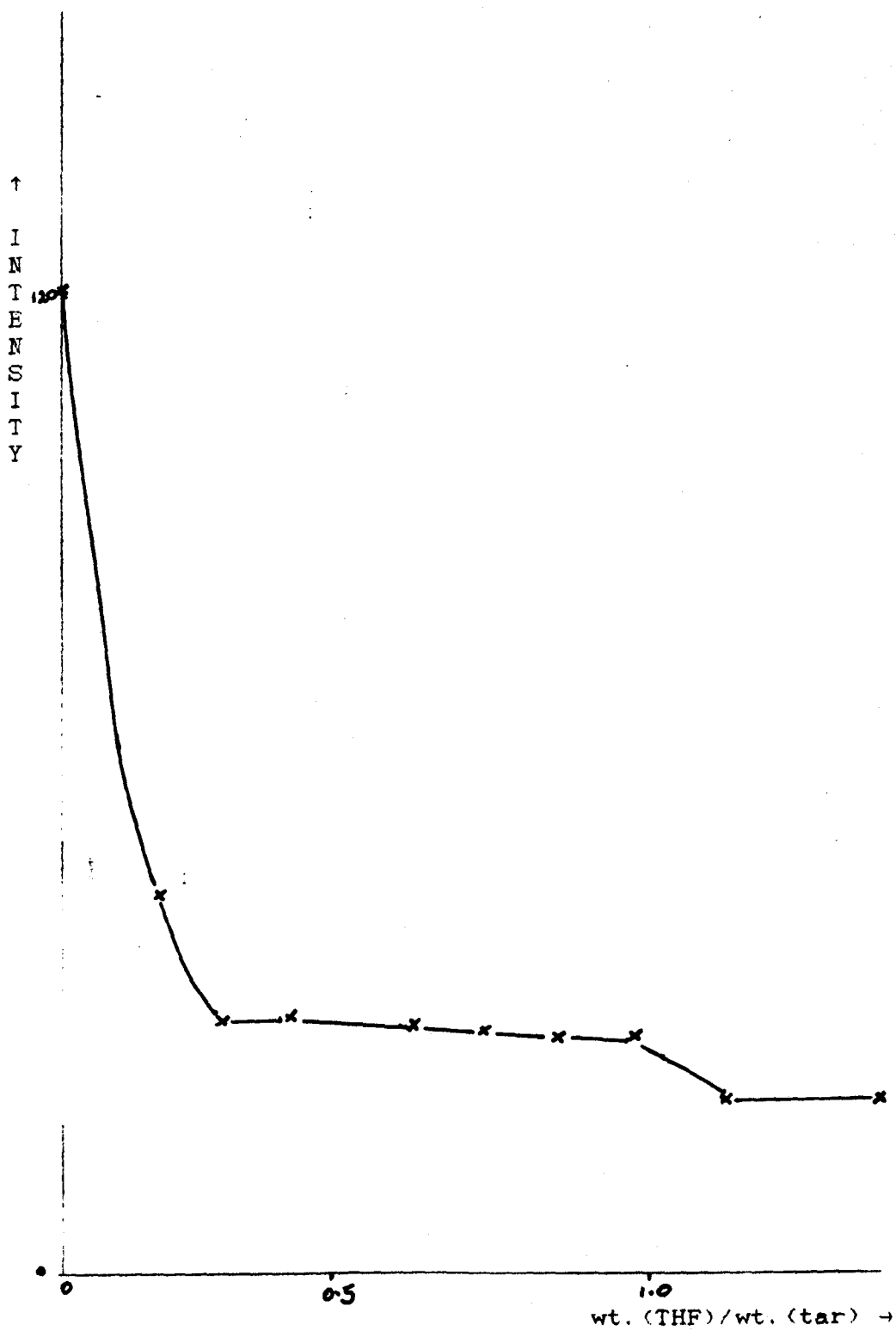


Figure 2(11): A graphical representation of the effect of solvent volume on the tar/THF esr signal intensity.

no further solvent addition had taken place.

Thus a second solvent study was undertaken, that is, to study the effect of time when a given volume of solvent is added to the tar. In this study, as earlier, a blank spectrum, of pure tar, was recorded. Then a measured volume of solvent ($\approx 1\text{ml}$) was added, at elapsed time, $t = 0$. Spectra were then recorded at timed intervals. Some examples of the results obtained are shown in *fig. 2(iii)*. It was noted from the graph that there was an initial loss of esr signal intensity, but, in all the cases studied, after 1800s (30mins.) no further loss in signal intensity was observed. For all the tars studied there was a residual esr signal which was never lost.

Larger volumes of solvent were added to the tar and an elapsed time study undertaken, but the results obtained were independent of added solvent volume. These results discredit those obtained from the earlier, variable solvent volume studies. Those results were probably due to an elapsed time effect.

x Manton Recycle Tar
 o Lynemouth Sales Tar
 Δ Lynemouth Recycle Tar
 □ Markham Main Sales Tar

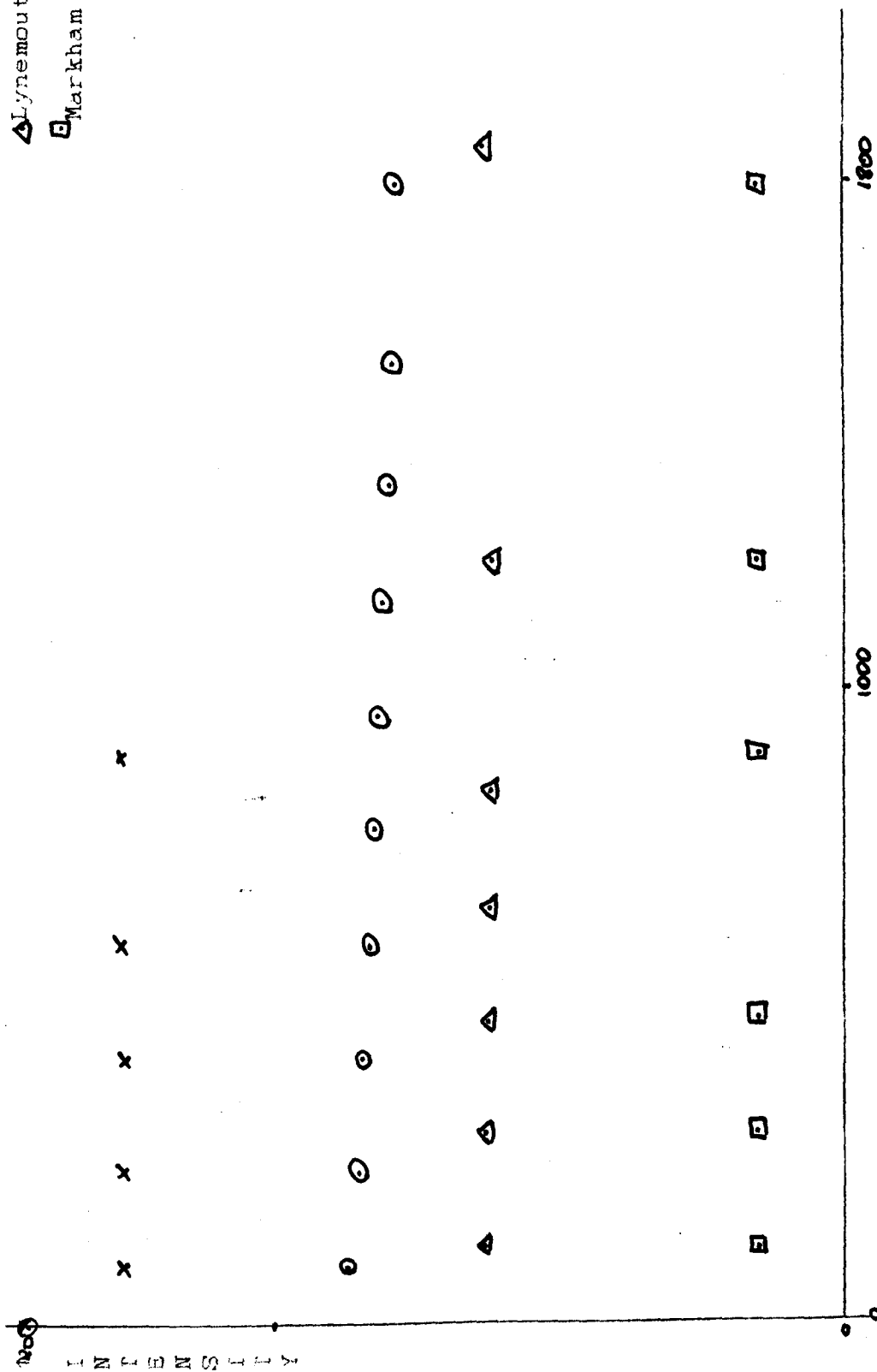


Figure 2(iii): A graphical representation of the effect of elapsed time, t, on the tar/THF esr signal intensity.

Chapter 3

3 ESR Study of Coals

3.1 Introduction

Elemental analyses for some of these coal samples and the NCB classification for all of these coals were supplied by British Gas and are given in *table 3(i)*. The NCB classification is a guide to the relative amounts of carbon and volatile matter within the coal. The first digit relates to the amount of carbon in the coal; the lower the number the higher the percentage of carbon present. The last two digits relate to the amount of volatile matter present; if this volatile matter is $> 32\%$, then the last two digits of the classification are 01; if the value is $> 36\%$, then these digits are 02. This classification is explained fully in reference 24.

3.2 Pure Coals

The esr spectra of the fresh coals were taken and the g-values and peak-to-peak line-widths were recorded; this data is presented in *table 3(ii)*. The signal intensity was also noted. Most of the coal samples studied showed a single broad resonance with no hyperfine; typical examples are shown in *fig. 3(i)*.

The coal samples studied were all approximately the same weight and the esr spectra all gave approximately the same signal intensity. However in one case, namely Henning

Table 3(1)

| <u>Sample</u> | <u>NCE</u> | <u>%C</u> | <u>%H</u> |
|--------------------------|---------------|-----------|-----------|
| | <u>Class.</u> | | |
| Pumpquant Coal | 101 | - | - |
| Manton Coal | 502 | 79.5 | 5.3 |
| Hucknall Coal | 602 | 79.6 | 5.5 |
| Manvers Swallowwood Coal | 602 | 79.0 | 5.4 |
| Lynemouth Coal | 702 | - | - |
| Markham Main Coal | 702 | 79.37 | 5.17 |
| Gedling Coal | 802 | 78.4 | 5.2 |
| Snibston Coal | 902 | 78.2 | 5.2 |
| Henning Coal | sub-bit. | - | - |
| Belle Ayr Coal | lignite | - | - |

Table 3(ii)

| <u>Sample</u> | <u>g-value</u> | <u>Line-width (G)</u> |
|--------------------------|----------------|-----------------------|
| Pumpquant Coal | 2.0028 | 4.6 |
| Manton Coal | 2.0023 | 5.0 |
| Hucknall Coal | 2.0023 | 1.0;5.5 |
| Manvers Swallowwood Coal | 2.0024 | 4.6 |
| Lynemouth Coal | 2.0024 | 6.0 |
| Markham Main Coal | 2.0024 | 5.5 |
| Gedling Coal | 2.0023 | 5.0 |
| Snibston Coal | 2.0025 | 4.5 |
| Henning Coal | 2.0036 | 6.0 |
| Belle Ayr Coal | 2.0035 | 6.2 |

- Gedling Coal
- - Manton Coal
- · - Manvers Swallowwood Coal
- · · Markham Main Coal

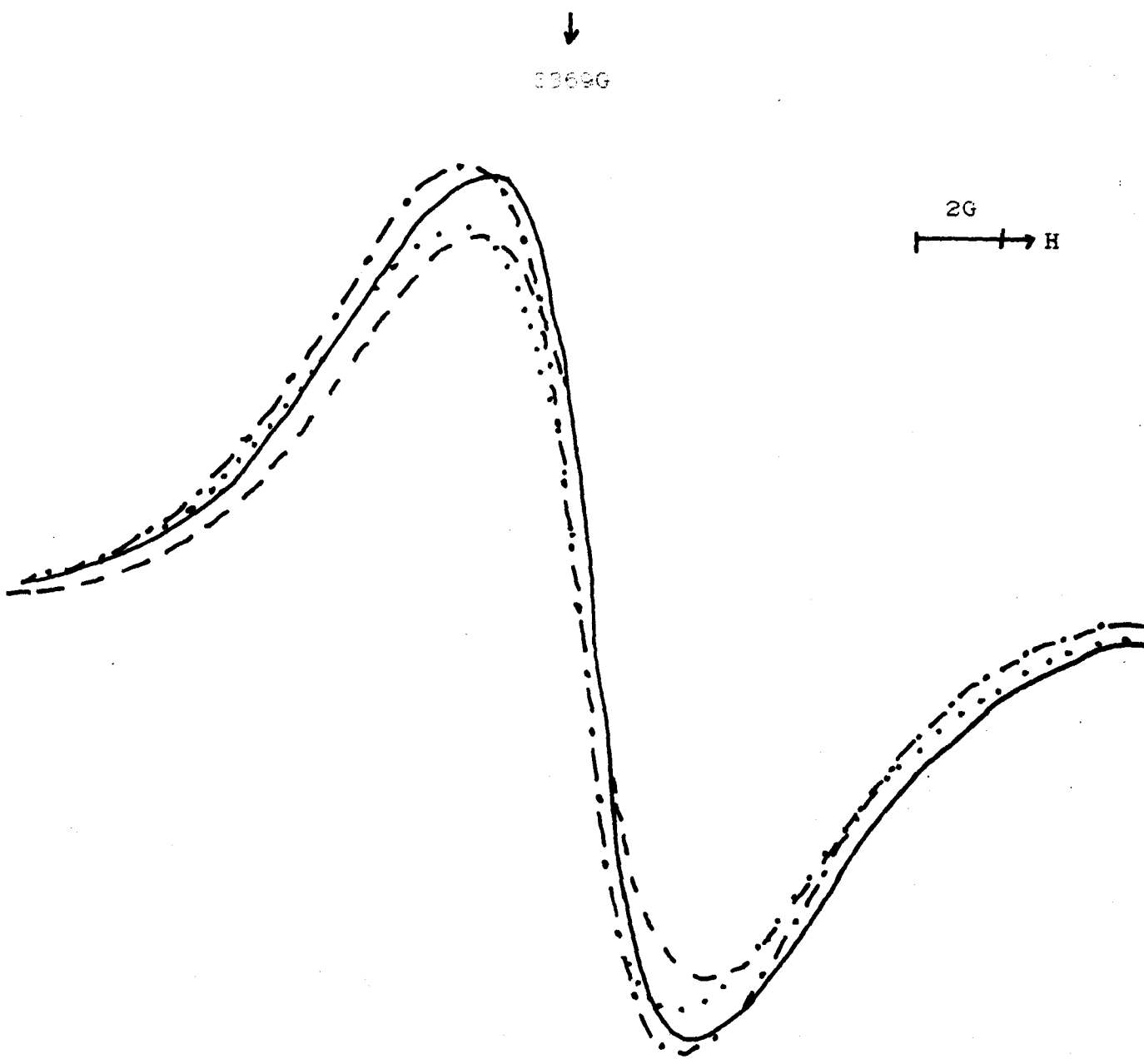


Figure 3(i): Typical esr spectra of coal.

Coal, an esr signal ca. 10^2 smaller than the other coals was obtained. This spectrum is shown in *fig. 3(ii)*. Most of the coals studied had a g-value close to the free electron value of 2.0023, see *table 3(ii)*. This is in agreement with other workers such as Khulbe et al.^{'44'} and Retcofsky;^{'57'} who showed that for coals with greater than 65%C, the g-value approaches free-spin. The coals studied, for which data is available, have 78-80%C. The remaining coals have higher g-values reaching a maximum of 2.0036G. These values are typical of g-values for neutral radicals of carbon, nitrogen and hydrocarbon ions.^{'58'}

The esr spectrum of one of the coals, Hucknall Coal, exhibited a narrow line in addition to the usual broad resonance; see Chapter 1. The spectrum is shown in *fig. 3(iii)a*. The spectrum is a sharp line ($\approx 1G$), superimposed on a broader signal, similar to that noted by Petrakis and Grandy.^{'57'}

The coal samples under study were then exposed to atmospheric oxygen for 24 hours and their spectra recorded. The g-values and line-widths are shown in *table 3(iii)*; it is noteworthy that these values are very similar to those obtained for same unexposed coal, this fact was also noted by Ohuchi et al.^{'59'} With Hucknall Coal, the narrow line broadens and merges with the broad line when air is admitted, as shown in *fig. 3(iii)b*. It was suggested by Petrakis and Grandy^{'50'} that this broadening was due to the presence of paramagnetic oxygen, which decreases the

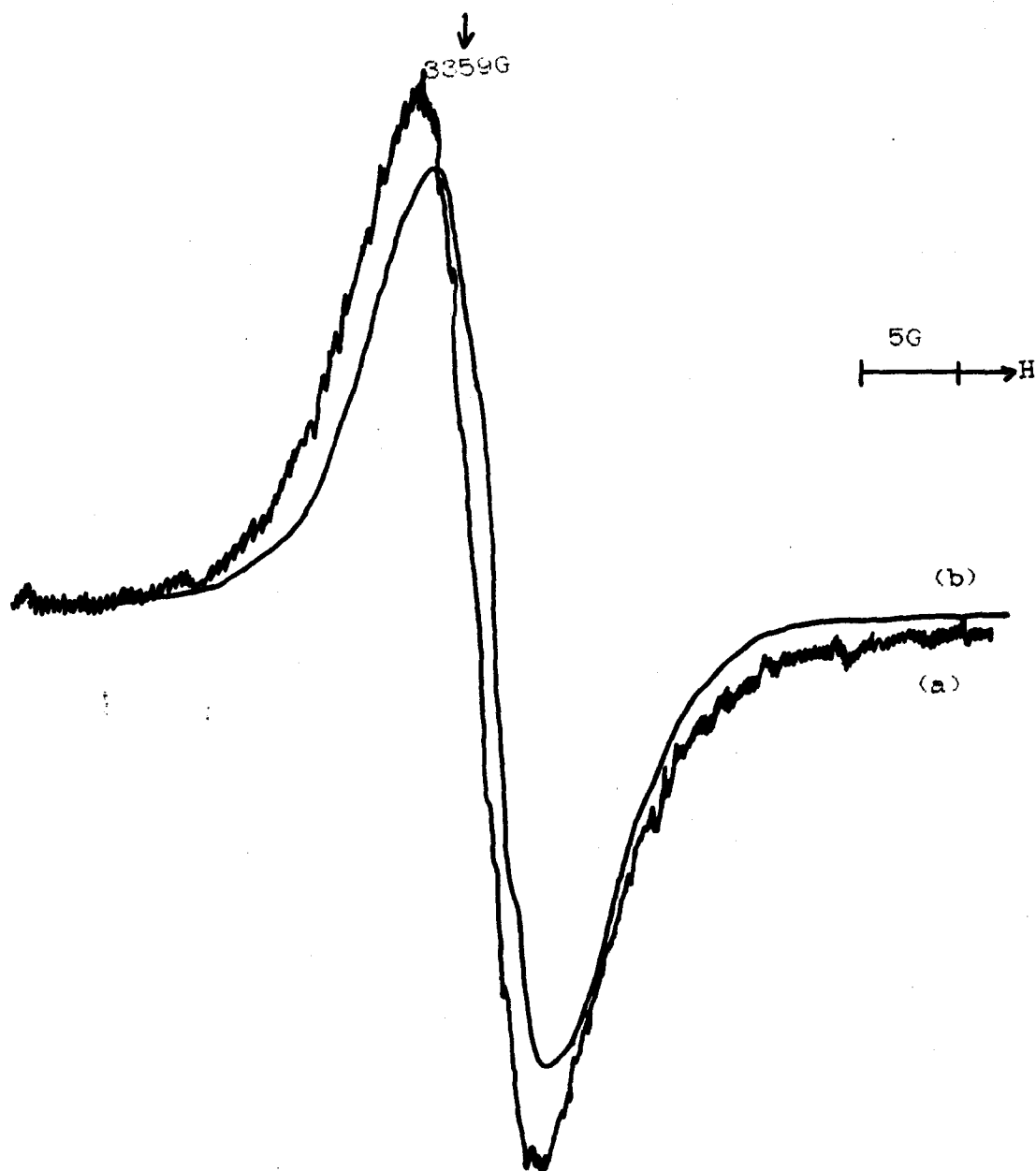


Figure 3(ii): ESR spectra of (a) pure Henning Coal (gain $\times 10^2$), (b) pure Lynemouth Coal.

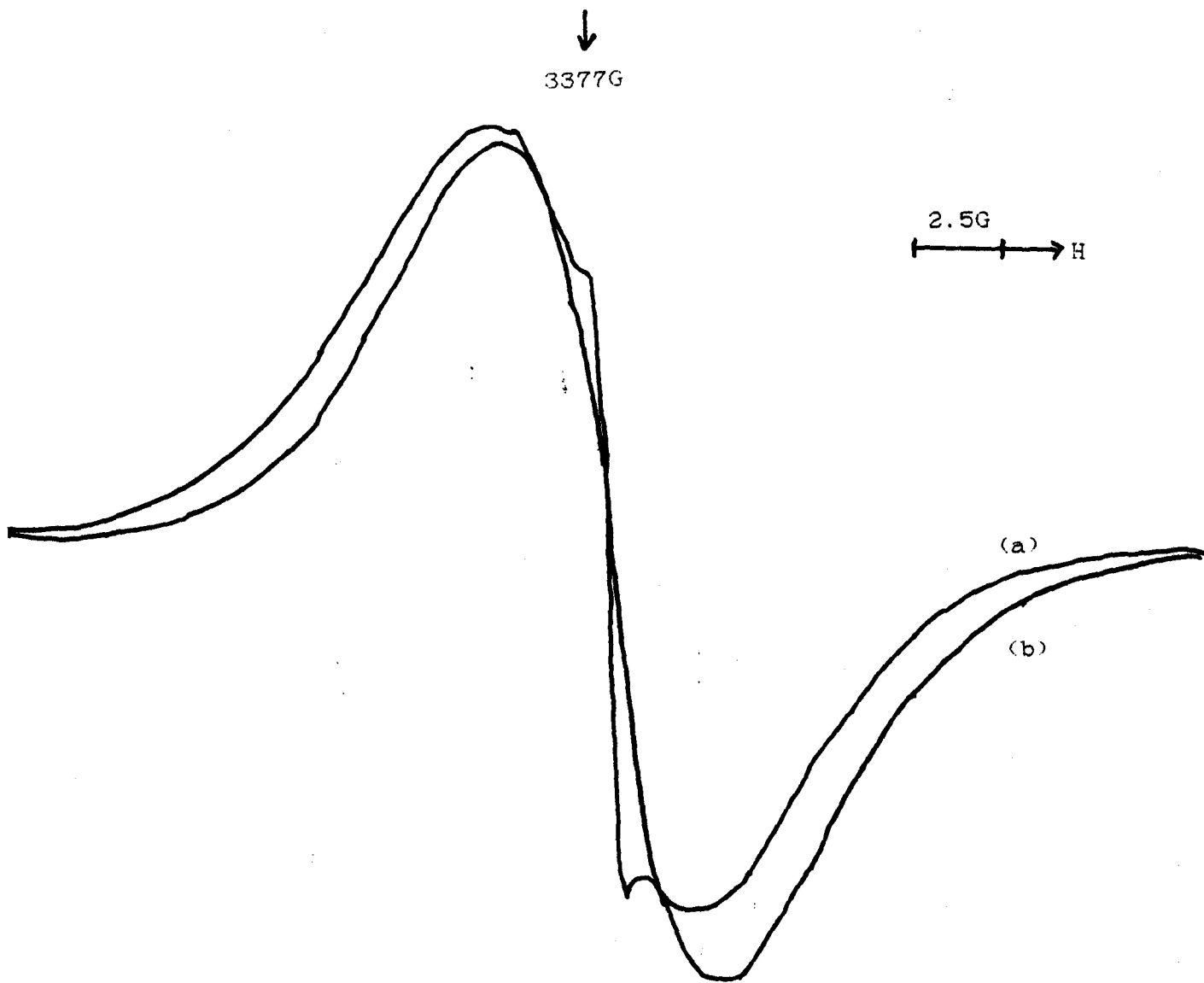


Figure 3(iii): ESR spectra of pure Hucknall Coal;
(a) fresh, (b) after exposure to atmospheric oxygen.

Table 3(iii)

| <u>Sample</u> | <u>g-value</u> (G) | <u>Line-width</u> (G) |
|--------------------------|--------------------|-----------------------|
| Pumpquant Coal | 2.0026 | 4.5 |
| Manton Coal | 2.0023 | 5.0 |
| Hucknall Coal | 2.0023 | 6.0 |
| Manvers Swallowwood Coal | 2.0024 | 5.0 |
| Lynemouth Coal | 2.0026 | 6.0 |
| Markham Main Coal | 2.0024 | 6.25 |
| Gedling Coal | 2.0023 | 5.0 |
| Snibston Coal | 2.0025 | 5.0 |
| Henning Coal | 2.0035 | 6.0 |
| Belle Ayr Coal | 2.0036 | 6.0 |

electron relaxation times and leads to the broadening of spectral lines. On evacuation, some evidence of the reappearance of the narrow line is obtained; but, despite long periods under a high vacuum, the total return of the original narrow line was not observed.

3.3 Solvent Addition

Having noted that solvents affect the esr signal of tar, in Chapter 2, a solvent study of coal was undertaken. The experiments were designed so as to study the effect of various solvents on the different coal samples. The solvents used were tetrahydrofuran (THF), acetonitrile (MeCN), dimethyl formamide (DMF), dimethyl sulphoxide (DMSO) and triethyl phosphineoxide (TEPO). These solvents gave a range of basicity and molecular size.

Preliminary studies showed that the addition of solvent to the coal altered only the esr signal intensity, all other parameters remained constant. The solvents used here were all used as available i.e. some dissolved oxygen was present (*oxygenated*). A systematic study was then undertaken, the coal/solvent mixtures being left to stand for 1 hour before the spectra were recorded, so as to eliminate the elapsed time effect, see Chapter 2.

The intensity of each esr signal was measured and since the esr line-width was unchanged, the intensity can be used as a measure of radical concentration. Spectra were

recorded for each coal with each solvent. An example of the spectra obtained for one coal with various solvents is shown in *fig. 3(iv)*. So as to compare the effect of different solvents on different coals, the initial intensities of the pure coal signals were standardised. From these standardised signals all the other signals could have their relative intensities calculated, and a graphical representation of all the results obtained is shown in *fig. 3(v)*. The first impression of the graph is that there seems to be no systematic variation of esr signal intensity with solvent addition, but closer study does reveal some interesting points worthy of note.

The first point of note is that on solvent addition the intensity of most of the signals decreased, though some remained constant and some increased. This confirms the expectation that there are different radicals present in the different coals and these different radicals react differently with the solvents. The decrease in signal intensity was expected and was due to the neutralisation of some of the free radicals by reaction with the solvents. The constancy of some of the signals suggests that some of the free radicals present in some of the coals are resistant to chemical attack by the solvents. However, the increase in intensity was unexpected and it was only observed with THF as the solvent; there seems no obvious reason for this increase, but Ohuchi *et al.*⁽²²⁾ also noted an increase in esr signal intensity. They postulated that

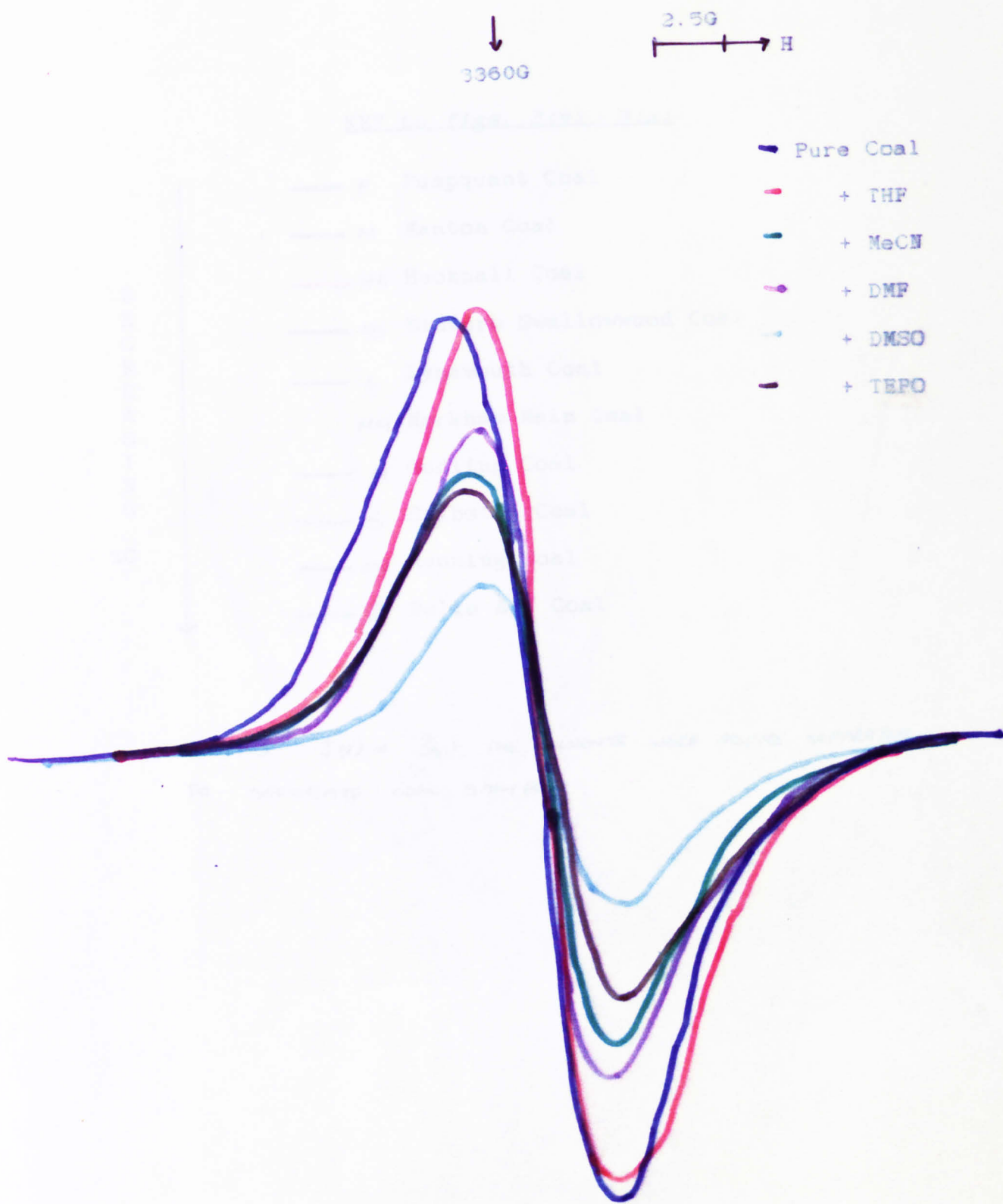


Figure 3(iv): The effect of dry oxygenated solvent addition on the esr spectrum of Lynemouth Coal.

KEY to figs. 3(v) - 3(x)

D
E
C
R
E
A
S
I
N
G
%C

-  P Pumpquant Coal
-  M Manton Coal
-  MK Hucknall Coal
-  MS Manvers Swallowwood Coal
-  L Lynemouth Coal
-  MM Markham Main Coal
-  G Gedling Coal
-  S Snibston Coal
-  HN Henning Coal
-  B Belle Ayr Coal

FOR FIGS 3(V) & 3(W) THE SOLVENTS WERE ADDED SEPARATELY
TO SEPERATE COAL SAMPLES

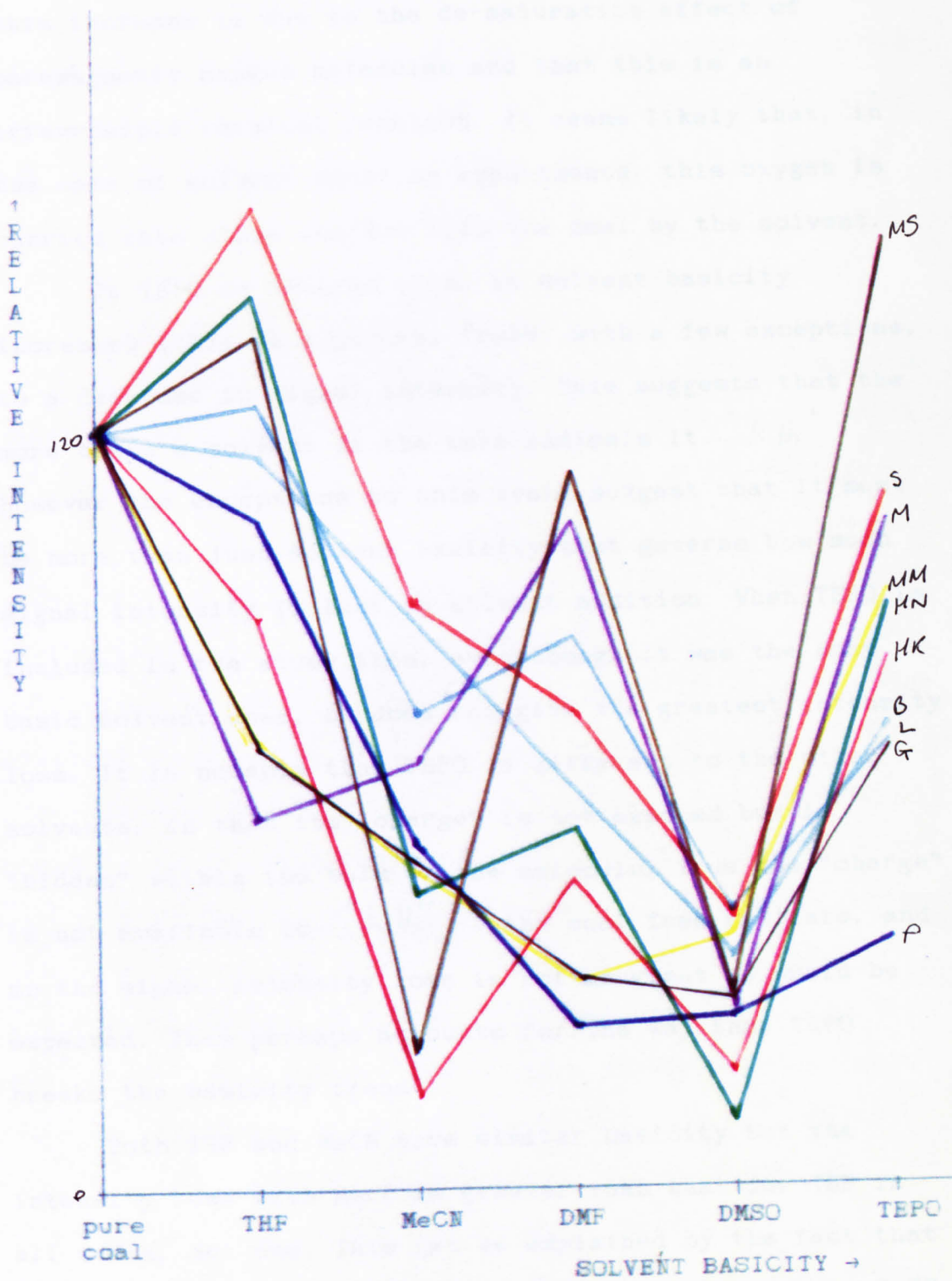


Figure 3(v): A graphical representation of the effect of oxygenated solvents on the coal esr signal intensity.

this increase is due to the de-saturation effect of paramagnetic oxygen molecules and that this is an irreversible chemical reaction. It seems likely that, in the case of solvent addition experiments, this oxygen is carried into close contact with the coal by the solvent.

If TEPO is ignored then, as solvent basicity increases there is a general trend, with a few exceptions, to a decrease in signal intensity. This suggests that the more basic a solvent is the more radicals it "kills". However the exceptions to this trend suggest that it must be more than just solvent basicity that governs how much signal intensity is lost on solvent addition. When TEPO is included in the study then, even though it was the most basic solvent used, it does not give the greatest intensity loss. It is notable that TEPO is different to the other solvents, in that its "charge" is not exposed but is "hidden" within the bulk of the molecule. Thus the "charge" is not available to "kill" the coal free radicals, and so the signal intensity loss is not as great as would be expected. This perhaps accounts for the way that TEPO breaks the basicity trend.

Both THF and MeCN have similar basicity but the intensity loss with MeCN is greater than that for THF in all cases, but one. This can be explained by the fact that MeCN is a much smaller molecule than THF and thus the MeCN molecules can penetrate further into the coal pores, have contact with more of the coal surface and thus neutralise

more of the free radicals. For all of the solvents except DMSO there is a wide spread of intensities. DMSO itself had a very similar effect on all the coals and a large decrease in intensity was seen in all cases, and this is probably due to the basicity of the solvent and its exposed "charge".

It is interesting that the traces of Markham Main Coal and Gedling Coal are very similar even though they are coals with different NCB classifications; Markham Main Coal and Lynemouth Coal, however, have the same NCB classification but they have very different traces. Also there is no direct correlation between the carbon content of the coal and the amount of signal intensity loss; both the coal with the highest %C and the coal with the lowest %C give a trace somewhere towards the middle of the series of lines.

As mentioned earlier it was thought that dissolved oxygen in the solvent could be causing some of the effects seen in that earlier study. The solubility of oxygen in the various solvents was likely to vary, however data of the relative solubility of oxygen in the solvents used was not available. Thus a further set of experiments were designed using de-oxygenated solvents. For this series of experiments the same solvents were used as before except for TEPO, since this solvent could not be conveniently de-oxygenated. The spectra were recorded and the intensities standardised as for the *oxygenated* samples, and a similar graphical representation is shown in *fig. 3(vi)*.

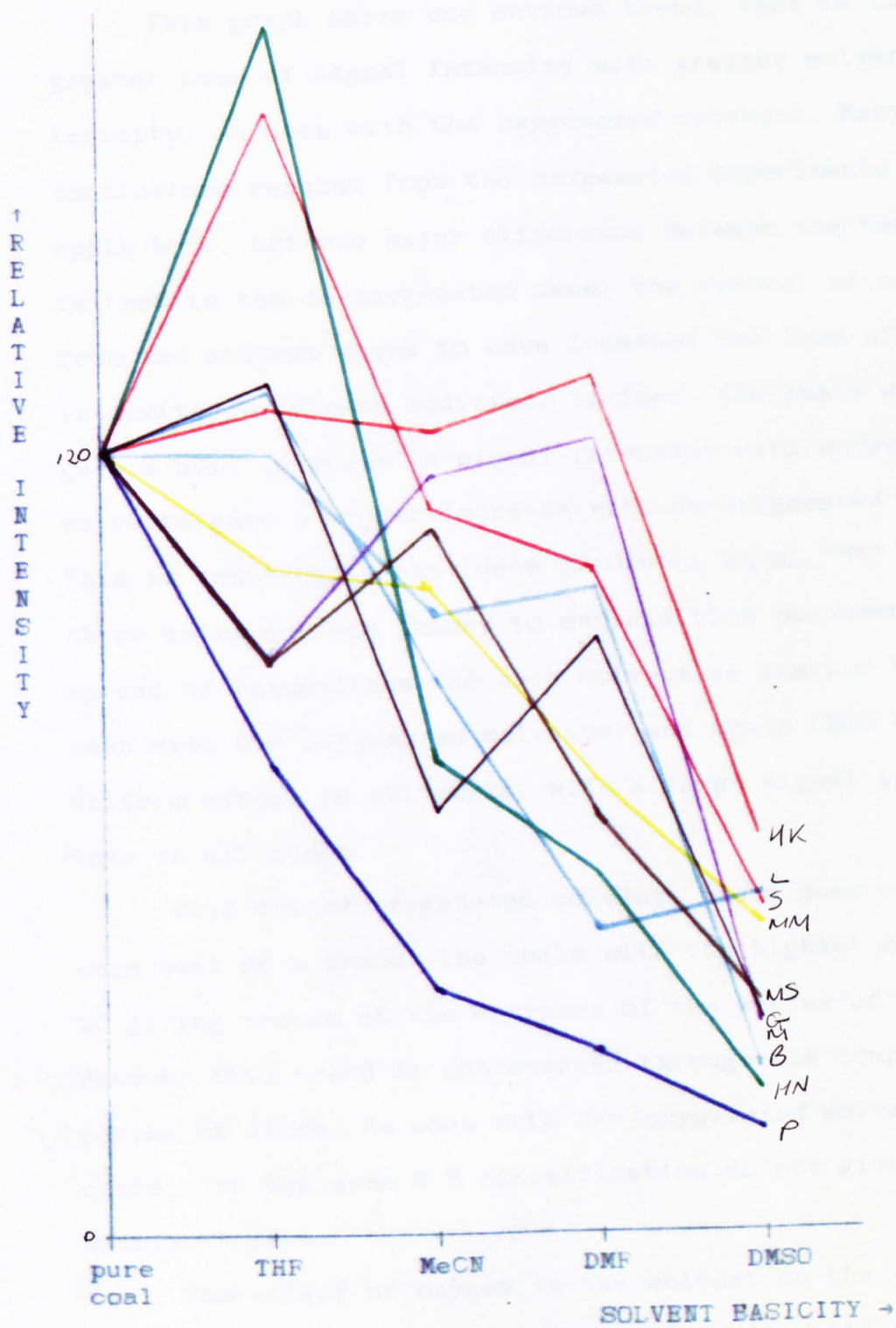


Figure 3(vi): A graphical representation of the effect of de-oxygenated solvents on the coal esr signal intensity.

This graph shows one obvious trend, that is the greater loss of signal intensity with greater solvent basicity, as seen with the *oxygenated* solvents. Many of the conclusions reached from the *oxygenated* experiments also apply here, but one major difference between the two cases is that in the de-oxygenated case, the removal of oxygen from the solvent seems to have lessened the loss of signal intensity on solvent addition. In fact, the coals which gave a nett increase in signal intensity with *oxygenated* solvents gave a bigger increase with de-oxygenated solvent. This is contrary to the ideas of Ohuchi *et al.*⁽⁵²⁾ and there is no current theory to explain this phenomenon. The spread of intensities for each solvent is similar to that seen with the *oxygenated* solvents, and again DMSO has a uniform effect on all coals, with a large signal intensity loss in all cases.

With the de-oxygenated solvents there does seem to be some sort of a trend, the coals with the highest and lowest %C giving traces at the extremes of the series of lines. However this trend is not carried through the complete series of lines. As seen with the *oxygenated* solvents the coals with the same NCB classification do not give the similar traces.

The effect of oxygen in the solvent on the *esr* signal intensity can be better observed by plotting the previously obtained results in a different way. Graphical representations of the effect of oxygen on the *esr* signal

intensity of all the coals with any particular solvent are shown in *figs. 3(vii) - 3(x)*.

Figure 3(vii) shows the effect of oxygen on the coal/THF signal intensity. The signal intensities are distributed evenly around the intensity of pure coal; for both the *oxygenated* and *de-oxygenated* solvents approximately half of the signal intensities have increased and half have decreased. The lines to the right hand side of the graph show the difference, for each coal, between the signal intensities after the addition of *oxygenated* and *de-oxygenated* solvents. As can be seen, the intensity differences vary greatly and there seems to be no trend as to the size of the difference and the %C of the coal. The largest difference, however, is due to a coal, Hucknall Coal, which has a relatively high hydrogen content, i.e. %H greater than any of the other coals. This trend is seen throughout these graphs. The coals which show the least difference between the two experiments also have signal intensities close to the original (pure coal) intensity, and due to the inaccuracy of esr intensity measurements ($\pm 10\%$) it is likely that these signals did not actually change on solvent addition.

The +/- signs on these vertical lines show which end of the line is due to *oxygenated* solvent (+) and which is due to *de-oxygenated* (-). As can be seen from these lines, some of the coals have an esr signal intensity that increases when the solvent is *de-oxygenated* and some have a

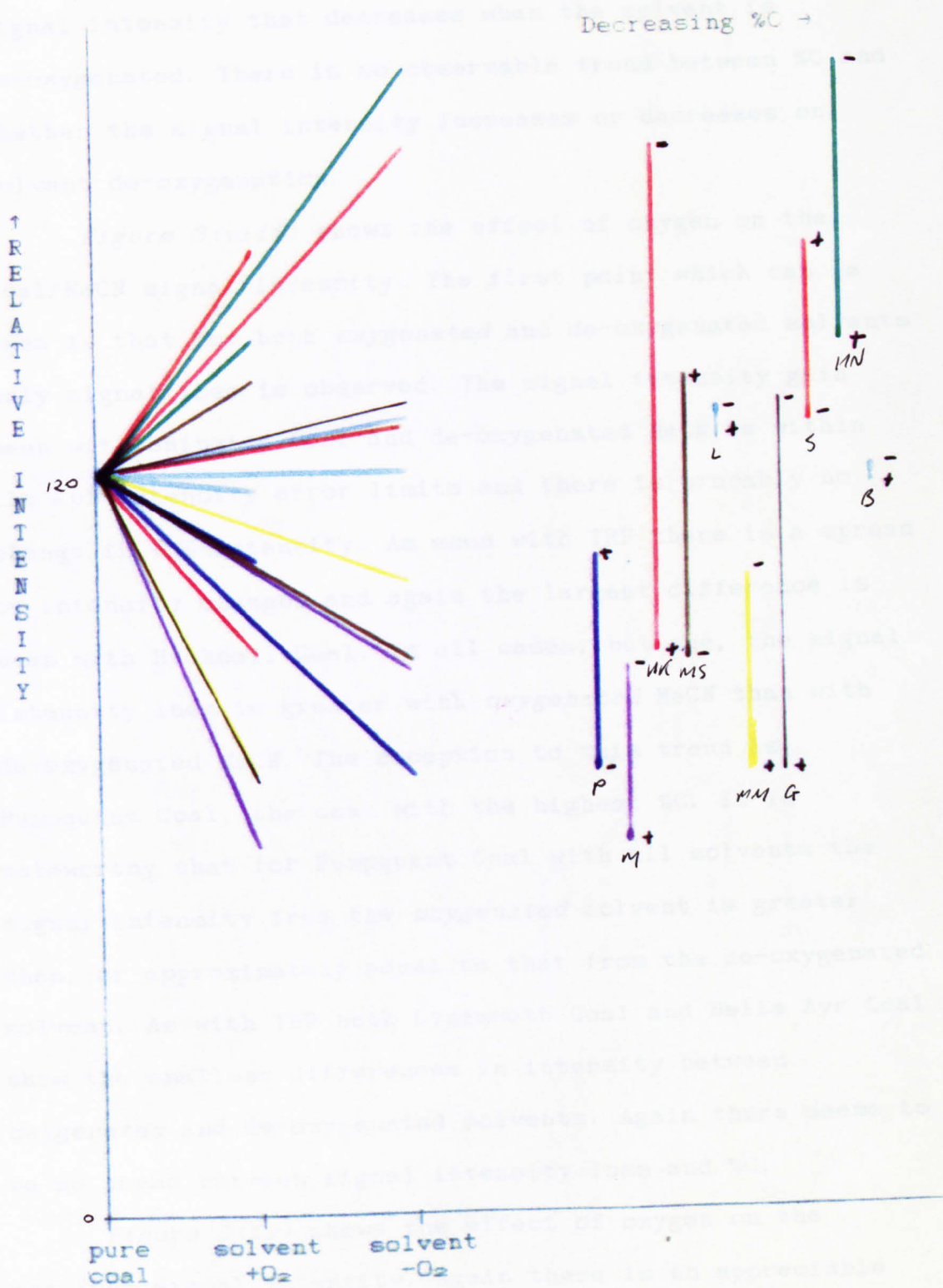


Figure 3(vii): A graphical representation of the effect of oxygen on the coal/THF esr signal intensity.

signal intensity that decreases when the solvent is de-oxygenated. There is no observable trend between %C and whether the signal intensity increases or decreases on solvent de-oxygenation.

Figure 3(viii) shows the effect of oxygen on the coal/MeCN signal intensity. The first point which can be seen is that for both oxygenated and de-oxygenated solvents only signal loss is observed. The signal intensity gain seen with Snibston Coal and de-oxygenated MeCN is within the 10% intensity error limits and there is probably no change in the intensity. As seen with THF there is a spread of intensity changes and again the largest difference is seen with Hucknall Coal. In all cases, but one, the signal intensity loss is greater with oxygenated MeCN than with de-oxygenated MeCN. The exception to this trend is Pumpquant Coal, the coal with the highest %C. It is noteworthy that for Pumpquant Coal with all solvents the signal intensity from the oxygenated solvent is greater than, or approximately equal to that from the de-oxygenated solvent. As with THF both Lynemouth Coal and Belle Ayr Coal show the smallest differences in intensity between oxygenated and de-oxygenated solvents. Again there seems to be no trend between signal intensity loss and %C.

Figure 3(ix) shows the effect of oxygen on the coal/DMF signal intensity. Again there is no appreciable signal intensity gain, however the greatest signal loss is less than that seen with MeCN. A spread of intensity

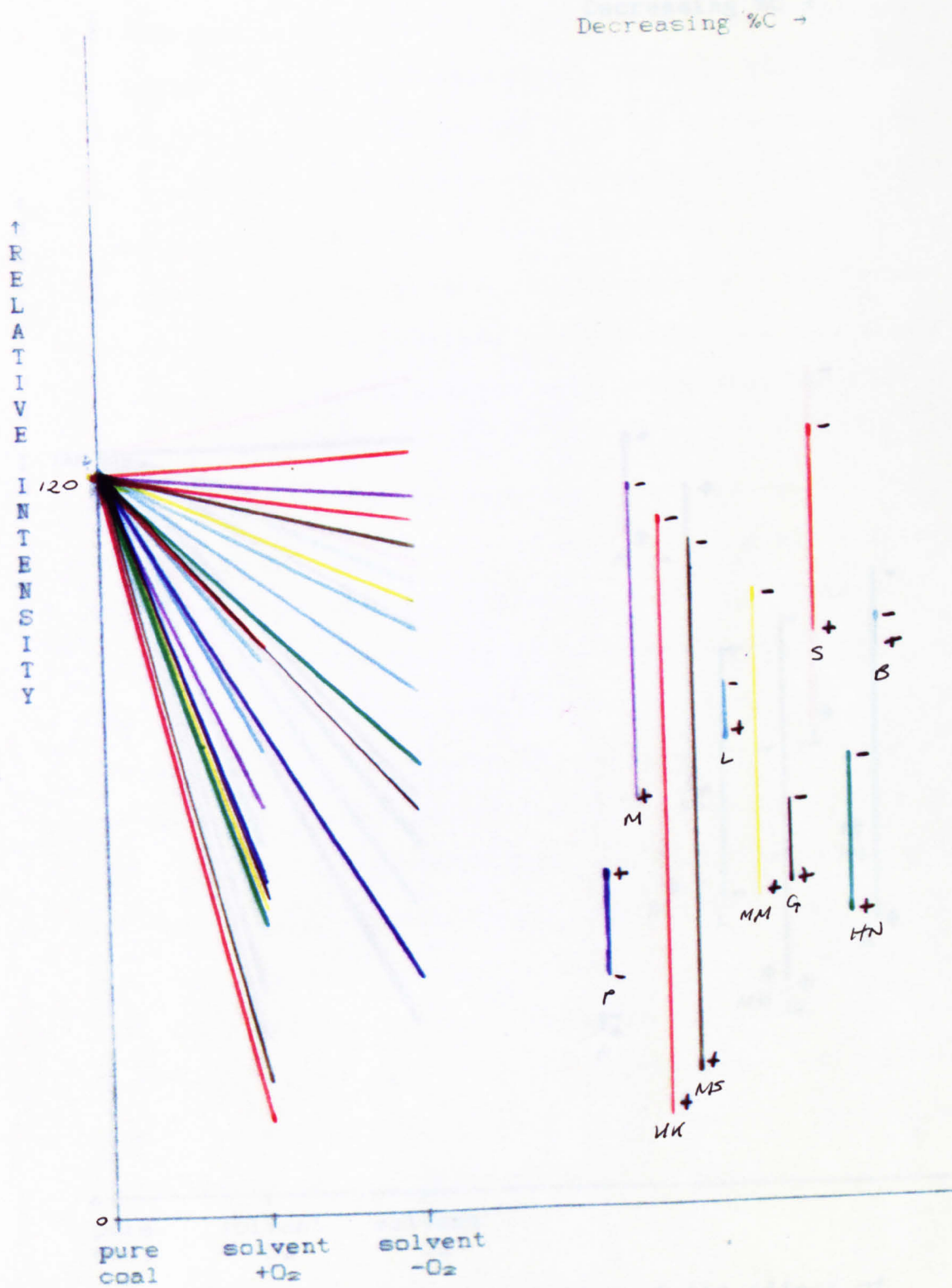


Figure 3(viii): A graphical representation of the effect of oxygen on the coal/MeCN esr signal intensity.

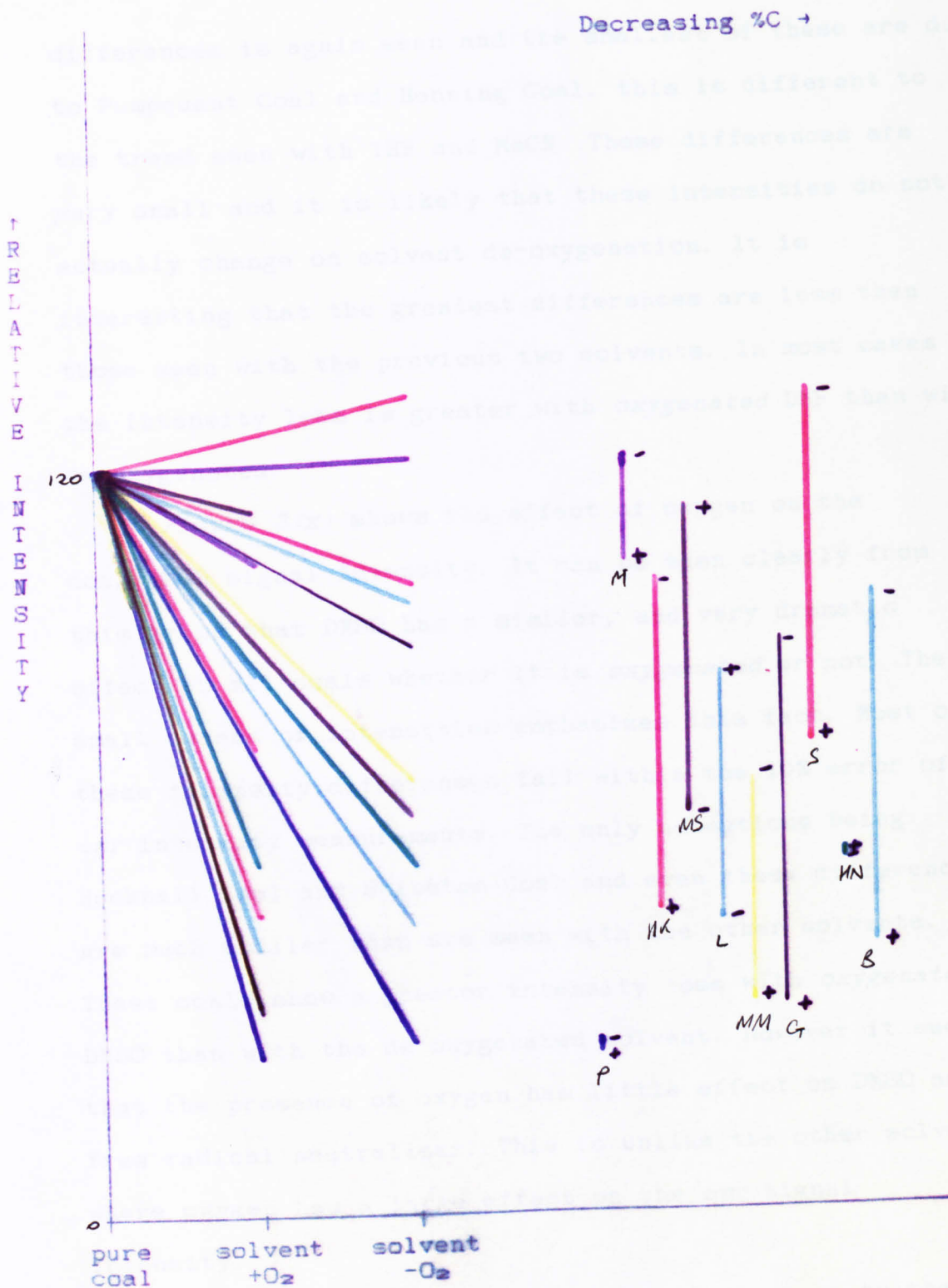


Figure 3(ix): A graphical representation of the effect of oxygen on the coal/DMF esr signal intensity.

differences is again seen and the smallest of these are due to Pumpquant Coal and Henning Coal, this is different to the trend seen with THF and MeCN. These differences are very small and it is likely that these intensities do not actually change on solvent de-oxygenation. It is interesting that the greatest differences are less than those seen with the previous two solvents. In most cases the intensity loss is greater with *oxygenated* DMF than with de-oxygenated.

Figure 3(x) shows the effect of oxygen on the coal/DMSO signal intensity. It can be seen clearly from this graph that DMSO has a similar, and very dramatic effect on all coals whether it is *oxygenated* or not. The small spread of intensities emphasizes this fact. Most of these intensity differences fall within the 10% error of esr intensity measurements. The only exceptions being Hucknall Coal and Snibston Coal and even these differences are much smaller than are seen with the other solvents. These coals show a greater intensity loss with *oxygenated* DMSO than with the de-oxygenated solvent. However it seems that the presence of oxygen has little effect on DMSO as a free radical neutraliser. This is unlike the other solvents where oxygen has a large effect on the esr signal intensity.

There seem to be no general conclusions as to the effect of solvents (*oxygenated* or de-oxygenated) on coals. Also the single broad esr resonance was not very

informative since the only way to decrease %C →
 intensity. An IR study was investigated in the hope that the
 multiple line IR spectra would be more informative.

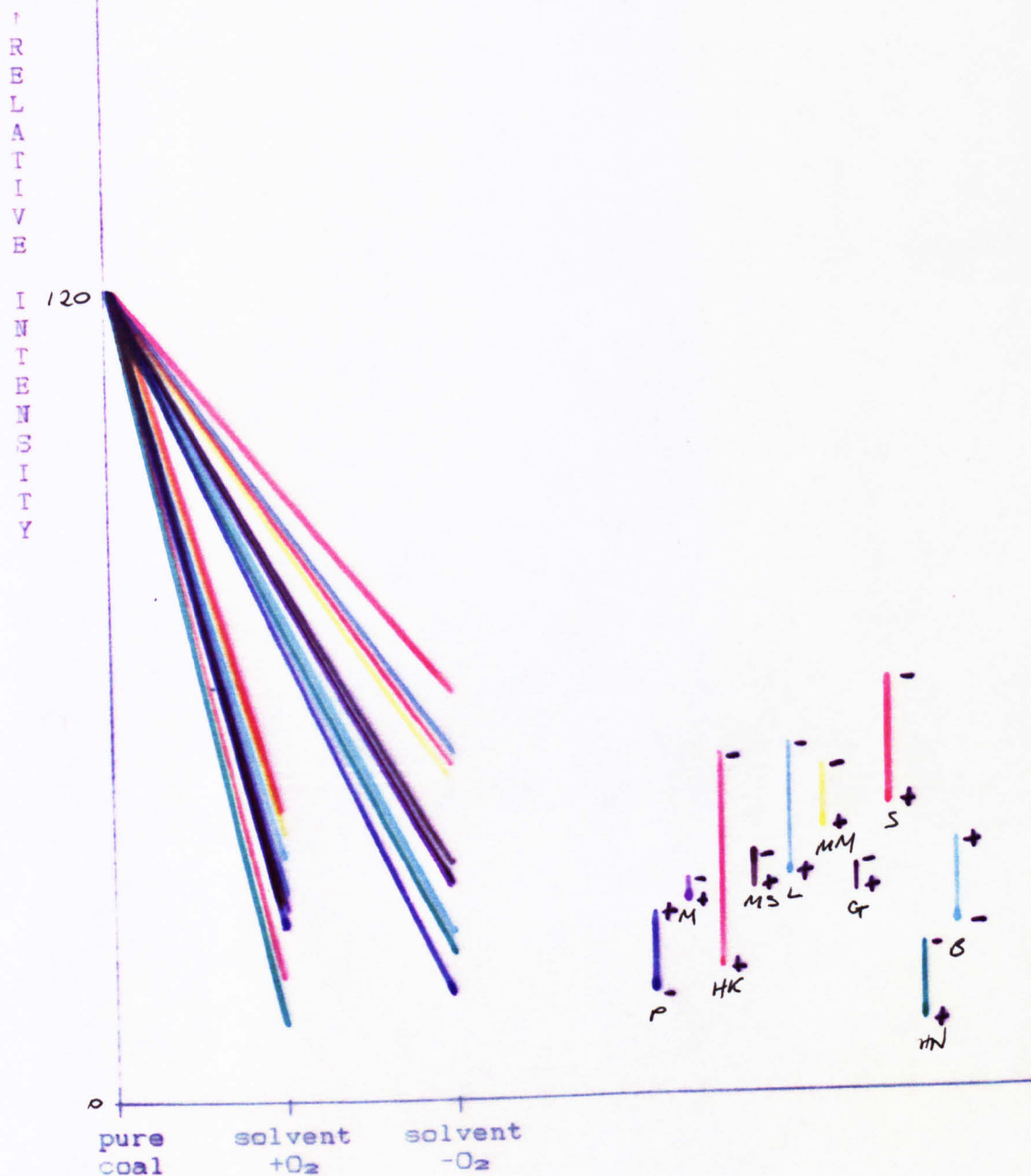


Figure 3(x): A graphical representation of the effect of oxygen on the coal/DMSO esr signal intensity.

informative since the only measurable variable was intensity. An ir study was instigated in the hope that the multiple line ir spectrum would be more informative.

Chapter 4

4 Ir Study of Coals

4.1 Pure Coals

Initially the coal samples were prepared as pressed discs, as described in Chapter 1.2. A variety of coal samples were selected and *ir* spectra of these coals were recorded; these are shown in *figs. 4(i) - 4(v)*, also shown in *fig. 4(i)* is the assignment of the spectral lines. As expected most of the coal spectra are similar, since the same functional groups are present in all the coals. However, the spectrum obtained from Pumpquant Coal, *fig. 4(v)*, is of much lower intensity than that from the other coals; presumably the anthracitic structure of this high %C coal is less transparent to *ir* light.

Problems with the production of complete discs and their very fragile nature were encountered, and because of these problems the spectra from coal films were examined, in the hope that these films could adequately replace the discs. These film spectra were then compared with the spectra obtained from the discs; since no reference to the use of coal films in *ir* spectroscopy could be found, their feasibility for the *ir* study of coal was unknown. A study of the use of coal pressed discs in *ir* spectroscopy had already been undertaken and details are given in reference 56. For the same coal the only noticeable difference between the two spectra from disc and film was the cut-off at $\approx 1000\text{cm}^{-1}$, and this was due to the CaF_2 *ir* plates used,

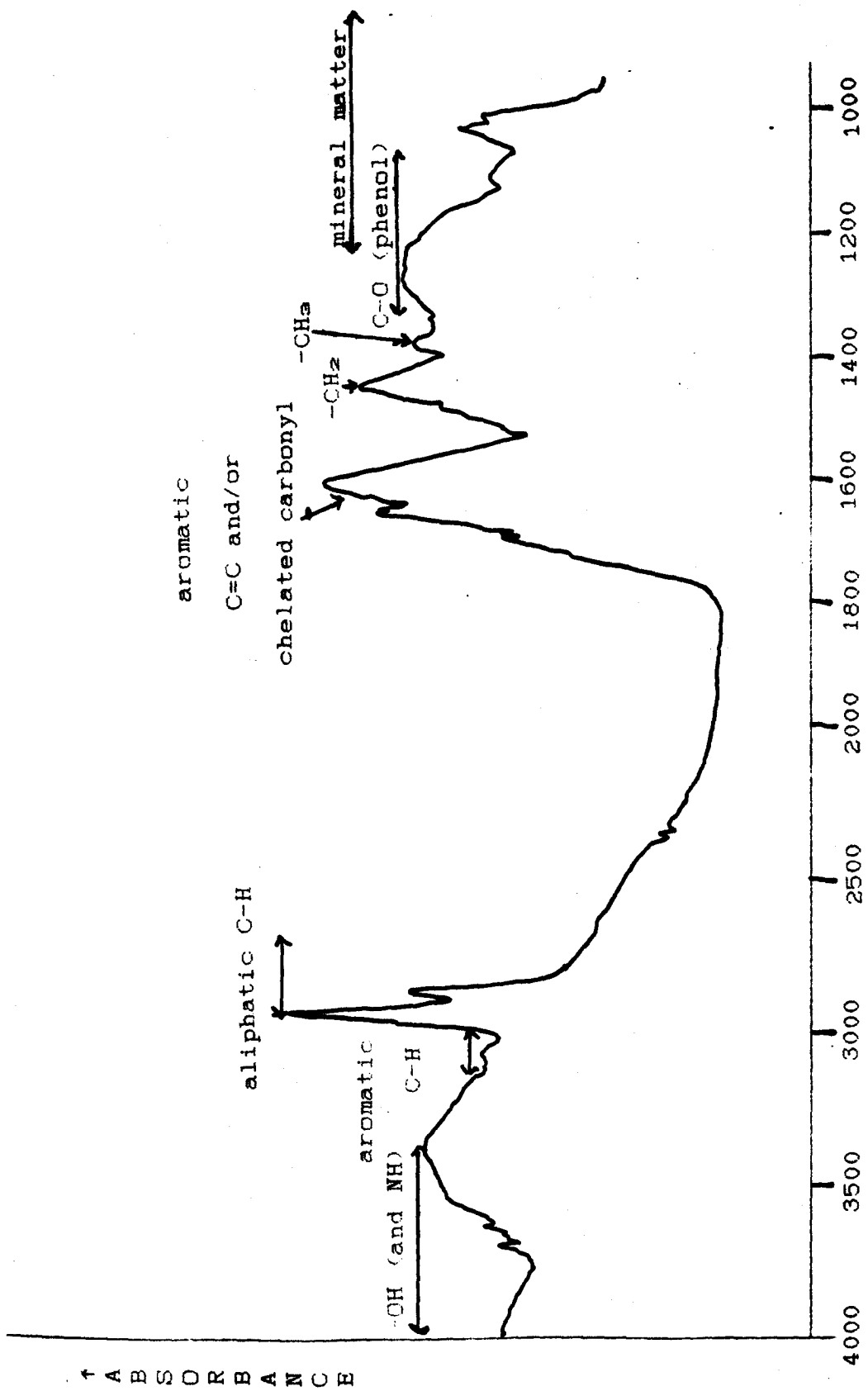


Figure 4(1): Ir spectrum of Snibston Coal disc showing the assignment of the observed bands.

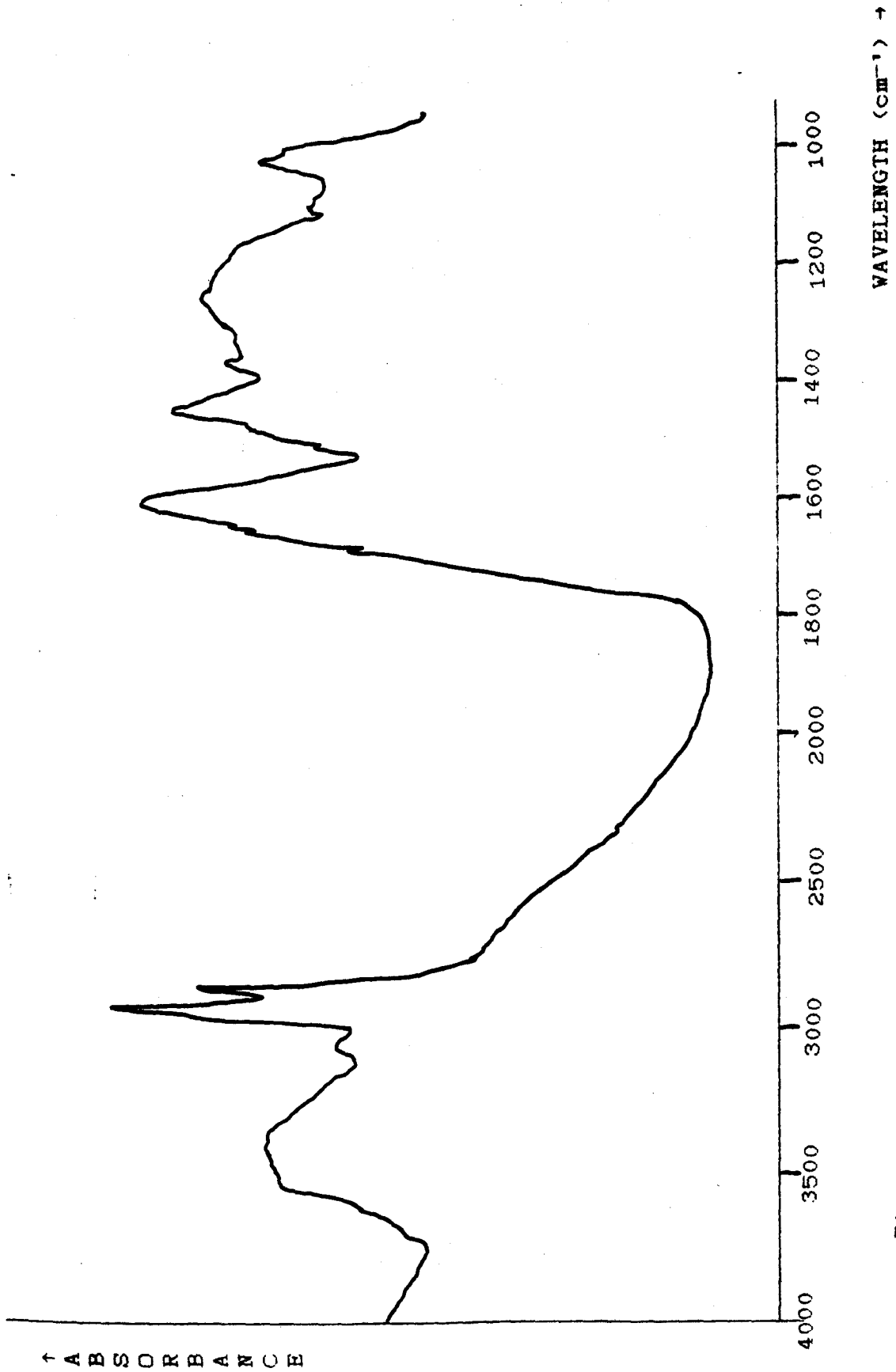


Figure 4(11): Ir spectrum of Gedling Coal disc.

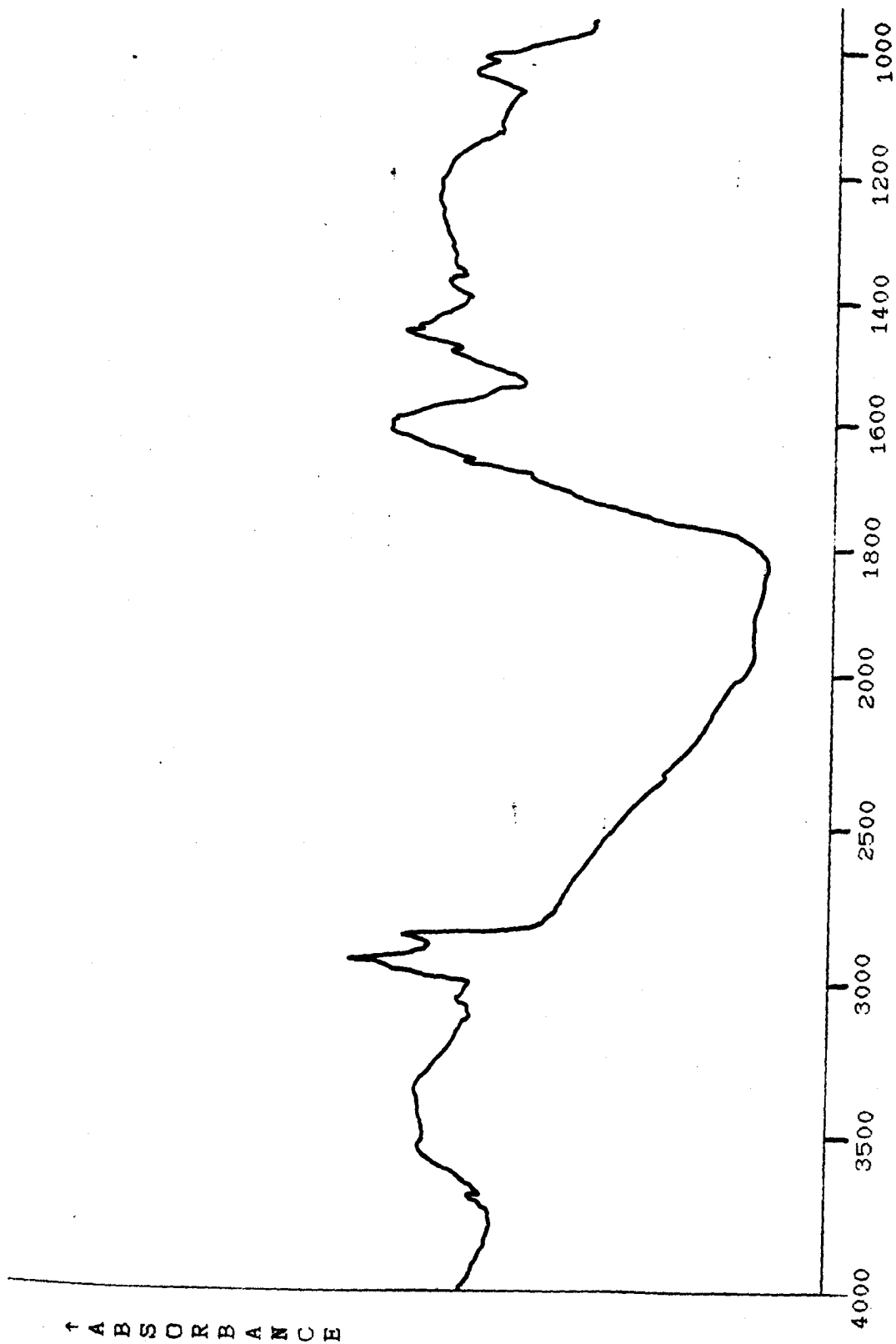


Figure 4(111): Ir spectrum of Markham Main Coal disc.

WAVELENGTH (cm⁻¹) →

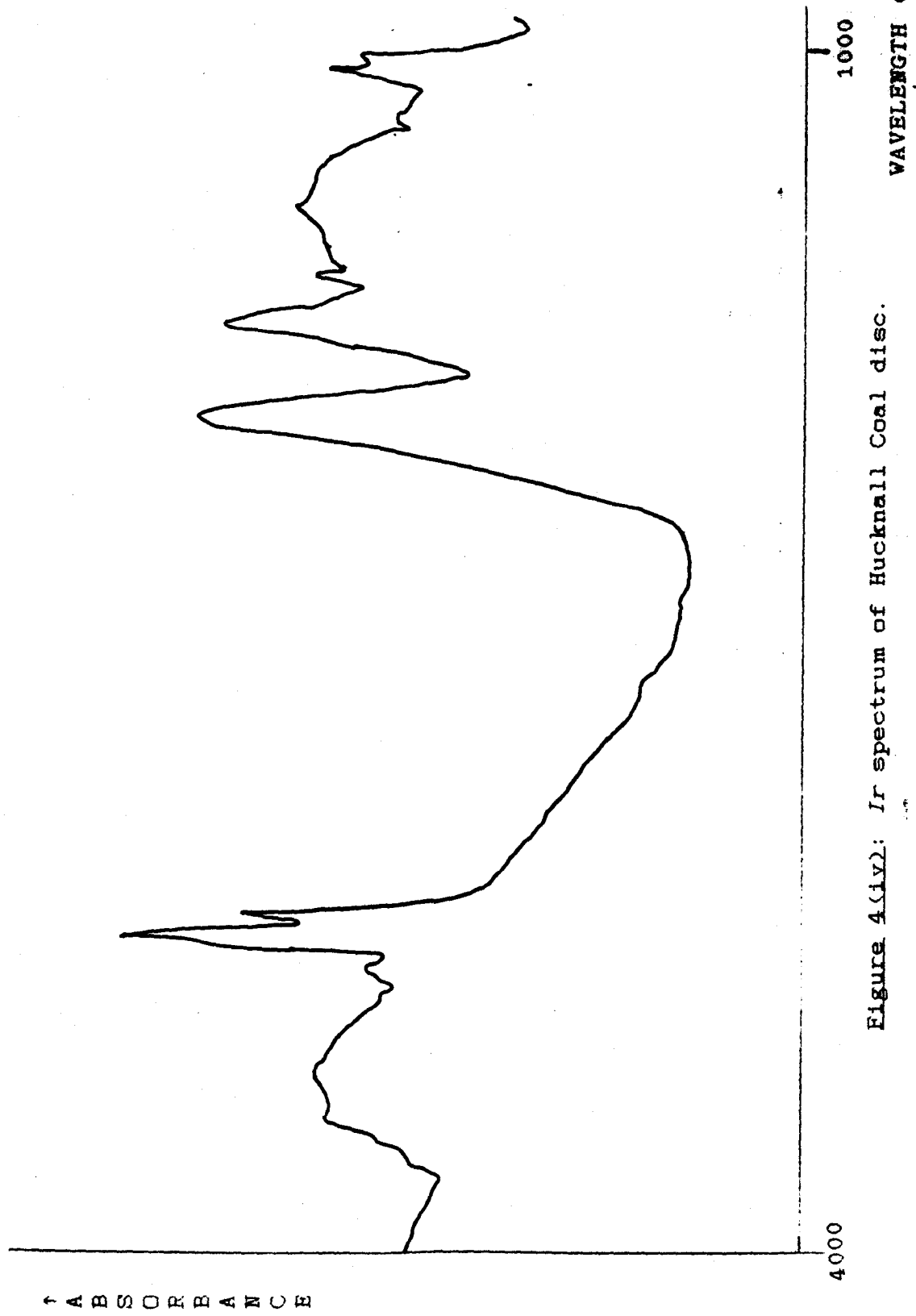


Figure 4(iv): Ir spectrum of Hucknall Coal disc.

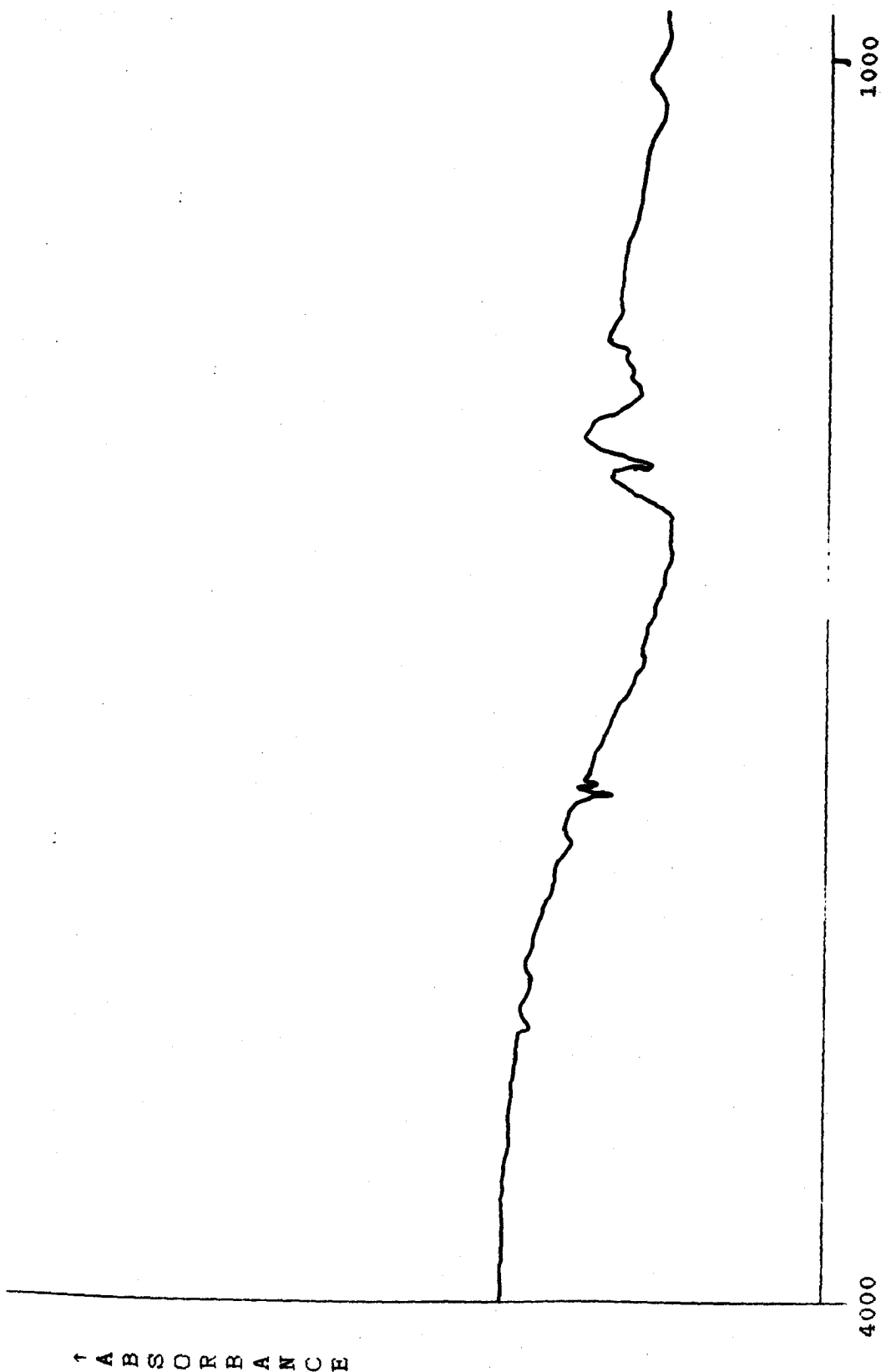


Figure 4(y): Ir spectrum of Pumpquant Coal disc.

WAVELENGTH (cm⁻¹) →

↑ ABSORBANCE

see *fig. 4(vi)*. The similarity of the spectral detail from pressed discs and films was very good and all further *ir* work was undertaken on coal films.

4.2 Solvent Addition

Two coals were selected for solvent study because these coals gave intense, reproducible spectra; these coals were Gedling Coal and Hucknall Coal. The solvents used were the same ones as used in the *esr* study of coals, i.e. THF, MeCN, DMF and DMSO.

A preliminary study was undertaken so as to assess which of the solvents would be the most suitable for *ir* study. Spectra of pure coal films were recorded and then these films were left in contact with solvent vapour for several hours, see Chapter 1.2. Spectra of the resulting films were taken and the results assessed. However, only one solvent, DMF, proved volatile enough to add solvent to the coals in the humidifying system used, and not too volatile, such that it was lost from the coal film before the spectrum could be recorded. An example of the spectra obtained before and after solvent addition is shown in *fig. 4(vii)*. The major differences between the two spectra are the large additional band at $\approx 1670\text{cm}^{-1}$, due to the carbonyl stretching frequency of DMF, and a shift in the broad band between 3700cm^{-1} and 3000cm^{-1} . All the further work described in this chapter uses DMF as the solvent.

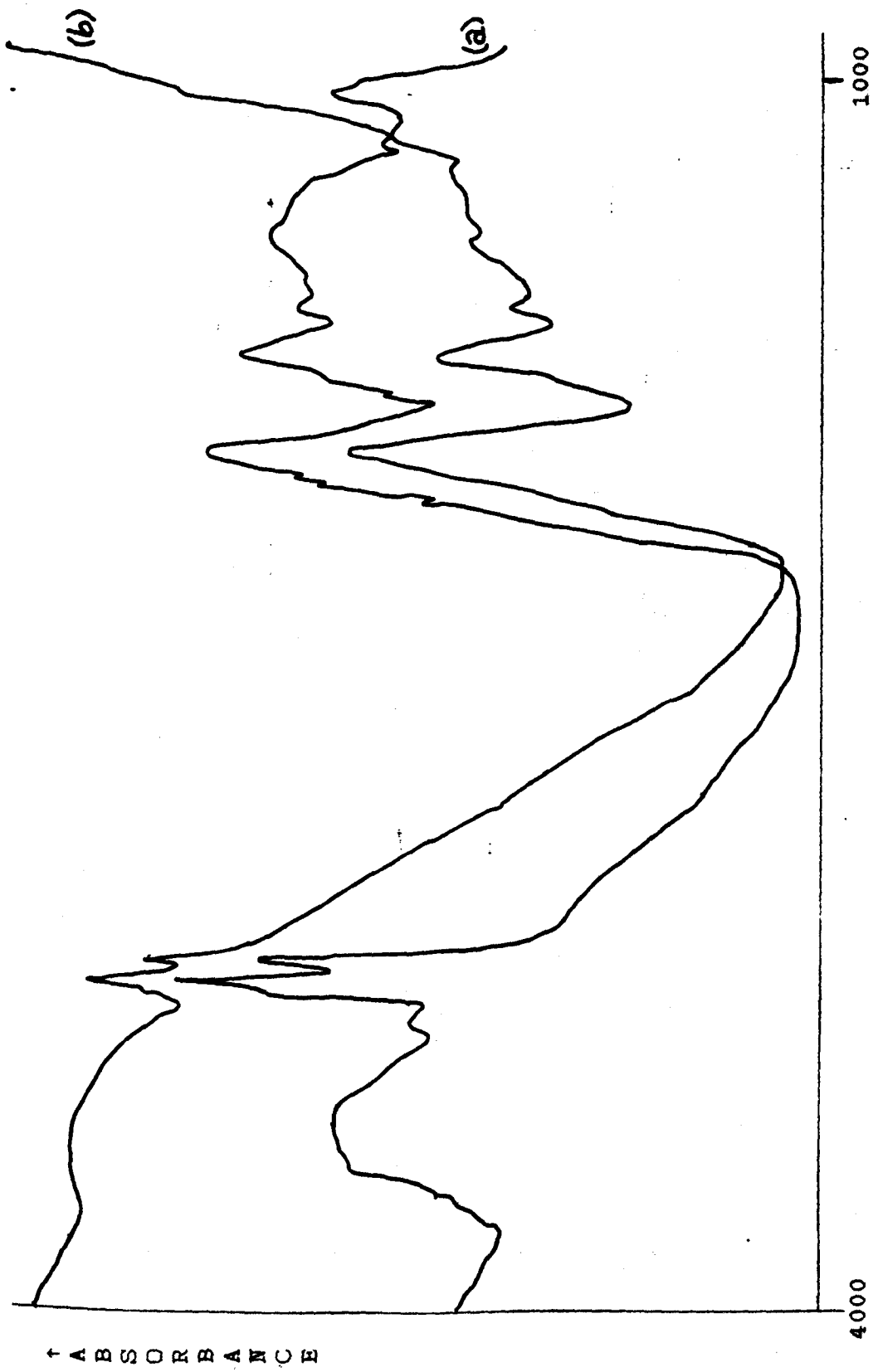


Figure 4(vi): Ir spectrum of Gedling Coal; (a) disc, (b) film.

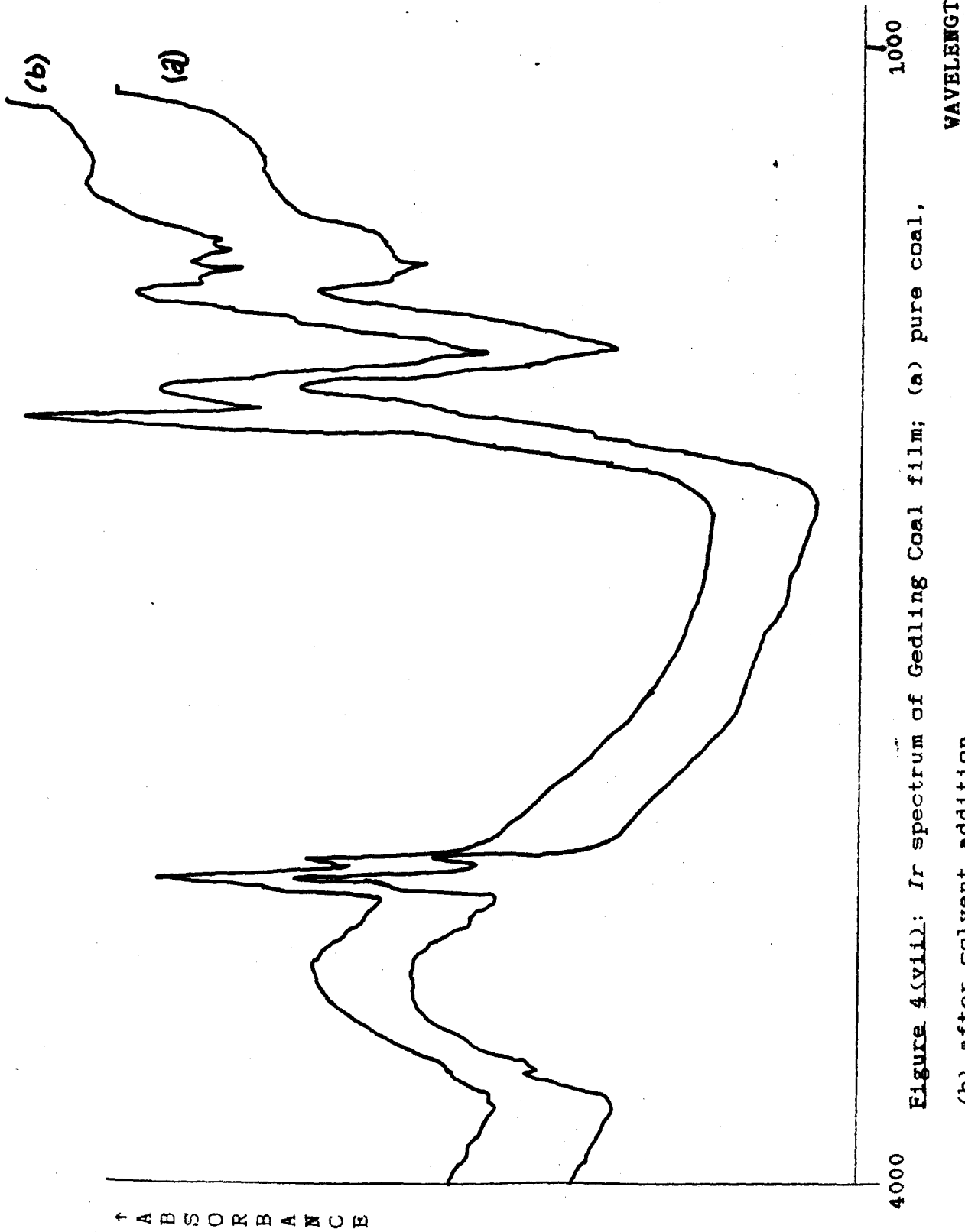


Figure 4(viii): Ir spectrum of Gedling Coal film; (a) pure coal,
 (b) after solvent addition.

Further experiments were then undertaken to study in more detail how the solvent altered the coal film spectrum, and how quickly this solvent addition took place. As earlier, a base spectrum was recorded and then at timed intervals the coal film was removed from the humidifier and its spectrum recorded, the film was then replaced in the humidifier and further solvent addition permitted. So as to study the reaction in more detail the two parts of the spectrum where previous change had been noted were expanded and studied separately.

The first part of the spectrum studied was in the range 1800cm^{-1} to 1500cm^{-1} . The spectra obtained for an elapsed time (t) range of up to 12960 mins. (9 days) are shown in *fig. 4(viii)*. As mentioned earlier the "growing" peak is due to the $>\text{C}=\text{O}$ stretch in the solvent. As can be seen, this peak is quite broad; some of the peak being due to pure solvent condensed onto the coal surface and some of the peak being due to solvent in the pores of the coal. Thus the position of the peak gives some indication as to the types of functional groups present in coal and "projecting into" the pores. The relative positions of the observed band and bands due to pure DMF in other pure solvents⁽⁶⁰⁾ are shown in *fig. 4(ix)*. The component of the observed signal due to pure DMF is thought to be in the area around 1680cm^{-1} , and at high concentrations of solvent this component gives a sharp edge to the band. Thus the other components of the band are centred towards the right

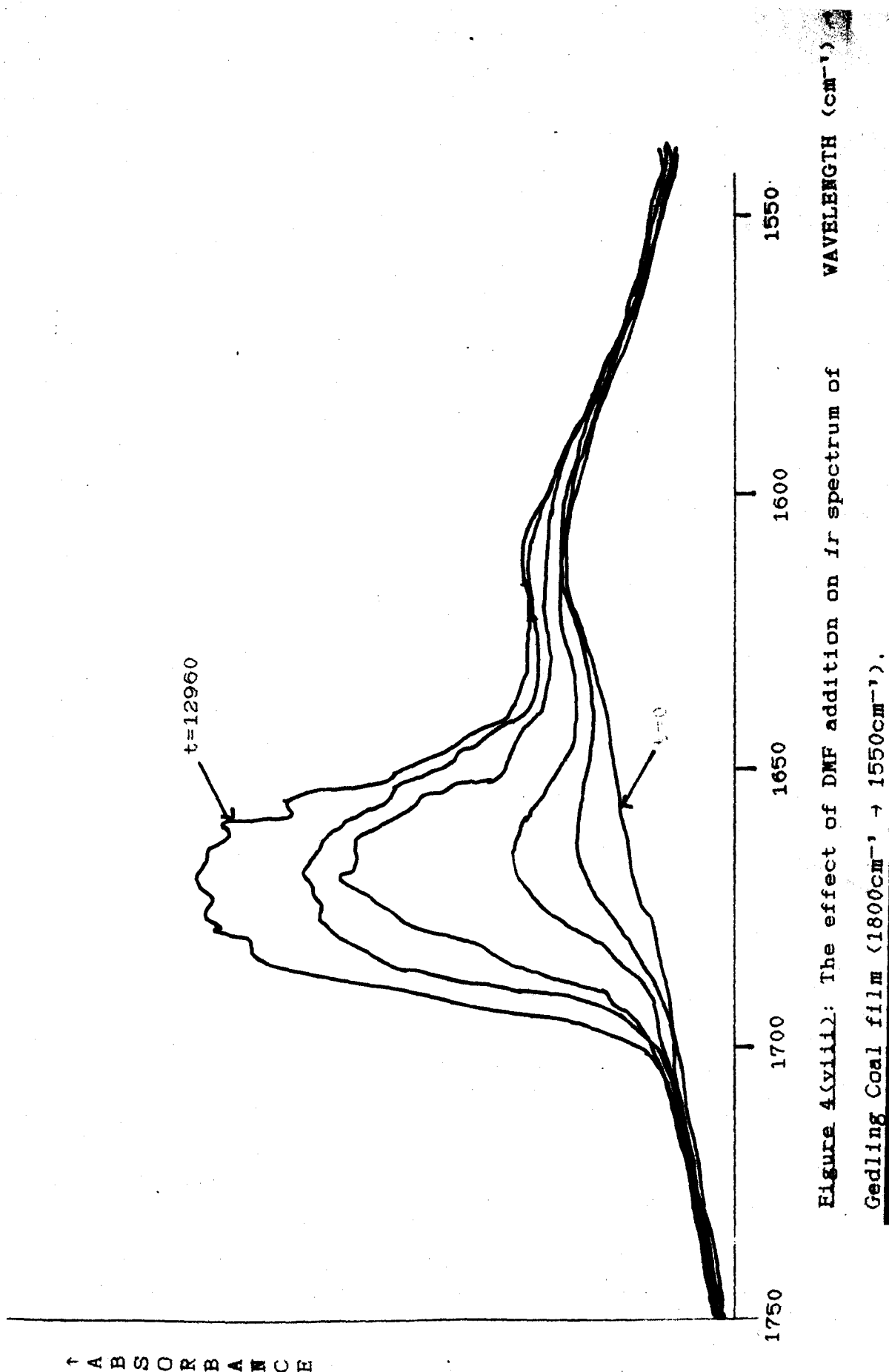


Figure 4(viii): The effect of DMF addition on ir spectrum of Gedling Coal film ($1800\text{cm}^{-1} \rightarrow 1550\text{cm}^{-1}$).

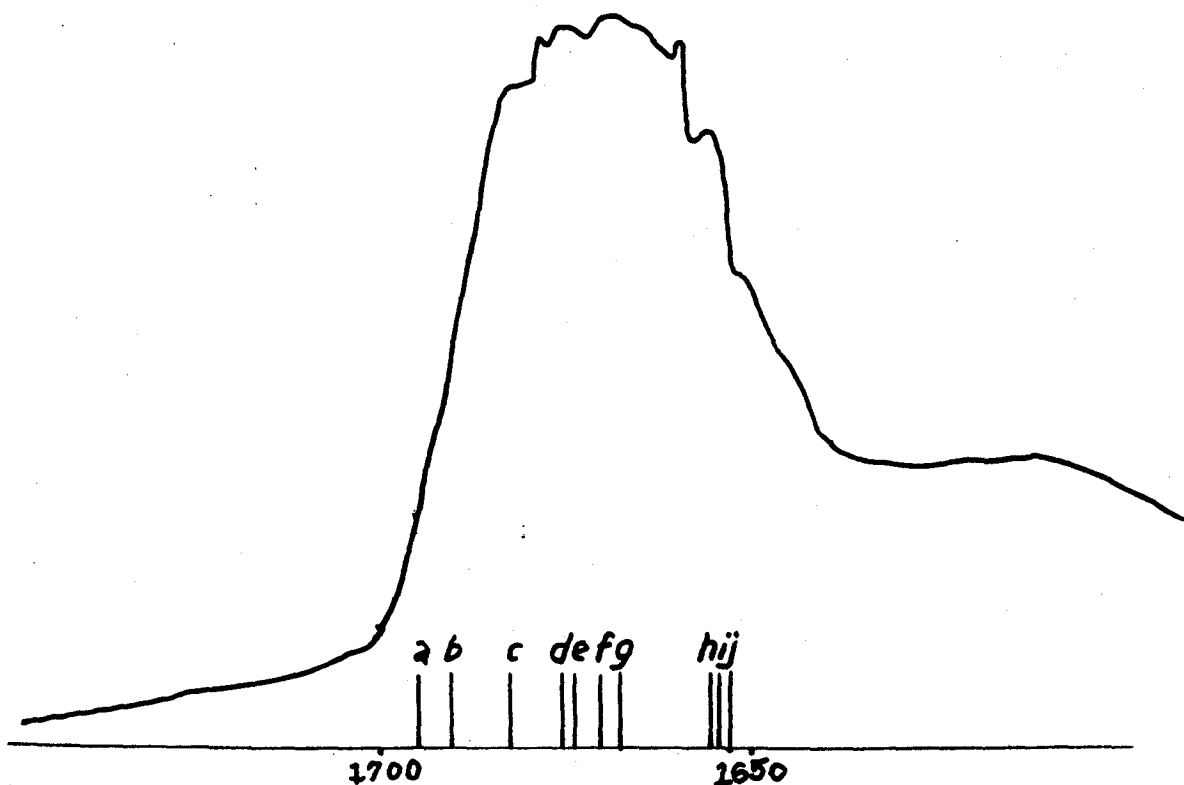


Figure 4(ix): Relative positions of observed band and DMF in various solvents.

| KEY | |
|------|------------------------|
| a. | Hexane. |
| b. | Triethylamine. |
| c. | Tetrahydrofuran. |
| d. | Acetonitrile. |
| e. | Dichloromethane. |
| f. | Dimethyl sulphoxide. |
| g/h. | Methanol. |
| i. | water. |
| j. | Hexafluoroisopropanol. |

hand side. This puts these components in the range of methanol and perhaps water. Both of these solvents are strongly hydrogen bonded, and this suggests that the inner surface of the coal pores is hydrogen bonding to the DMF added to the coal. From this it can be inferred that there are weak hydrogen bonds present in the pure coal pores and on addition of solvent these weak bonds are broken and replaced by stronger hydrogen bonds to the solvent. Thus elsewhere in the *ir* spectrum it should be possible to observe a nett loss in signal, due to the loss of these weak hydrogen bonds.

A study of the region 4000cm^{-1} to 2500cm^{-1} was undertaken, as a change in this region of the spectrum was noticed in the initial study. The spectra obtained during an elapsed time study are shown in *fig. 4(x)*. It can be seen from these spectra that there is a loss of signal, in the range 3700cm^{-1} to 3200cm^{-1} , on addition of solvent. This loss of signal is in the area of the spectrum where the water O-H stretching frequency is observed. ⁽⁶⁰⁾ It is postulated that this signal loss is due to the breaking of relatively weak hydrogen bonds to water prior to the formation of stronger hydrogen bonds to DMF.

A short initial study of solvent action on Hucknall Coal was undertaken. The region of the spectrum studied was 1800cm^{-1} to 1550cm^{-1} and the spectra obtained are shown in *fig. 4(xi)*. The results are very similar to those obtained with Gedling Coal, and most of the same conclusions can be

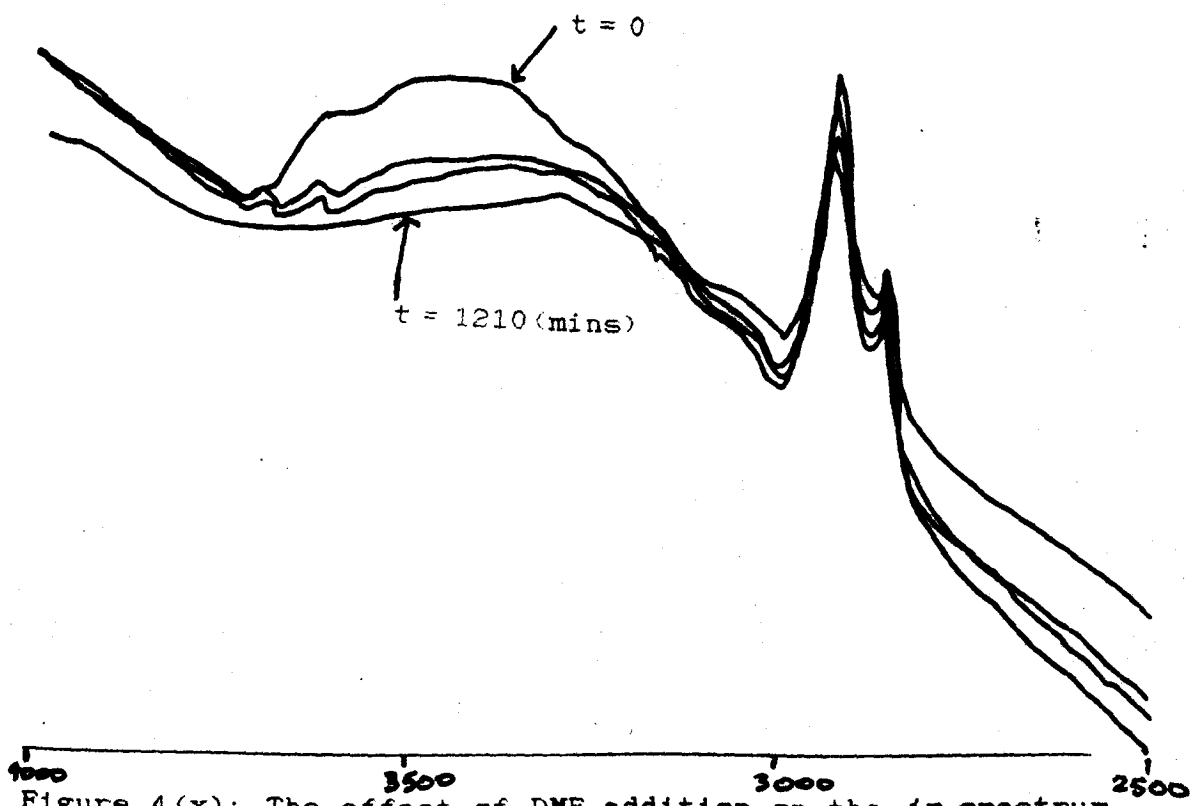
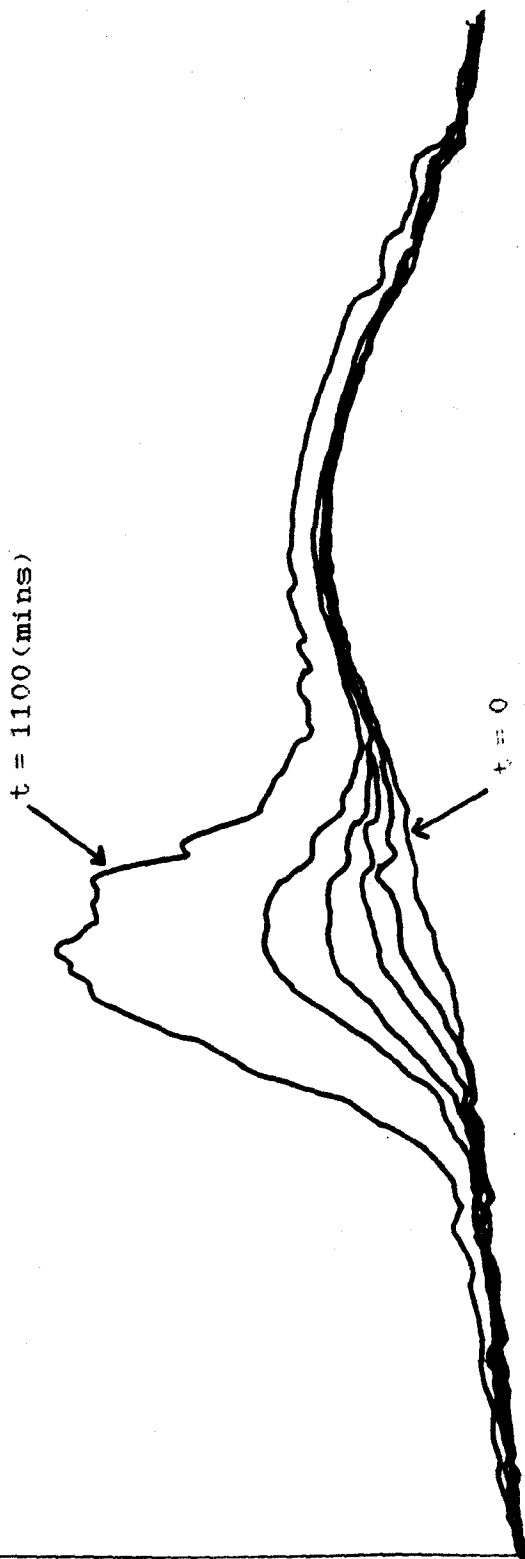


Figure 4(x): The effect of DMF addition on the ir spectrum of Gedling Coal film ($4000\text{cm}^{-1} \rightarrow 2500\text{cm}^{-1}$).

↑ A B S O R B A N C E



1750 Figure 4(x1): The effect of DMF addition on ir spectrum of
Hucknall Coal film (1800cm⁻¹ → 1550cm⁻¹).
1550 WAVELENGTH (cm⁻¹) →

drawn. It is interesting to note, however, that the rate of solvent addition is much faster with Hucknall Coal than with Gedling Coal.

References
to Part I

REFERENCES TO PART I

1. L. Petrakis and D.W. Grandy; "Coal Science and Technology :5", 1983, Elsevier, Amsterdam.
2. R. C. Neavel; "Coal Structure", 1981, Amer. Chem. Soc., Washington D.C.
3. D.E.G. Austin, D.J.E. Ingram, P.H. Given, C.R. Binder and L.W. Hill; "Coal Science", 1966, Amer. Chem. Soc., Washington D.C.
4. P.B. Hirsch; "Res. Conf. on Science in the Use of Coal", 1958, Inst. of Fuel, London.
5. T. Green, J. Kovac, D. Brenner and J.W. Larsen; "Coal Structure", (Ed. R.A. Meyers), 1982, Academic Press.
6. A. Marzec, M. Juzwa, K. Betlej and M. Sobkowiak; *Fuel Process. Technol.*, 1979, 2, 35.
7. J. Szeliga and A. Marzec; *Fuel*, 1983, 62, 1229.
8. J.S. Gethner; *Prepr., Div. Org. Coatings and Plastics Amer. Chem. Soc.*, 1980, 43, 413.
9. J.S. Gethner; *J. Chem. Soc. Faraday Trans. 1*, 1985, 81, 991.
10. K.M. Thomas; private communication.
11. T.K. Green and J.W. Larsen; *Fuel*, 1984, 63, 1538.
12. D. Brenner; *Fuel*, 1985, 64, 167.
13. J.R. Nelson, O.P. Mahajan and P.L. Walker; *Fuel*, 1980, 59, 831.
14. J.R. Nelson; *Fuel*, 1983, 62, 112.
15. D. Brenner; *Fuel*, 1983, 62, 1347.

16. P.R. Reucroft and K.B. Patel; *Fuel*, 1983, **62**, 279.
17. R.E. Winans, R.G. Scott, R.L. McBeth and R. Hayatsu; *Prepr., Div. Pet. Chem., Amer. Chem. Soc.*, 1980, **25(2)**, 262.
18. L. Petrakis, D.W. Grandy and G.L. Jones; *Chemtech.*, 1984, **14(1)**, 52.
19. J. Uebersfeld, A. Etienne and J. Combrisson; *Nature*, 1954, **174**, 614.
20. D.J.E. Ingram, J.G. Tapley, R. Jackson, R.L. Bond and A.R. Murnaghan; *Nature*, 1954, **174**, 797.
21. B. Commoner, J. Townsend and G.E. Pake; *Nature*, 1954, **174**, 689.
22. H.L. Retcofsky, G.P. Thompson, R. Raymond and R.A. Friedel; *Fuel*, 1975, **54**, 126.
23. H.L. Retcofsky, J.M. Stark and R.A. Friedel; *Anal. Chem.*, 1968, **40**, 1699.
24. H. Tschalmer and E. de Ruiter; "Chemistry of Coal Utilisation", Suppl. Vol., (Ed. H.H. Lowry), 1963, Wiley, New York.
25. S. Toyoda and H. Honda; *Carbon*, 1966, **3**, 527.
26. S. Toyoda and H. Honda; *J. Fuel Soc. Japan*, 1965, **44**, 697.
27. S. Toyoda, S. Sugawara and H. Honda; *J. Fuel Soc. Japan*, 1966, **45**, 876.
28. W.R. Ladner and R. Wheatley; *Brit. Coal Util. Res. Assoc. Monthly Bull.*, 1965, **29(7)**, 201.
29. C.L. Kwan and T.F. Yen; *Anal. Chem.*, 1979, **51(8)**, 1225.

30. L. Petrakis and D.W. Grandy; *Anal. Chem.*, 1978, 50(2), 303.
31. S. Duber and A.B. Wieckowski; *Fuel*, 1982, 61, 433.
32. V.P. Berveno; *Solid Fuel Chem.*, 1982, 16(1), 51.
33. A.G. Kotov and V.P. Berveno; *Solid Fuel Chem.*, 1983, 17(3), 30.
34. S. Schlick, M. Narayana and L. Kevan; *Fuel*, 1983, 62, 1250.
35. R. Chauvin, P. Chiche, M.F. Quinton and J. Uebersfeld; *Carbon (Oxford)*, 1969, 7(2), 307.
36. H.L. Retcofsky, M.R. Hough, M.M. Maguire and R.B. Clarkson; "Coal Structure", 1981, Amer. Chem. Soc., Washington D.C.
37. L. Petrakis and D.W. Grandy; *Prepr., Div. Fuel Chem., Amer. Chem. Soc.*, 1978, 23(4), 147.
38. L. Petrakis and D.W. Grandy; *Amer. Inst. Phys., Conf. Proc.*, 1981, 70(1), 101.
39. S. Duber and A.B. Wieckowski; *Fuel*, 1984, 63, 1641.
40. C. Yokokawa; *Fuel*, 1969, 48, 29.
41. H.L. Retcofsky, M.R. Hough and R.B. Clarkson; *Prepr., Div. Fuel Chem., Amer. Chem. Soc.*, 1979, 24(1), 83.
42. M.O. Kestner and A.A. Kober; *Alternative Energy Sources 2*, 1979, 2(7), 2943.
43. J.S. Gethner; *Fuel*, 1985, 64, 1443.
44. K.C. Khulbe, A. Manogian, B.W. Chan, R.S. Mann and J.A. MacPhee; *Fuel*, 1983, 62, 973.
45. H.L. Retcofsky; *D.O.E. Symp. Ser.*, 1978, 46, 79.

46. C. Yokakawa; *Fuel*, 1968, **47**, 273.
47. E. de Ruiter and H. Tschamler; *Brennstoff-Chemie*, 1961, **42**(9), 32.
48. L. Petrakis and D.W. Grandy; *Fuel*, 1981, **60**, 120.
49. H.L. Retcofsky, G.P. Thompson, M. Hough and R.A. Friedel; *Amer. Chem. Soc., Symp. Ser.*, 1978, **71**, 142.
50. D.W. Van Krevelen; "Coal", 1961, Elsevier Publishing Co., New York.
51. R.A. Friedel and J.A. Queiser; *Fuel*, 1959, **38**, 369.
52. S.K. Chakrabartty and N. Berkowitz; *Fuel*, 1974, **53**, 240.
53. S.K. Chakrabartty and N. Berkowitz; *Fuel*, 1976, **55**, 362.
54. C.G. Cannon and G.B.B.M. Sutherland; *Trans. Faraday Soc.*, 1945, **41**, 279.
55. C.G. Cannon and G.B.B.M. Sutherland; *Nature*, 1945, **156**, 240.
56. The British Carbonisation Research Association, Carbonisation Research Report **64**, 1979.
57. H.L. Retcofsky; "Chemistry of Coal Utilisation", Second Supp. Vol., (Ed. M.A. Elliot), 1981, Wiley, New York.
58. H.L. Retcofsky, J.M. Stark and R.A. Friedel; *Chem. Ind. (London)*, 1967, **31**, 1327.
59. H. Ohuchi, M. Shiotani and J. Sohma; *Fuel*, 1969, **48**(2), 187.
60. G. Eaton; Leicester University, Ph.D. thesis.

Part II

Mono and Dicarbonyl

Radical Cations

Chapter 5

5 INTRODUCTION

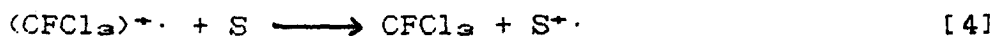
5.1 Background

It was postulated by Retcofsky *et al.*⁽⁶¹⁾ that some of the free radicals in coal could be due to semiquinone like moities. This provides a tenuous link between the foregoing work, and this study of radical cations, which centred originally on quinone radical cations.

Radiolysis of a molecule can give rise to its radical cation, its radical anion or both. Careful selection of the appropriate solvent can give the desired selectivity so that the radical cation or radical anion can be uniquely produced.

The solvents that have been used to produce radical cations are usually halogenated; for example tetrachloromethane (CCl_4), tetrabromomethane (CBr_4)⁽⁶²⁾ and especially trifluorochloromethane (CFCl_3).⁽⁶³⁾ Both CCl_4 and CBr_4 give solvent signals near to free spin, which tend to obscure the esr features from the substrate molecules. CFCl_3 , however, gives only very weak esr signals near to free spin; these signals being assigned to minor impurities and not to CFCl_3 -derived radicals.

The essential mechanism of the CFCl_3 matrix for producing the radical cations can be summarised by the following set of reactions, where S is the solute molecule whose cation is to be studied.



The concentration of S is chosen to be small enough (usually 0.1% mole fraction or smaller) to avoid direct irradiation of S, so that the excitation leads almost totally to the direct ionisation of the matrix molecules. The radical $(\text{CFCl}_3)^{\cdot+}$ produced in reaction [1] is known to migrate rapidly over a number of solvent molecules, reaction [3], until it encounters a molecule of S in reaction [4].⁽⁶⁴⁾ The ionisation potential of CFCl_3 , being 11.9eV,⁽⁶⁵⁻⁶⁾ allows solute molecules with ionisation potentials less than 11.9eV to be ionised. Since the C-Cl bond is susceptible to cleavage, reaction [2], the *esr* signals from $\text{CFCl}_2\cdot$ might be expected to interfere with those of the radical cations of the solute molecules under study. Fortunately, since the $\text{CFCl}_2\cdot$ radical in frozen CFCl_3 polycrystalline matrices is randomly orientated, its *esr* signal is dispersed over a wide range of magnetic field. Because of the rapid mobility of $(\text{CFCl}_3)^{\cdot+}$, no *esr* features from this radical are detected. Hence the distinct advantage that CFCl_3 has over other solvents is that the *esr* signal of the solute cation is not significantly affected by the superimposing signals of the neutral matrix radicals. Moreover, since the melting point of CFCl_3 is 162K, there is an ample temperature range between 77K and

the melting point of CFCl_3 which permits the study of the effect of temperature upon the *esr* spectra.

The disadvantages of using CFCl_3 as a solvent for the production of radical cations are slight. The use of dilute solutions reduces intermolecular interactions; but hydrogen atom transfer, '67' matrix-adduct formation, '68' and rearrangement reactions '69' have been reported. It will be evident from the results presented herein that in the majority of cases only the primary radical cations are formed.

This radical cation study is broadly divided into four parts. The detection of the radical cations from monocarbonyl derivatives, cyclic carbonyls, acyclic dicarbonyls and aldehydic carbonyls. Interpretations of their *esr* spectra are offered, including discussions on electronic and structural information derived from the spectra.

5.2 Experimental

The simplicity and versatility of CFCl_3 as a general solvent for the production of radical cations is exemplified by the convenient method of preparation of samples. The following experimental section describes a general radiolytic method for the production of all the radical cations studied here.

Dilute solutions of CFCl_3 (0.1% mole fraction) were

cooled to 77K producing small polycrystalline masses. Samples, with the exception of methylglyoxal, glyoxal and formaldehyde, were of the best grades available commercially and these were purified, if necessary, by standard procedures. Their purities being checked by nmr spectroscopy. The samples of methylglyoxal, glyoxal and formaldehyde were prepared in collaboration with Dr. C. J. Rhodes. The samples were prepared by distilling the water from the commercially available product under vacuum. The residue was then heated with phosphorus pentoxide in a sublimation apparatus and the pure compound collected on a cold finger at 195K.

The CFCl_3 was obtained from B.D.H. Chemicals Limited at 99.9% purity and was used as obtained. Although the CFCl_3 supplied was 99.9% pure, residual impurity signals were still obtained in all the systems described herein. However, these "solvent" features were insignificant compared with those from the substrate radicals. All glassware used for preparative purposes was flamed to remove any traces of organic solvents, such as acetone.

All samples were exposed to ^{60}Co γ -rays at 77K in a Vickers radiation source to doses up to 0.5Mrad (dose rate 0.7Mrad/hour), the results being independent of dose in this range. ESR spectra were recorded on a Varian E109 X-band spectrometer calibrated with a Bruker B-H12E field probe, which was standardised with a sample of diphenylpicrylhydrazyl (DPPH), and a Bruker ER-200D SRC Q-band

spectrometer.

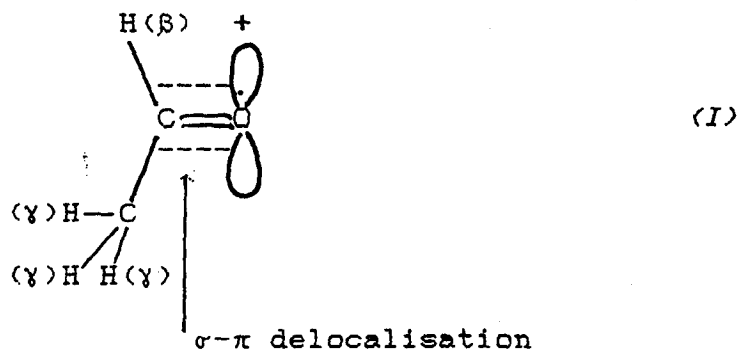
Samples were annealed by decanting the coolant and recooling to 77K whenever significant spectral changes were detected. This process was continued until the samples melted, at ca. 160K, all features then being lost irreversibly. Samples X-irradiated at 4K received doses up to 0.5Mrad (dose rate 0.4Mrad/hour) from an irradiation chamber built and designed in these laboratories. The X-irradiation at 4K and spectral recording at 10K were achieved by using liquid helium, via a transfer system, to cool the sample, and an Oxford Instruments liquid helium cryostat.

Chapter 6

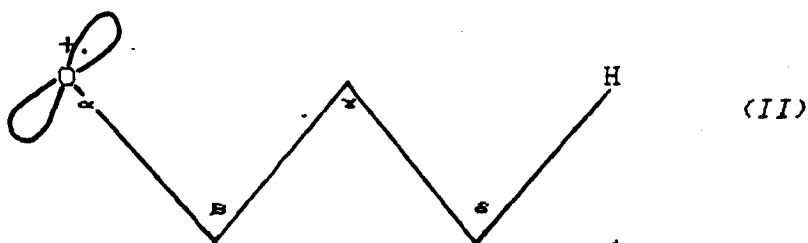
6 ACYCLIC CARBONYLS

6.1 Introduction

In contrast with the acetaldehyde cation, described in chapter 8, which exhibits a very large coupling to the aldehydic (β) proton, acetone gives an unresolved singlet; the methyl proton splitting being ca. 1.5G, as revealed byENDOR spectroscopy.⁷⁰ The structure of these cations is undoubtedly that shown in (I), the SOMO being the in-plane 2p orbital on oxygen, with large delocalisation into the adjacent C-H or C-C σ -bonds by σ - π overlap (hyperconjugation).



Although coupling to γ -protons is very small, that to δ -protons can be quite large; as shown by Snow and Williams,⁷¹ for a variety of aldehydes and ketones. This coupling is especially noticeable when the radical is in the optimum in-plane W-plan structure, (II). This work is supported by that of Boon *et al.*,⁷² who found that dilute CFCl_3 solutions of several simple aldehydes and



ketones gave esr features clearly assignable to their radical cations. The ketone cations only exhibited resolved proton couplings to δ -protons, if present. Otherwise, they were characterised by asymmetric singlet features with slight g-value variation. An example of the latter case is acetone, Me_2CO^+ , which gives a large asymmetric singlet in its esr spectrum. This chapter is concerned only with ketone cations, aldehydes being dealt with in chapter 8.

6.2 Acyclic Monocarbonyl

Methyl ethyl ketone

The spectrum obtained at 77K, *fig. 6(i)*, can be interpreted as a doublet of triplets and this is assigned to the δ -protons in the ethyl chain, *(III)*.

It is summarised that the protons are not all equivalent because of the limited rotation of the remote methyl group at 77K; ie H_A and H_B are equivalent but inequivalent to H_C . It is noteworthy that, for many radical cations, methyl groups exhibit well defined, fixed conformations rather than exhibiting free rotation at 77K, as is normally observed for neutral radicals. On annealing,

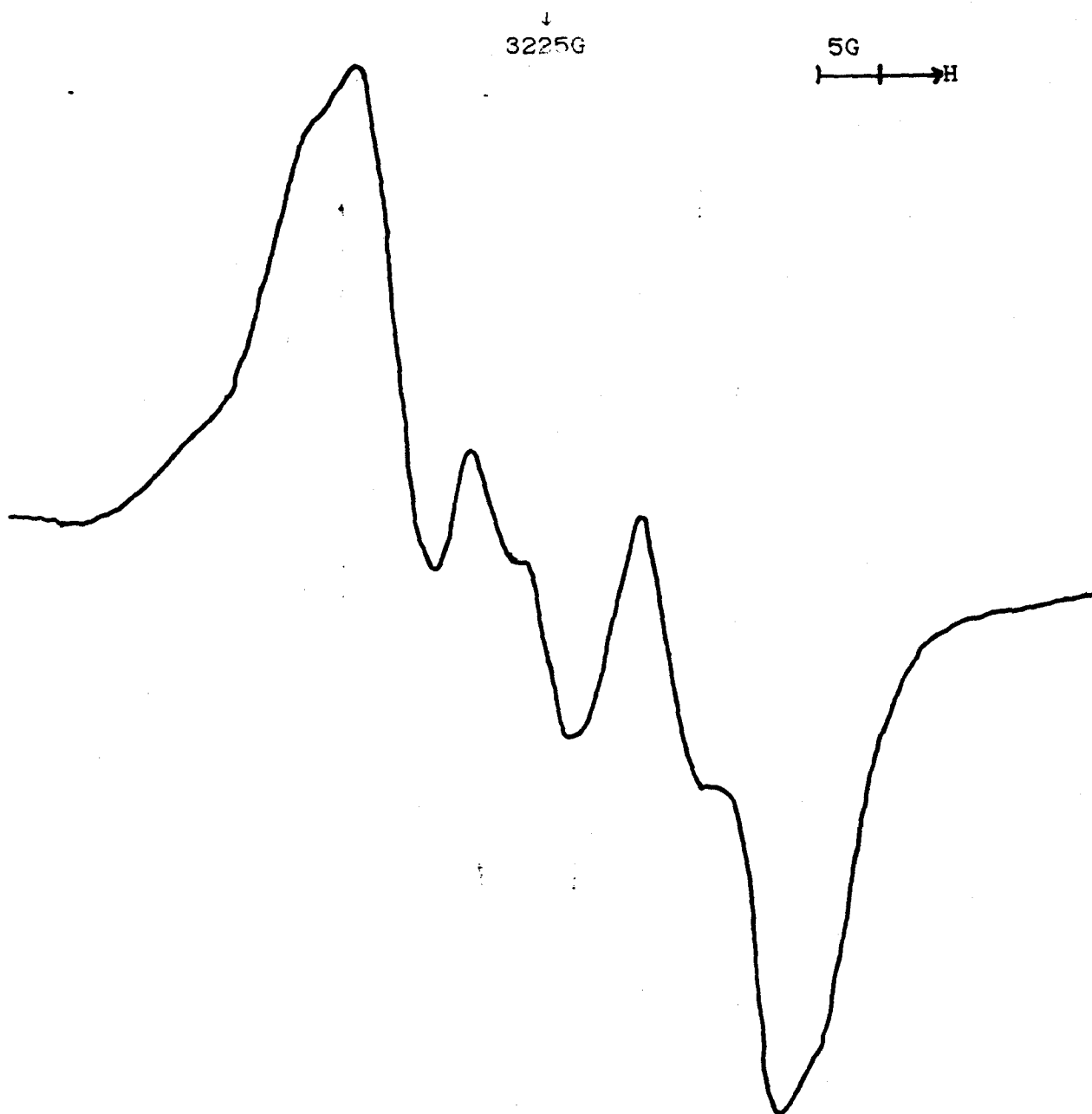


Figure 6(i): First-derivative X-band esr spectrum of methyl ethyl ketone in CFCl_3 , after exposure to ^{60}Co γ -rays at 77K, showing features assigned to its radical cation, at 77K.

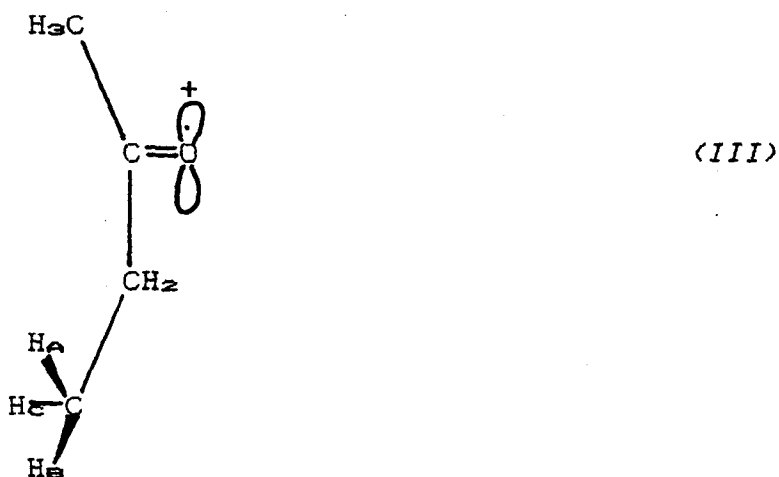


fig. 6(ii), the signal collapses into a quartet of binomial distribution. At this elevated temperature the methyl group is rotating and all the protons become equivalent. Protons from the γ -methyl group are not seen, as expected, by analogy with acetone.

6.3 Acyclic Dicarbonyls

2,3-butanedione

The spectrum obtained at 77K was a broad asymmetric singlet, similar to that obtained for acetone. There are δ -protons, but they apparently do not adopt the W-plan structure, and therefore do not couple with the spin. Alternatively, the delocalised structure of the cation may inhibit spin transfer to the methyl protons. It was noticed here, and can be seen throughout the radical cation work that coupling to protons δ to the spin does not seem to

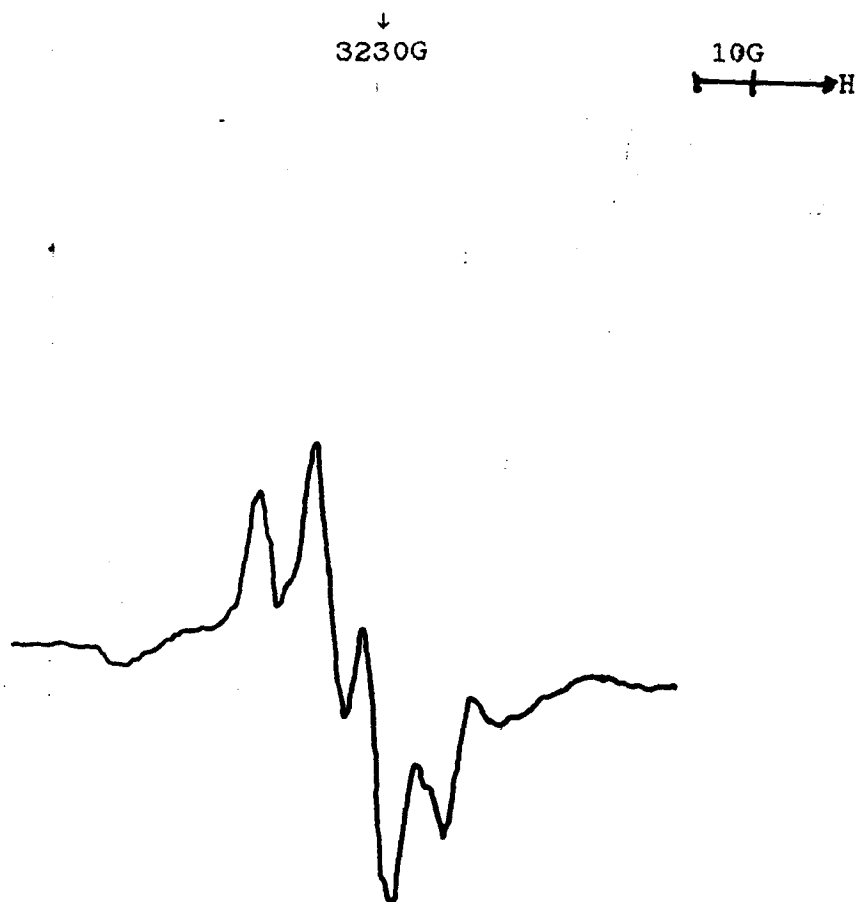


Figure 6(ii): First-derivative X-band esr spectrum of methyl ethyl ketone in CFCl_3 , after exposure to ^{60}Co γ -rays at 77K, showing features assigned to its radical cation, at ca. 140K.

occur if the coupling would be via a carbonyl group.

2,4-pentanedione

The spectrum at 77K showed a distorted doublet, *fig. 6(iii)a*. This is assigned to the rearranged cation, (IV).



The doublet is assigned to the central proton, H_a , since the hyperfine coupling is typical of that of a single α -proton. It should be noted here that the central protons in the parent compound are acidic protons. The presence of a positive charge on the cation will increase this acidity and thus one of these central protons is intramolecularly transferred. Similar rearrangements have been reported by Rideout and Symons in their work with ester cations.^{67a} If the parent cation had been formed then no coupling would be seen, since there would be no protons δ to the spin.

In an attempt to produce the parent radical cation, solutions were exposed to X-rays at 4K and the resulting spectra studied at 10K. The results obtained were the same as those from the 77K study. Thus this rearrangement takes place at very low temperatures and is probably an example

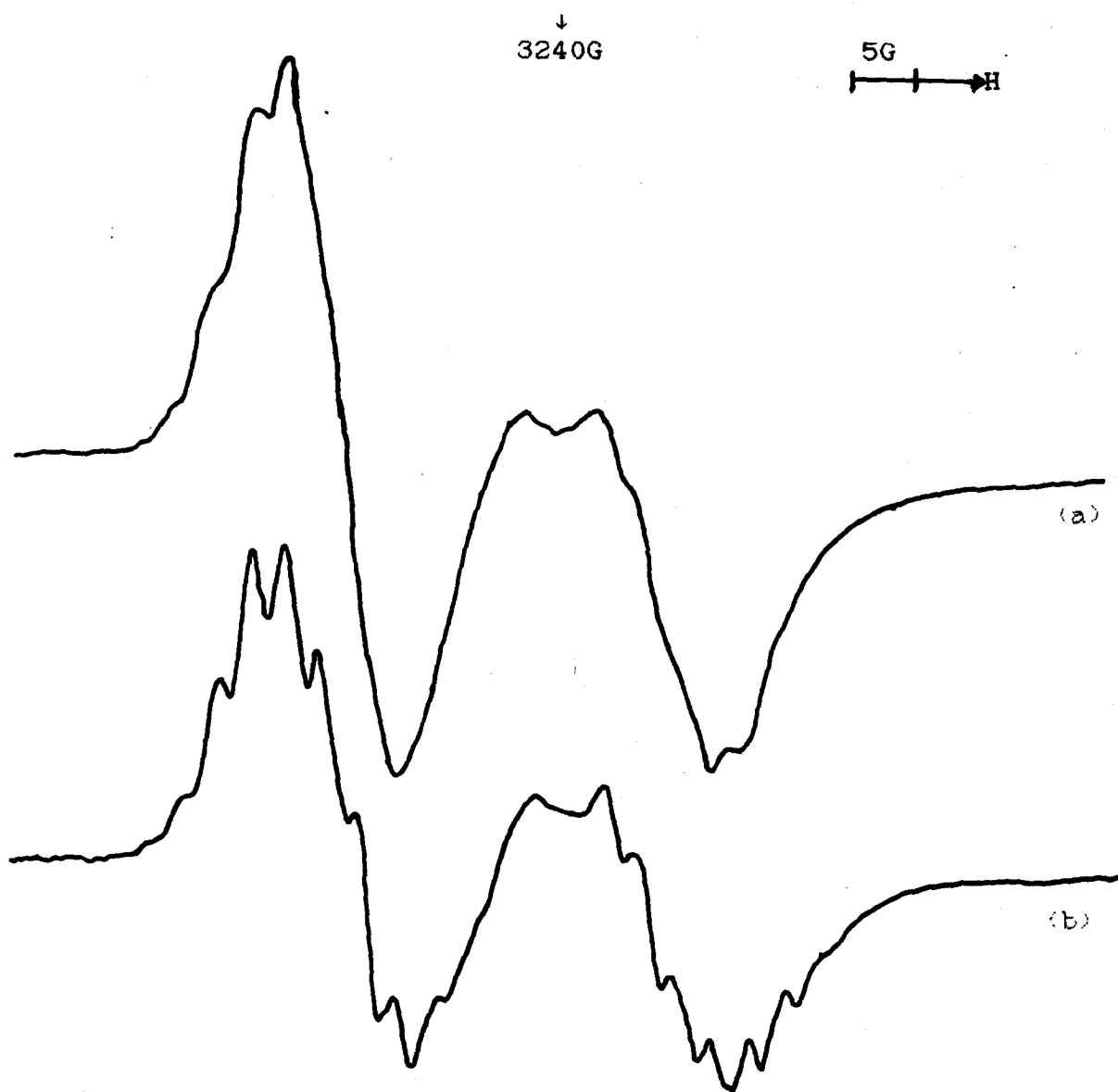
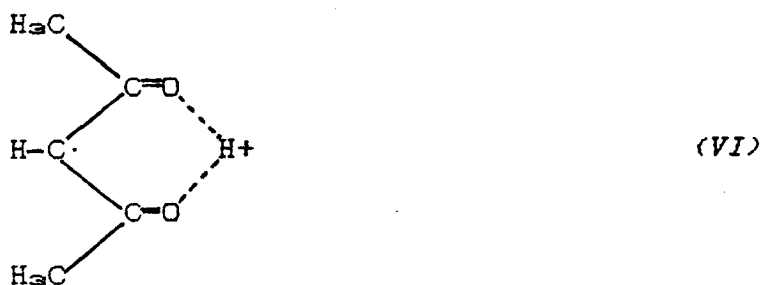
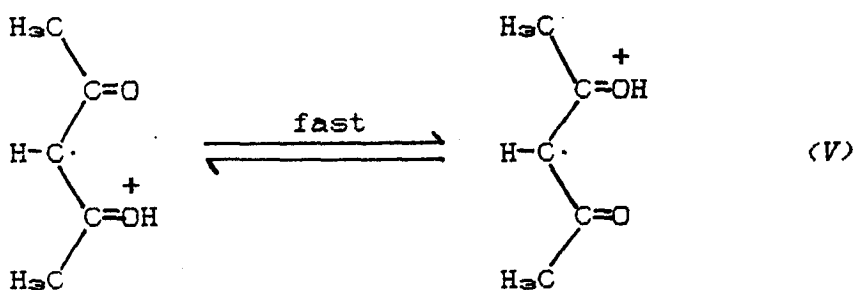


Figure 6(iii): First-derivative X-band *esr* spectra of 2,4-pentanedione in CFCl_3 , after exposure to ^{60}Co γ -rays at 77K, showing features assigned to its radical cation; (a) at 77K, (b) at ca. 140K.

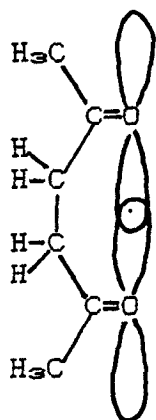
of "proton tunnelling". (74-8)

A spectrum was taken whilst the sample was annealing, *fig. 6(iii)b*, and this spectrum showed extra hyperfine splitting on the doublet seen at 77K. This hyperfine splitting is a septet; and can be assigned to the two methyl groups, rotating such that all the protons become equivalent. In order that all the protons on the methyl groups appear equivalent, it is suggested that either: the lone acidic proton, H_a , is exchanging rapidly between the two oxygen atoms, (V), or this proton is shared equally between the two oxygen atoms, (VI).

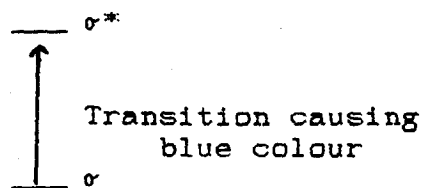
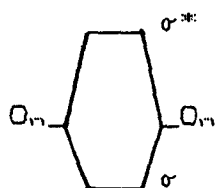


2,5-hexanedione

It was noted that the sample, after exposure to ^{60}Co γ -rays at 77K, was bright blue; all the other radical cations studied were white or off-white in colour after irradiation. The spectrum obtained at 77K was a triplet of triplets, *fig. 6(iv)*. The triplets are assigned to the central methylene protons; one of each pair being strongly coupled and one of each pair being weakly coupled. The small hyperfine coupling constants suggest a cyclised structure with the lone electron localised onto the two oxygen atoms, (VII).



(VII)



The postulated cyclised structure also explains the intense blue colour, since intense near-visible bands are

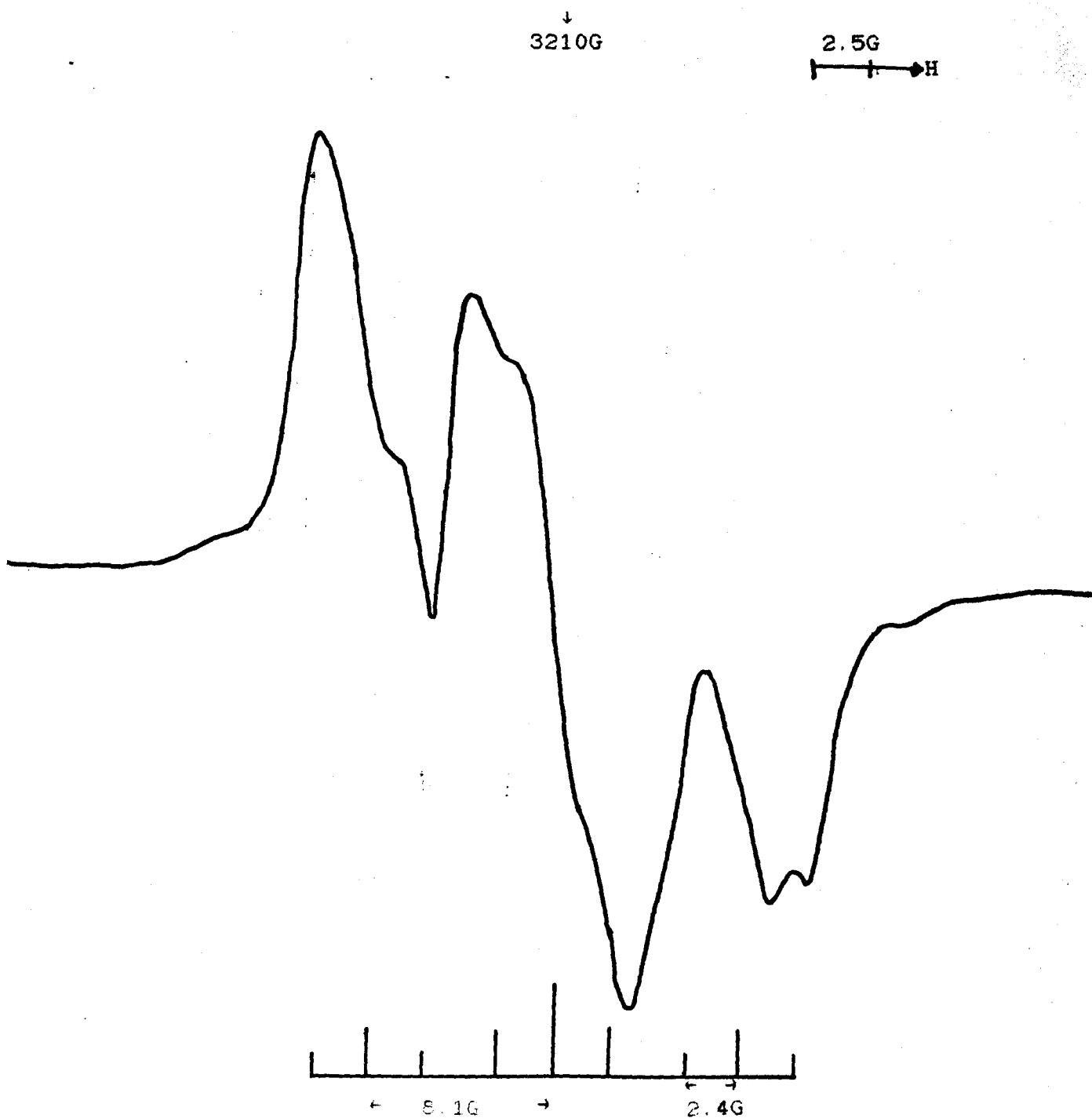


Figure 6(iv): First-derivative X-band esr spectrum of 2,5-hexanedione in CFCl_3 , after exposure to ^{60}Co γ -rays at 77K, showing features assigned to its radical cation, at 77K.

frequently found for the $\sigma \rightarrow \sigma^*$ transition of such radicals. (76) At ca. 129K a quintet of binomial distribution was observed, (also reported in reference 76). The sum of the hyperfine coupling constants for the two sets of spectra are the same, see table 6, suggesting that at the higher temperature the central protons are rapidly exchanging, a time-averaged value being observed.

2,3-hexanedione

The spectrum of this compound was an uninformative singlet. Presumably the spin is delocalised onto the two oxygen atoms, as with 2,3-butanedione, but no evidence for delocalisation into the propyl group was obtained. Also it seems that attack on the remote C-H protons does not occur. As with 2,3-butanedione it seems that the delocalised dicarbonyl unit fails to pass spin density onto the δ -protons.

Table 6

Esr Parameters For Acyclic Mono and Dicarboxyl Radical Cations.

| Cation (in CFC1 ₃) | T (K) | 1H Hyperfine Coupling Constants (G) | |
|---|---------------|-------------------------------------|---------------------------|
| | | α H | δ H |
| $\begin{array}{c} \text{H}_3\text{C} \quad + \\ \quad \diagdown \\ \quad \text{C}=\text{O} \\ \quad \diagup \\ \text{CH}_3\text{H}_2\text{C} \end{array}$ | 77 ca. 140 | | (2H)10, (1H)22 (3H)11 |
| $\begin{array}{c} \text{H}_3\text{C} \quad + \\ \quad \diagdown \\ \quad \text{C}=\text{O} \\ \quad \diagup \\ \quad \text{C}=\text{O} \\ \quad \diagdown \\ \text{H}_3\text{C} \end{array}$ | 77 | singlet | |
| $\begin{array}{c} \text{H}_3\text{C} \\ \quad \diagdown \\ \quad \text{C}=\text{O} \\ \quad \diagup \\ \text{HC} \\ \quad \diagdown \\ \quad \text{C}=\text{OH}^+ \\ \quad \diagup \\ \text{H}_3\text{C} \end{array}$ | 77 ca. 140 | (1H)23 (1H)23 | (6H)2.5 |
| $\begin{array}{c} \text{H}_3\text{C} \quad + \\ \quad \diagdown \\ \quad \text{C}=\text{O} \\ \quad \diagup \\ (\text{H}_2\text{C})_2 \\ \quad \diagdown \\ \quad \text{C}=\text{O} \\ \quad \diagup \\ \text{H}_3\text{C} \end{array}$ | 77 129 (†) | | (2H)8.1, (2H)2.4 (4H)5 |
| $\begin{array}{c} \text{H}_3\text{C} \quad + \\ \quad \diagdown \\ \quad \text{C}=\text{O} \\ \quad \diagup \\ \quad \text{C}=\text{O} \\ \quad \diagdown \\ \text{H}_3\text{CH}_2\text{CH}_2\text{C} \end{array}$ | 77 | singlet | |

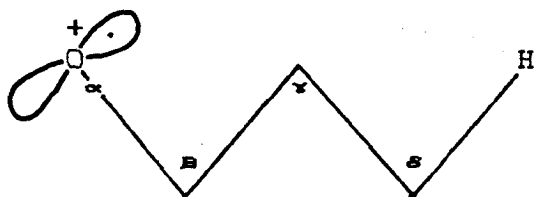
† see reference 76

Chapter 7

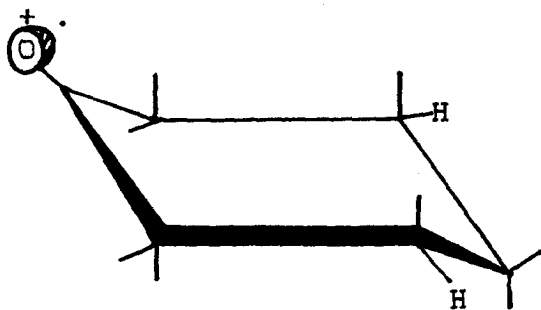
7 CYCLIC CARBONYLS

7.1 Introduction

As mentioned earlier, in chapter 6, no strong coupling to γ -protons is seen in ketones, but as Snow and Williams⁽⁷⁾ have shown, the δ -protons can give well resolved splittings when in the in-plane W-plan structure, (VIII); although average splittings remain small.



This is exemplified by the remarkably large coupling of the two δ -protons for the cation of cyclohexanone, depicted in (IX).



It seems to be a general rule for the carbonyl cations that whilst γ -proton coupling has not yet been resolved, except using endor methods, that to the δ -protons can be

relatively large for optimum conformations. ⁽⁷²⁾

7.2 Saturated Cyclic Monocarbonyl

Cyclobutanone

It was hoped that the cation of this compound would also exhibit coupling to two equivalent protons. In the event however, the 77K spectrum was too poorly defined to interpret. It was clearly related, however, to that seen at ca. 140K, *fig. 7(i)*, which is assigned to the ring opened cation, $\text{H}_2\text{C}\overset{\cdot}{\text{C}}\text{H}_2\text{CH}_2\text{C}\equiv\text{O}$. Presumably ring-strain is sufficient to cause C-C bond breakage in this case. This has been reported already by Boon *et al.* ⁽⁷²⁾

7.3 Saturated Cyclic Dicarboxyls

1,4-cyclohexanedione

The spectrum at 77K, *fig. 7(ii)*, showed a quintet of binomial distribution. This shows that four of the eight available protons couple to the spin. Comparing this result with that for the cyclohexanone radical cation, see earlier, it can be deduced that for cyclohexanedione, the signal should be assigned to the coupling of the spin to the four equatorial protons. Thus a five line spectrum is seen.

There are two reasonable interpretations of this spectrum; either the spin is localised onto one oxygen

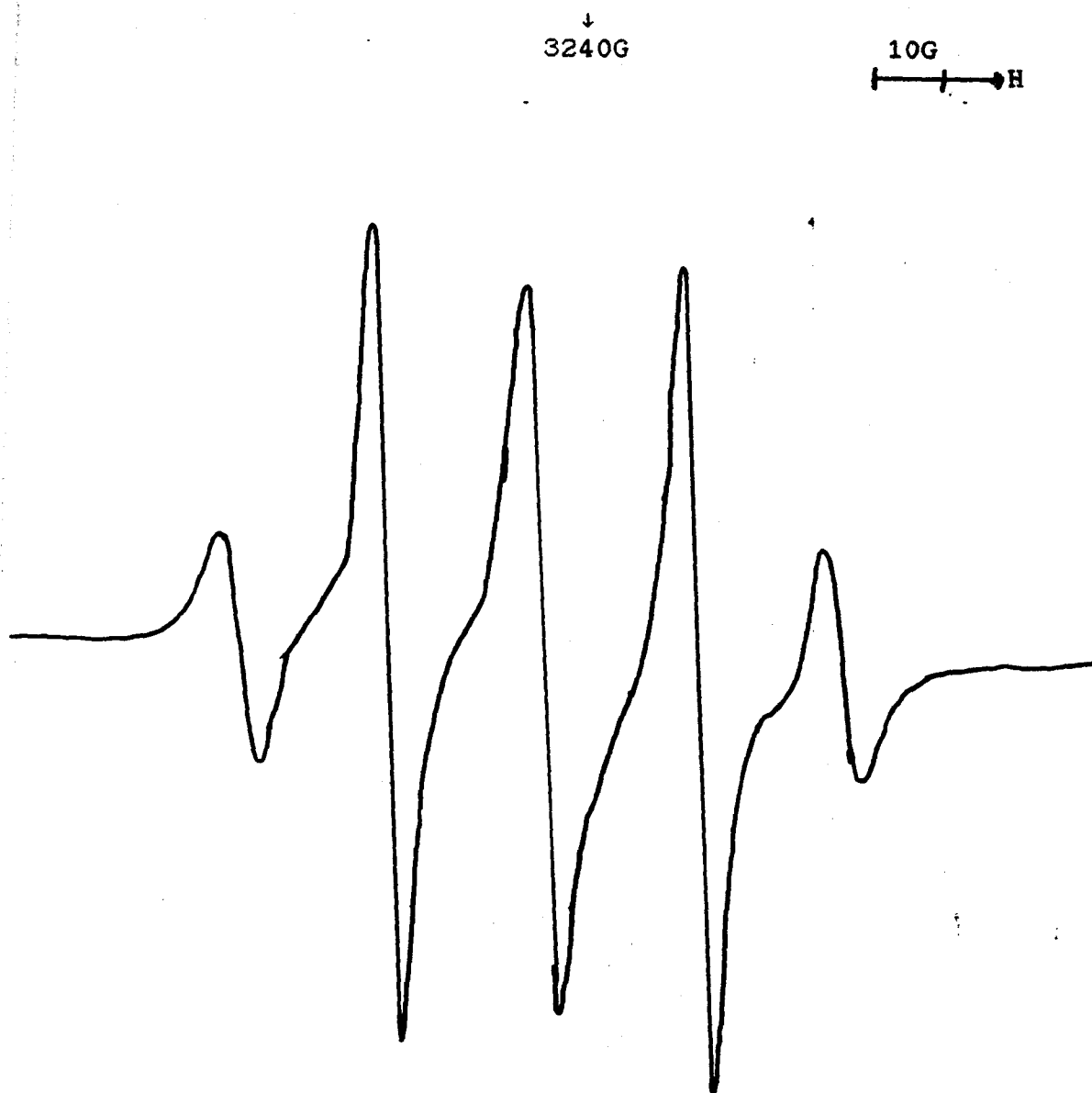


Figure 7(1): First-derivative X-band esr spectrum of cyclobutanone in CFCl_3 , after exposure to ^{60}Co γ -rays at 77K, showing features assigned to its rearranged radical cation, at ca. 140K.

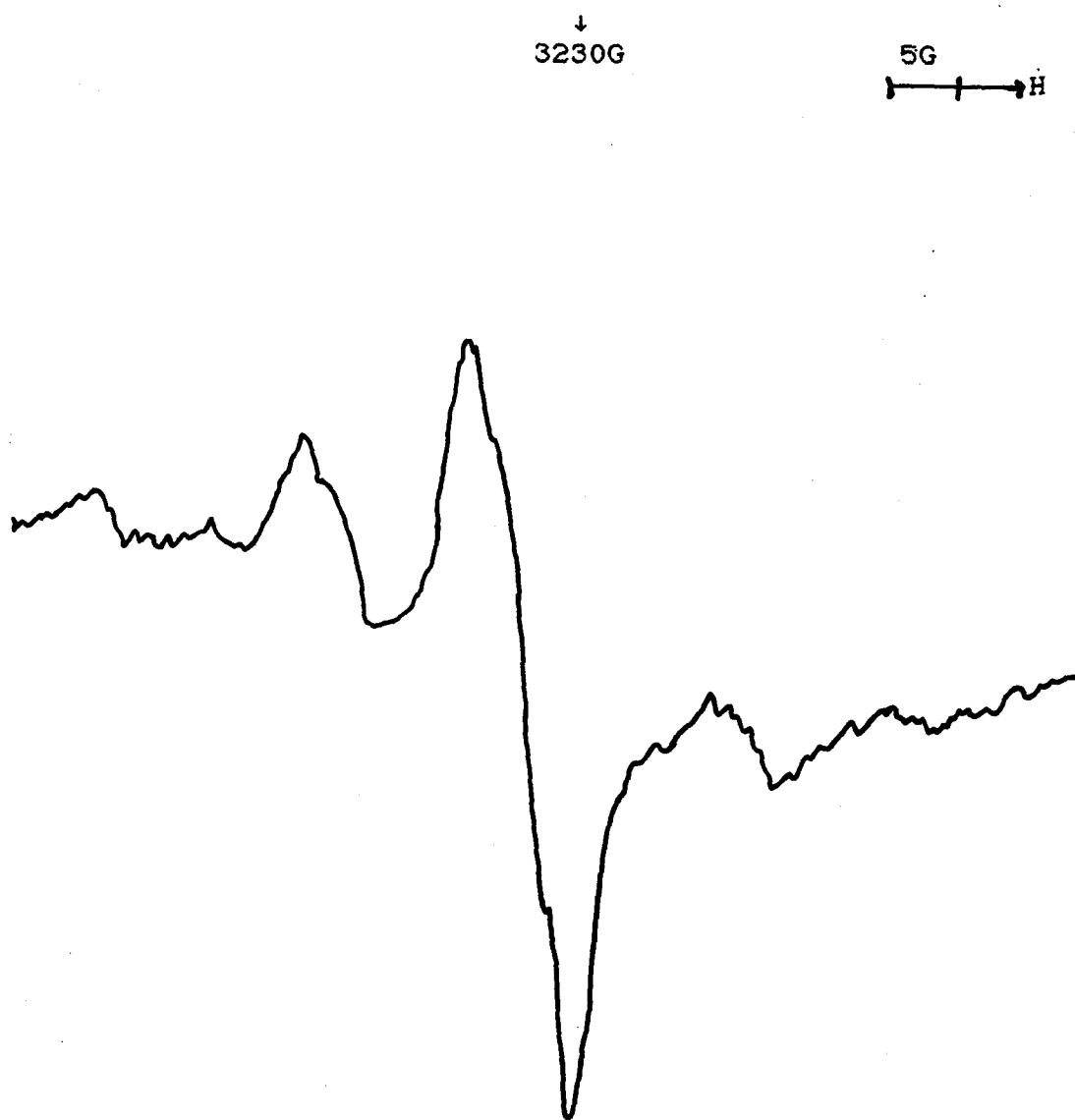


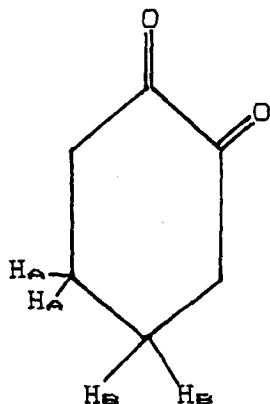
Figure 7(ii): First-derivative X-band esr spectrum of 1,4-cyclohexanedione in CFCl_3 , after exposure to ^{60}Co γ -rays at 77K, showing features assigned to its radical cation, at 77K.

equivalent protons are seen and five lines are observed in the *esr* spectrum. On cooling, again, the axial/equatorial interconversion is slowed, but since it is already slow no change is seen in the *esr* spectrum.

An experiment was undertaken to resolve this problem. The sample was irradiated at 77K, but the signal observed at 10K. The spectrum obtained at 10K, *fig. 7(iii)*, also gave a quintet, similar to that obtained at 77K. Thus the structure of the cation is the delocalised system, (XI), and the spin is shared between the two oxygen atoms, with slow axial/equatorial interconversion.

1,2-cyclohexanedione

The spectrum obtained at 77K, *fig. 7(iv)a*, is very complex and difficult to interpret. The spectrum expected was a triplet, or a triplet of triplets, i.e. coupling to H_A and/or H_B , (XII).



(XII)

Each pair was expected to be equivalent since it was

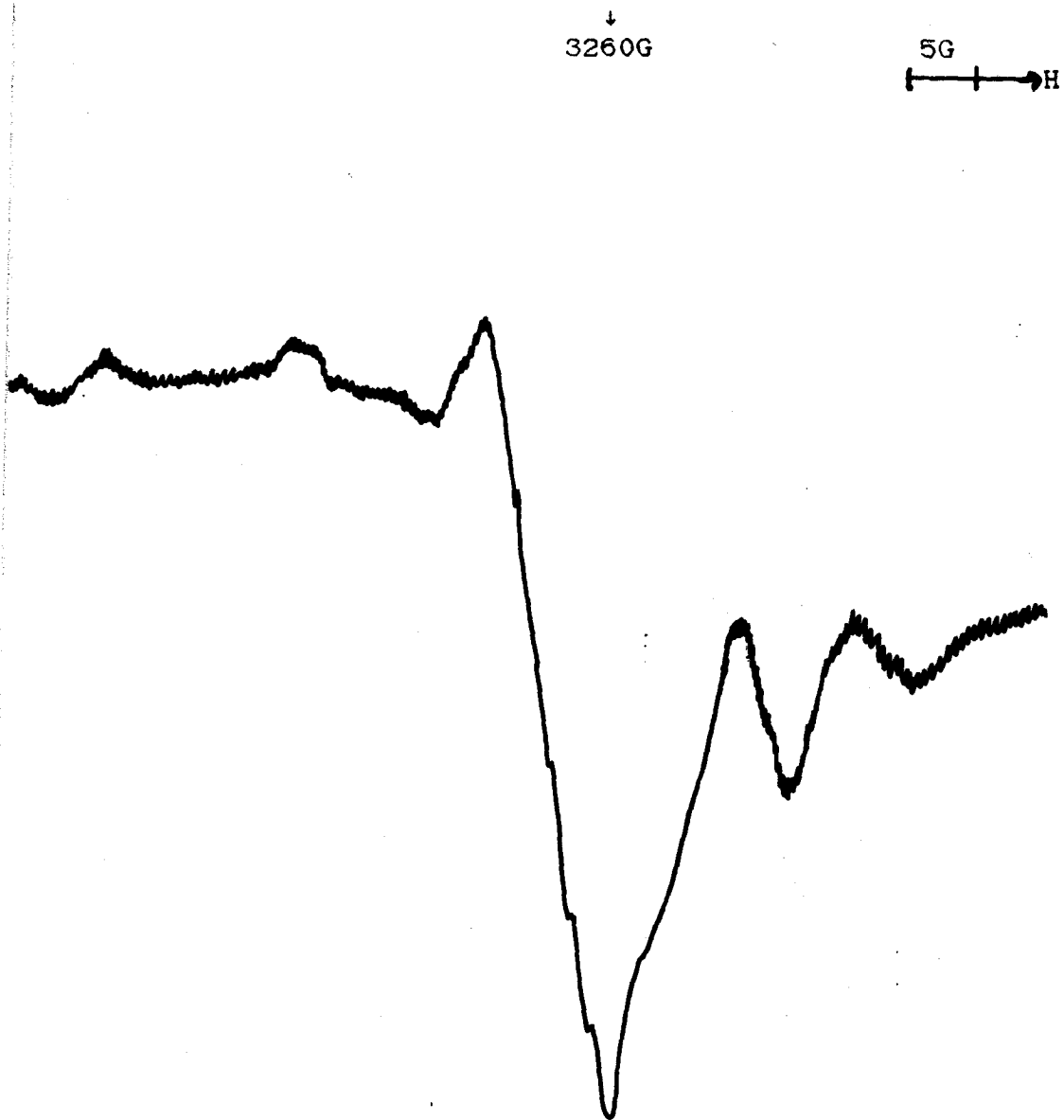


Figure 7(iii): First-derivative X-band esr spectrum of 1,4-cyclohexanedione in CFCl_3 , after exposure to ^{60}Co γ -rays at 77K, showing features assigned to its radical cation, at 10K.

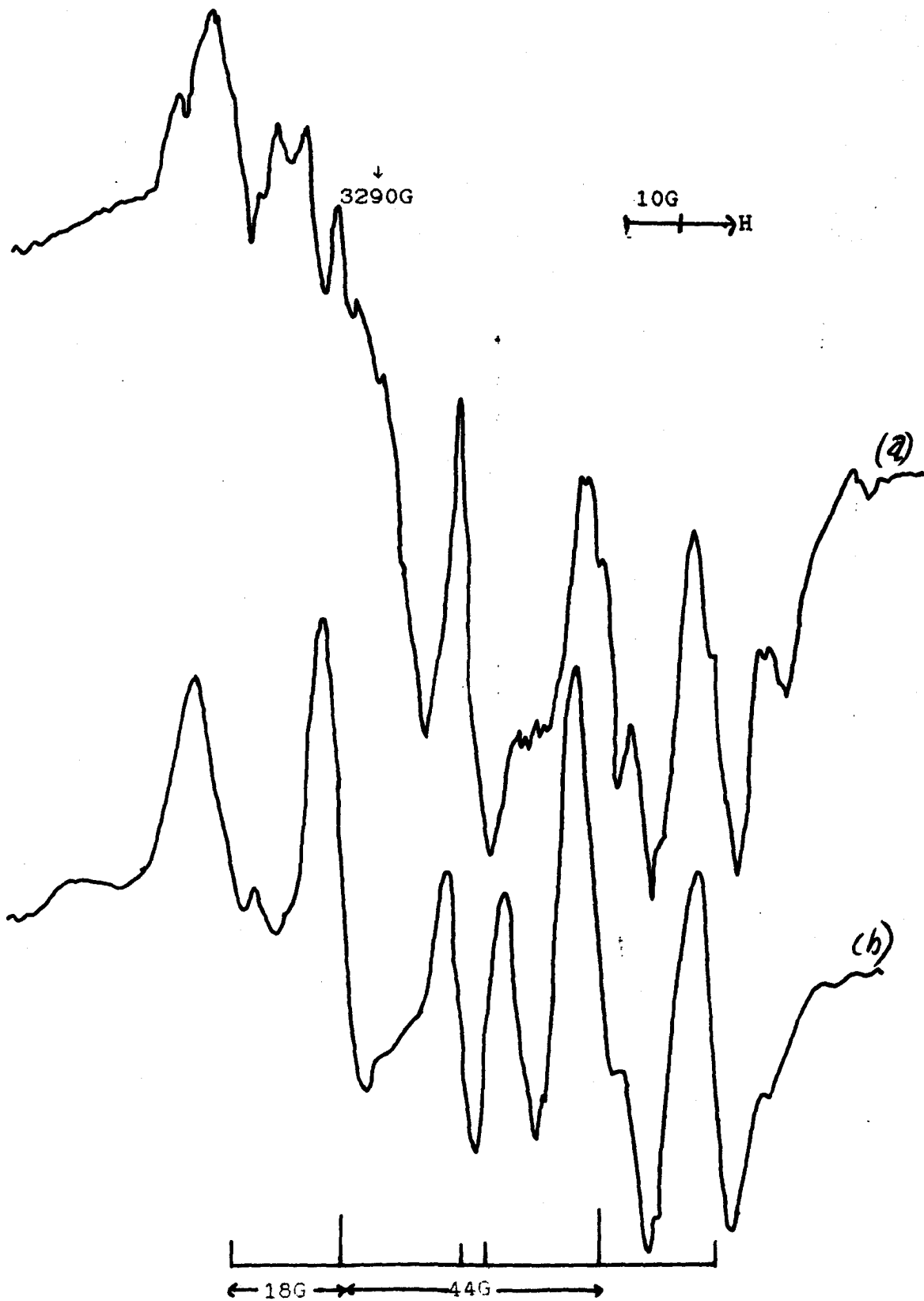


Figure 7(iv): First-derivative X-band esr spectra of 1,2-cyclohexanedione in CFCl_3 , after exposure to ^{60}Co γ -rays at 77K, showing features assigned to its radical cation; (a) at 77K, (b) at ca. 140K.

thought that the dicarbonyl unit would be planar.

Some g anisotropy could be seen in the 77K spectrum by the existence of sharp, clearly defined lines upfield of free spin and broader lines downfield of free spin. No strong σ^* -bonding exists, since σ^* -bonding is expected to give rise to relatively small proton splittings and possibly a visible colour. The value of ΔH for this compound is greater than that of 1,4-cyclohexanedione, see table 7, for which no O-O σ^* -bonding is possible.

In the spectrum taken during the anneal, *fig. 7(iv)b*, no strong central feature is seen; both a triplet and a triplet of triplets require a strong central line in their spectra. So the analysis of the spectrum cannot be lines due to a pair, or two pairs, of protons. The anneal spectrum appears to be a doublet of triplets, which could be due to a single proton and a pair of protons in different environments. It is possible that the dicarbonyl unit is twisted, as noted in the radical anion⁷⁷ of this compound. This could lead to inequivalence of the protons, and thus the resulting spectrum.

1.3-cyclohexanedione

Here the 77K spectrum was also complex and difficult to interpret, but in the anneal the spectrum became clearer and a definite triplet was seen, *fig. 7(v)*. As with 1,4-cyclohexanedione either a localised or a delocalised

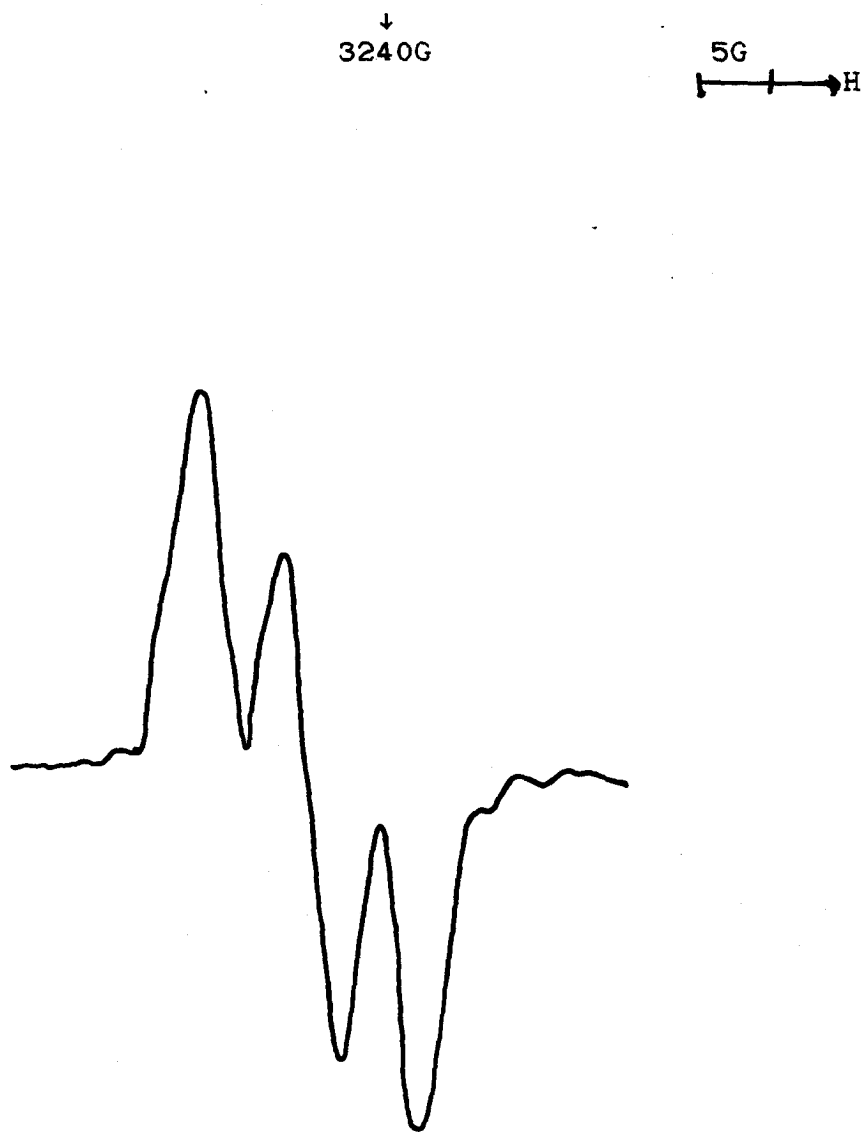
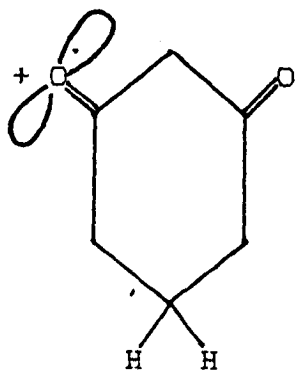
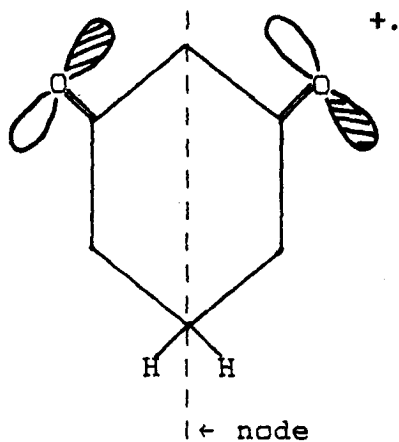


Figure 7(v): First-derivative X-band esr spectrum of 1,3-cyclohexanedione in CFCl_3 , after exposure to ^{60}Co γ -rays at 77K, showing features assigned to its radical cation, at ca. 140K.

spin could give rise to the observed spectrum. For the localised structure, (XIII), there are two δ -protons and normal delocalisation should occur.



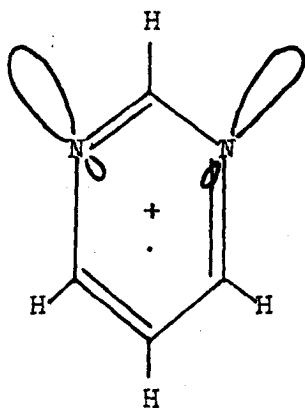
(XIII)



(XIV)

If the conformation is fixed, such that one proton is close to the planar W-plan structure, then a coupling of 20-30G might be expected, that to the other proton being small. For the delocalised structure, (XIV), these two protons are δ to both carbonyl oxygens. Since the combination of orbitals on oxygen is most likely to be antibonding, as indicated in (XIV), there should be a symmetry node passing through this methylene group. In which case the coupling to both protons should be negligible. Therefore the localised structure, (XIII), is strongly favoured for this radical cation. The electron transfer between the two oxygen atoms would leave the proton coupling unchanged, and hence our spectra are not able to distinguish between fast and slow electron transfer.

It is interesting to compare these results with those for the 1,3-diazabenzene radical cation, (XV).



(XV)

Here localised and delocalised structures are possible as with 1,3-cyclohexanedione. The cation of 1,3-diazabenzene undergoes an asymmetrical distortion, such that the electron is confined to one nitrogen atom. (78)

5,5-dimethyl-1,3-cyclohexanedione

The spectrum here showed a single line, and there was no coupling between the spin and any protons present. This result was expected, and confirms that the two coupled protons for unsubstituted cation must indeed be those in the 5-position.

1,3-cyclopentanedione

An attempt was made to prepare the radical cation of this compound, but it was totally insoluble in CFCl_3 , the solvent used, so no results were obtained.

7.4 Unsaturated Cyclic Carbonyls

para-benzoquinone

The spectrum at 77K, *fig. 7(vi)*, shows a quintet of binomial distribution, similar to that for 1,4-cyclohexanedione, its saturated analogue. Here, again, a lower temperature experiment was undertaken. The spectrum at 10K, *fig. 7(vii)*, also gave a binomial quintet, thus favouring the delocalised σ -structure.

2,6-dimethyl-para-benzoquinone

The results for this cation fit in well with those for the parent compound, p-benzoquinone. The spectrum assigned to the radical cation of this derivative, *fig. 7(viii)*, is a triplet, due to the coupling of the spin to two equivalent protons. Again, there are two possible interpretations of this spectrum, a π -model and a σ -model. The π -interpretation, which puts spin density into the π -system of the aromatic ring, requires a large hyperfine coupling constant for the methyl groups and this is not seen. The σ -interpretation, in which the spin density is delocalised through the σ -bonds of the whole molecule, puts lower spin density onto the oxygen atoms than in the unsubstituted compound, since the spin is shared over more bonds with the presence of the methyl groups. This σ -model predicts a slightly reduced hyperfine coupling constant for ring protons. This seems to be the case, in accord with the

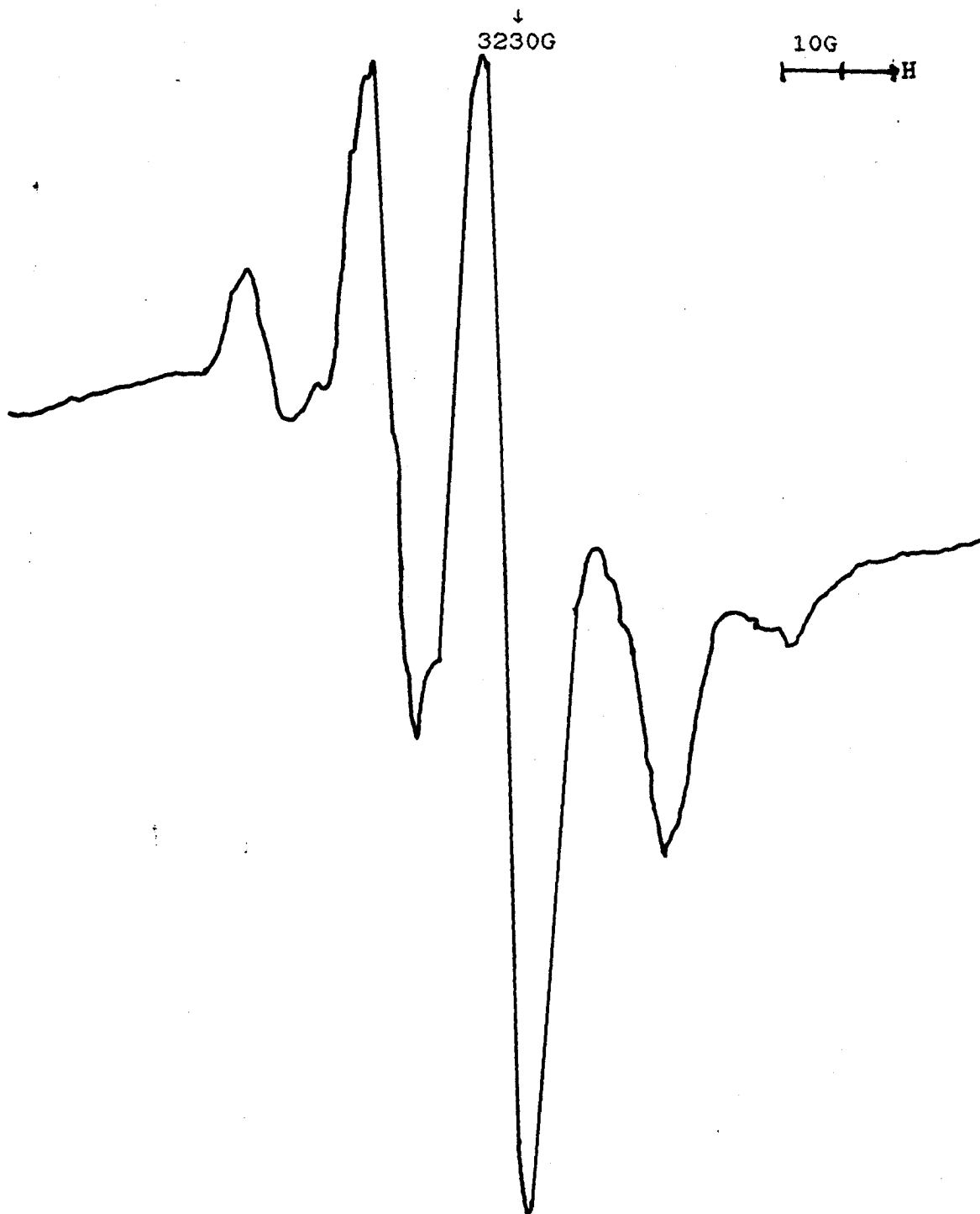


Figure 7(vi): First-derivative X-band esr spectrum of p-benzoquinone in CFCl_3 after exposure to ^{60}Co γ -rays at 77K, showing features assigned to its radical cation, at 77K.

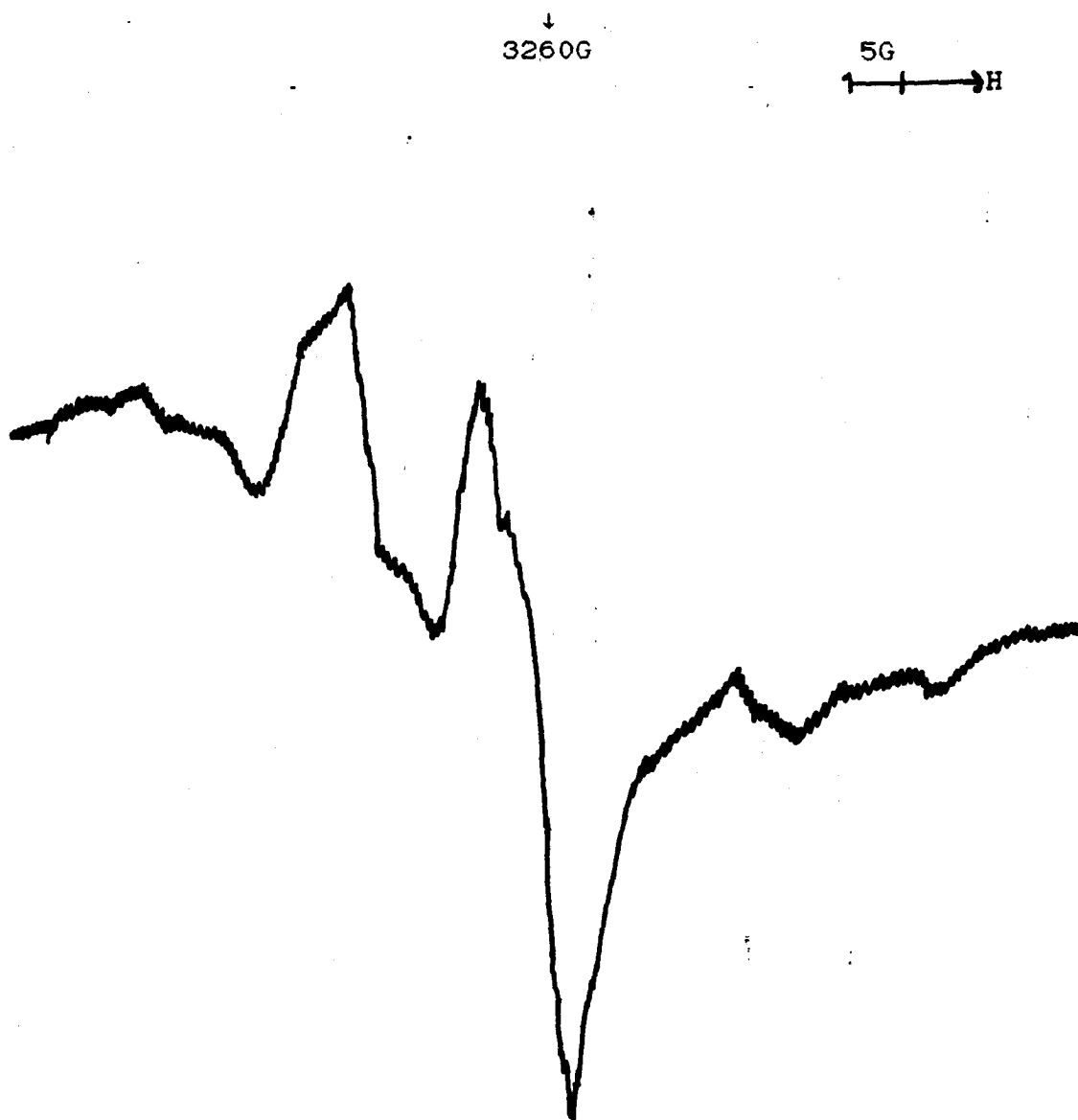


Figure 7(vii): First-derivative X-band esr spectrum of p-benzoquinone in CFCl_3 , after exposure to ^{60}Co γ -rays at 77K, showing features assigned to its radical cation, at 10K.

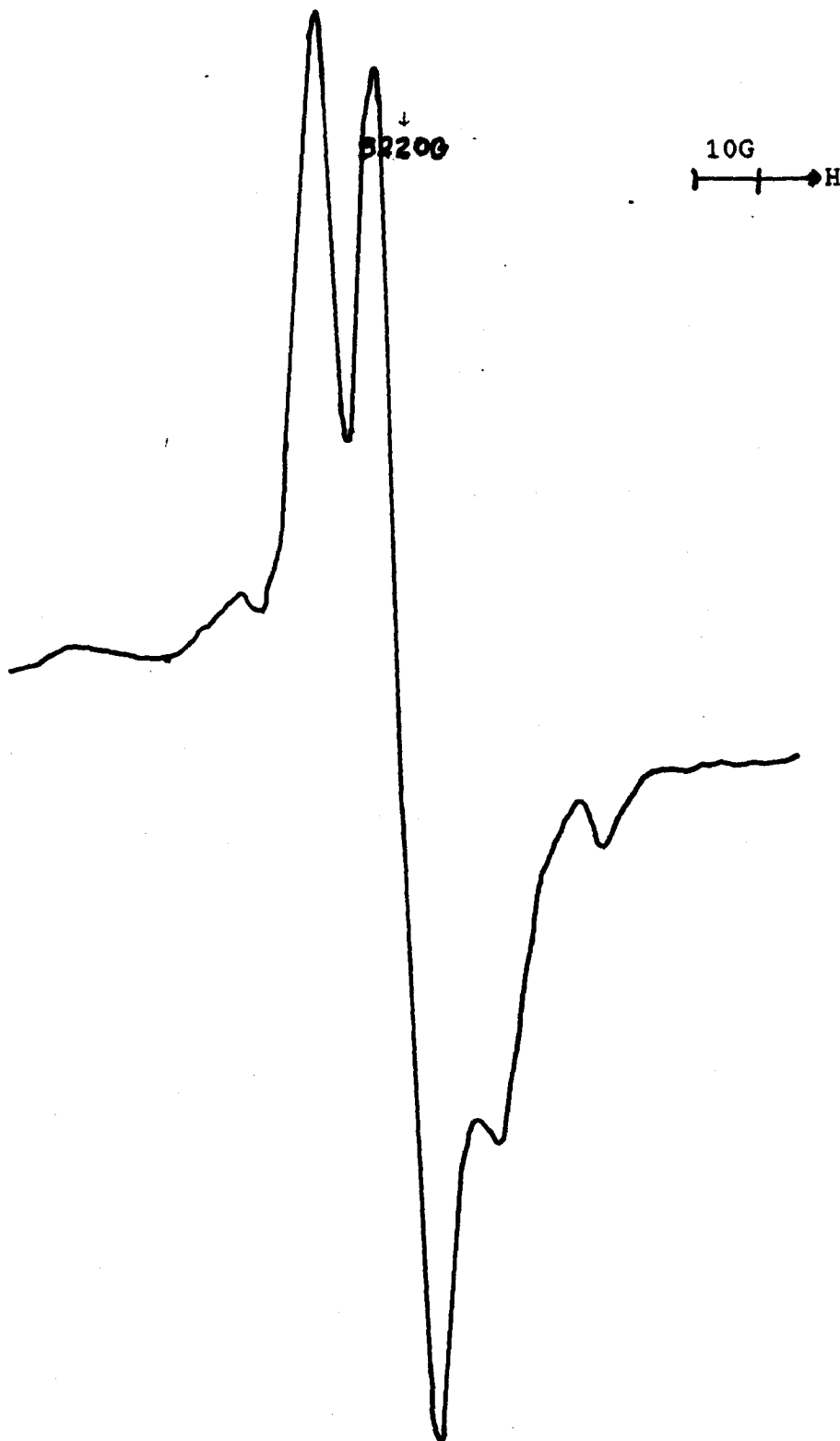
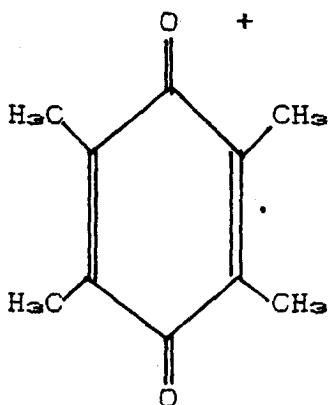


Figure 7(viii): First-derivative X-band esr spectrum of 2,6-dimethyl-p-benzoquinone in CFCl_3 , after exposure to ^{60}Co γ -rays at 77K, showing features assigned to its radical cation, at 77K.

σ -model, see table 7. Thus it appears that again the σ -interpretation gives the best structure.

2,3,5,6-tetramethyl-para-benzoquinone

The expected spectrum of this compound was a singlet, since no couplings to the protons in the methyl groups were observed in 2,6-dimethyl-p-benzoquinone. The observed spectrum was, however, more complex. Although very difficult to interpret, because the features are broad and asymmetric, an approximate fit can be obtained using a quintet of triplets, *fig. 7(ix)*. This suggests a contribution from four protons in one environment and two protons in a different one. This combination is very difficult to understand if a σ -delocalised model is used. The σ -model requires a specific delocalisation onto the in-plane proton of the methyl groups. The π -delocalised model, however, requires none of this and leads to a single-sided radical, (XVI).



(XVI)

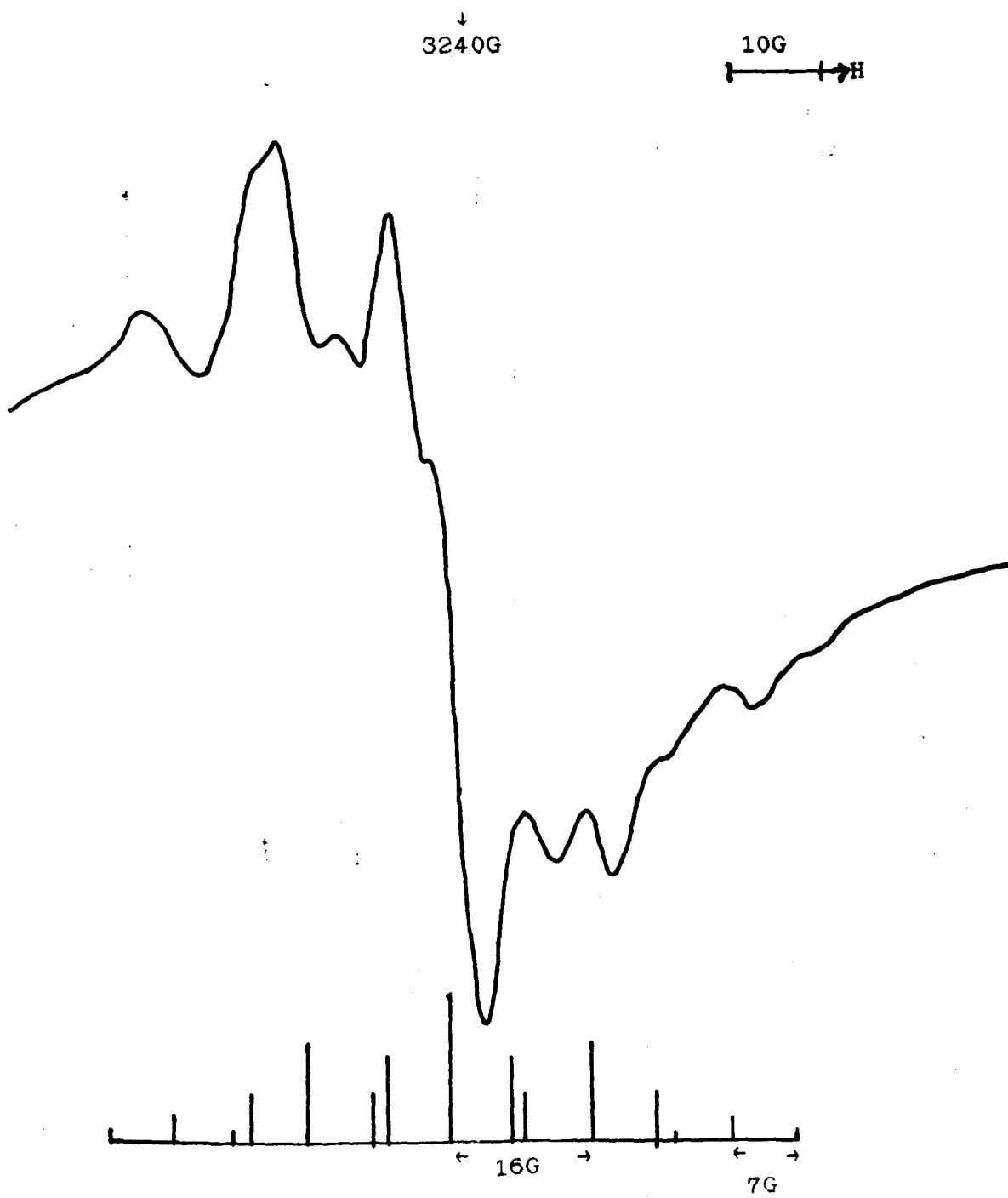
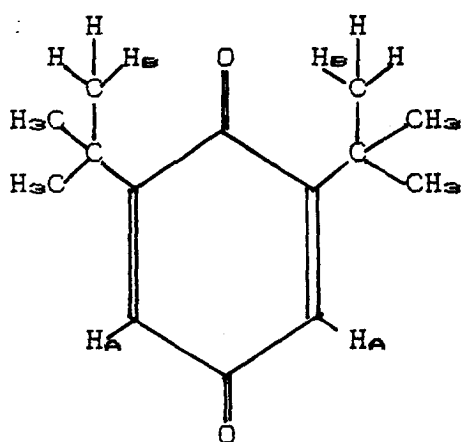


Figure 7(ix): First-derivative X-band esr spectrum of 2,3,5,6-tetramethyl-p-benzoquinone in CFC_{12} , after exposure to ^{60}Co γ -rays at 77K.

An orbital inversion to give the π -delocalised radical cation would not be unreasonable because of the stabilising effect of the four methyl groups. But, by analogy with such radical cations as those of toluene and p-xylene, ⁽⁷⁹⁾ we would expect to detect coupling to all twelve protons and this is not seen. A further study is needed to determine the structure of the radical cation.

2,6-di-tertiary-butyl-para-benzoquinone

The spectrum obtained at 77K, *fig. 7(x)*, is interpreted as a triplet of triplets. One triplet, $A(^1H_A) = 11G$, is assigned to the ring protons and the other triplet, $A(^1H_B) = 20G$, is assigned to two protons from the t-butyl groups, (XVII).



(XVII)

Thus there is some delocalisation of spin into the t-butyl units. In a spectrum taken during the anneal, the signal collapsed into a quintet, $A(^1H) = 14G$. This is explained by

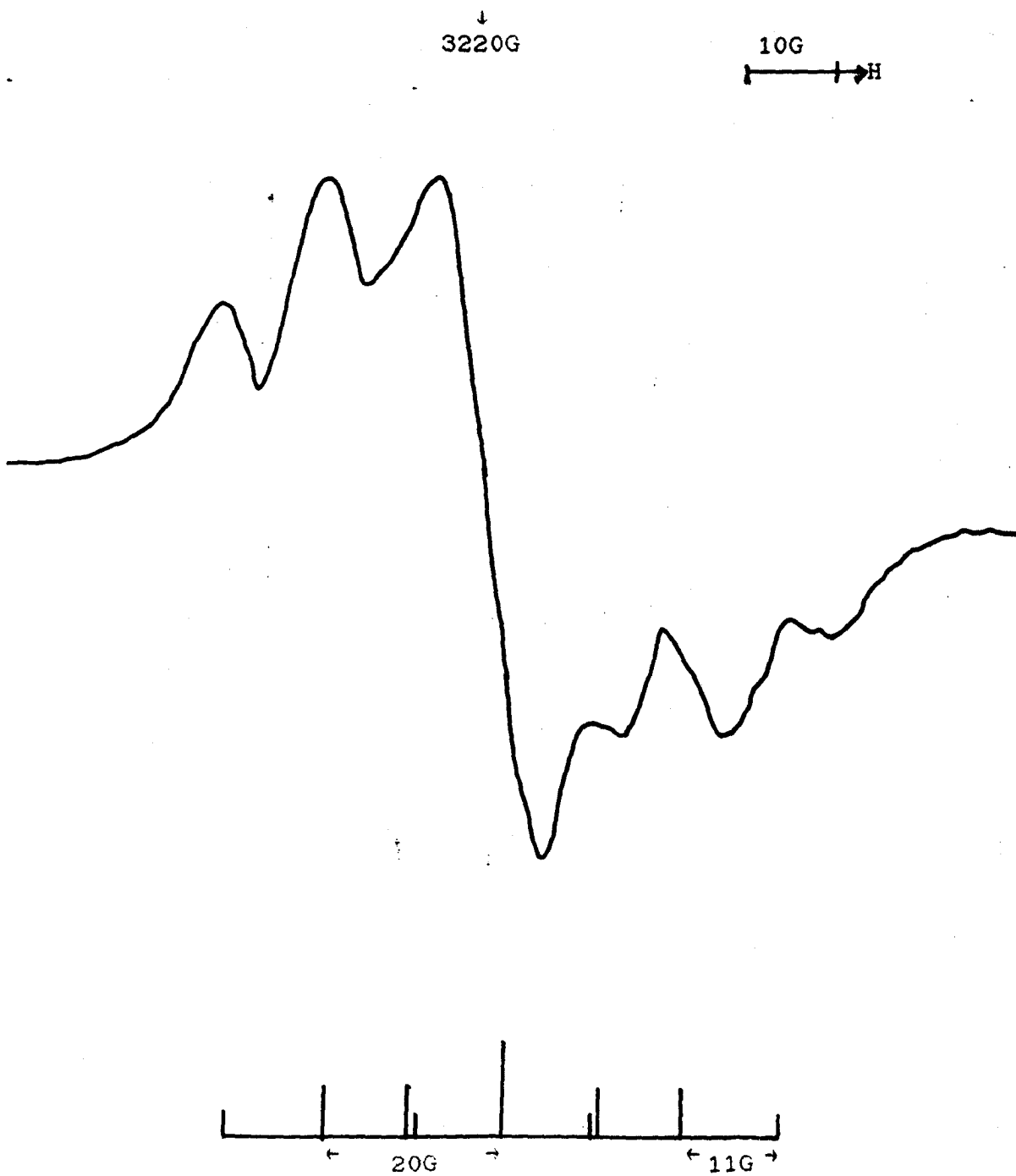
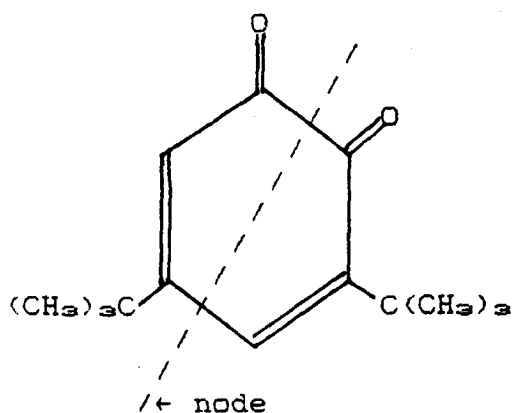


Figure 7(x): First-derivative X-band esr spectrum of 2,6-di-tertiary-butyl-p-benzoquinone in CFCl_3 , after exposure to ^{60}Co γ -rays at 77K, showing features assigned to its radical cation, at 77K.

the fact that the heating occurring during the anneal causes the hyperfine coupling constant of the lone proton to increase to 14G, and alongside this the t-butyl group is achieving some rotation and thus its proton hyperfine coupling constant is decreasing, by a time averaging effect. Thus the two sets of hyperfine coupling constants converge and, by chance, they achieve the same numerical value at this temperature.

3,5-di-tertiary-butyl-ortho-benzoquinone

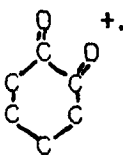
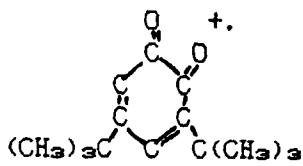
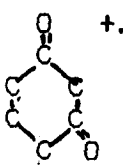
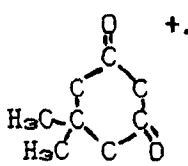
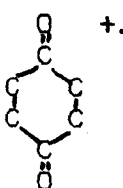
Unfortunately the observed spectrum for this compound was a singlet, and it is noteworthy that there is an absence of δ -proton coupling and thus the odd electron must be confined to the σ^* -orbital between the two oxygen atoms and not delocalised over the whole molecule. The dicarbonyl unit is probably planar and thus the electron would be confined to an antibonding orbital between the two oxygen atoms, (XVIII), and thus would not couple strongly to the protons.



It would have been interesting and useful to study the parent, unsubstituted o-benzoquinone as a comparison, but this compound was unavailable. The saturated analogue, in contrast to the singlet obtained herein, gave a complex spectrum. This spectrum is attributed to splittings caused by the dicarbonyl unit being twisted, and thus the lone electron can couple strongly to the protons. In this, the unsaturated case, the dicarbonyl unit is expected to be planar and thus the lone electron is confined within the dicarbonyl unit.

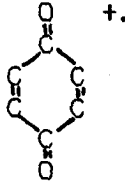
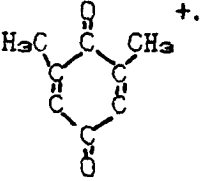
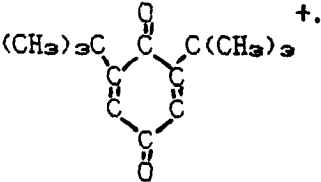
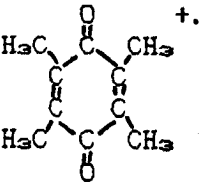
Table 7

Esr Parameters For Cyclic Mono and Dicarbonyl Radical Cations.

| Cation (in CFC1 ₂) | T (K) | $\delta^1\text{H}$ Hyperfine Coupling Constant (G) |
|---|---------------|--|
| $\cdot\text{H}_2\text{CCH}_2\text{CH}_2\text{C}\equiv\text{O}^+$ | ca. 140 | (4H)22 |
|  | ca. 140 | (2H)18, (1H)44 |
|  | 77 | singlet |
|  | 77 ca. 140 | (1H)12, (1H)0 (2H)6 |
|  | 77 | singlet |
|  | 77 10 | (4H)20 (4H)18 |

cont...

Table 7

| Cation | T (K) | $\delta^1\text{H}$ Hyperfine Coupling Constant (G) |
|---|---------------|--|
|  | 77 10 | (4H)18 (4H)15 |
|  | 77 | (2H)11 |
|  | 77 ca. 140 | (2H)11, (2H)20 (4H)14 |
|  | 77 | (2H)7, (4H)16 |

Chapter 8

8 Aldehydic Carbonyls

8.1 Introduction

In contrast to the radical cations of acetone and 2,3-butanedione, in CFCl_3 , which exhibit no proton couplings and thus their esr spectra are asymmetric singlets, the radical cation of formaldehyde has recently been well defined in inert gas media.⁽⁸⁰⁾ The unsolvated species showing strong coupling to the β -protons with $A(^1\text{H}) = 132.7\text{G}$ and $g = 2.0036$. Formation of the parent radical cation of formaldehyde has not been reported in a CFCl_3 matrix or any related medium. Also radical cations of the dicarbonyl derivatives of formaldehyde, glyoxal and methylglyoxal have not been previously studied by esr spectroscopy.

8.2 Aldehydic Monocarbonyl

Formaldehyde

The spectrum obtained at 77K, *fig. 8(i)*, was a complex central region and two sets of widely spaced lines, marked α , separated by 320G. The parent radical cation is probably present but is obscured by other features in the central region, and thus is unresolved. These α features are assumed to be the $M_1 = \pm 1$ lines of a triplet of 160G. These α lines appeared to be further split into four lines all of approximately equal intensity. On annealing the

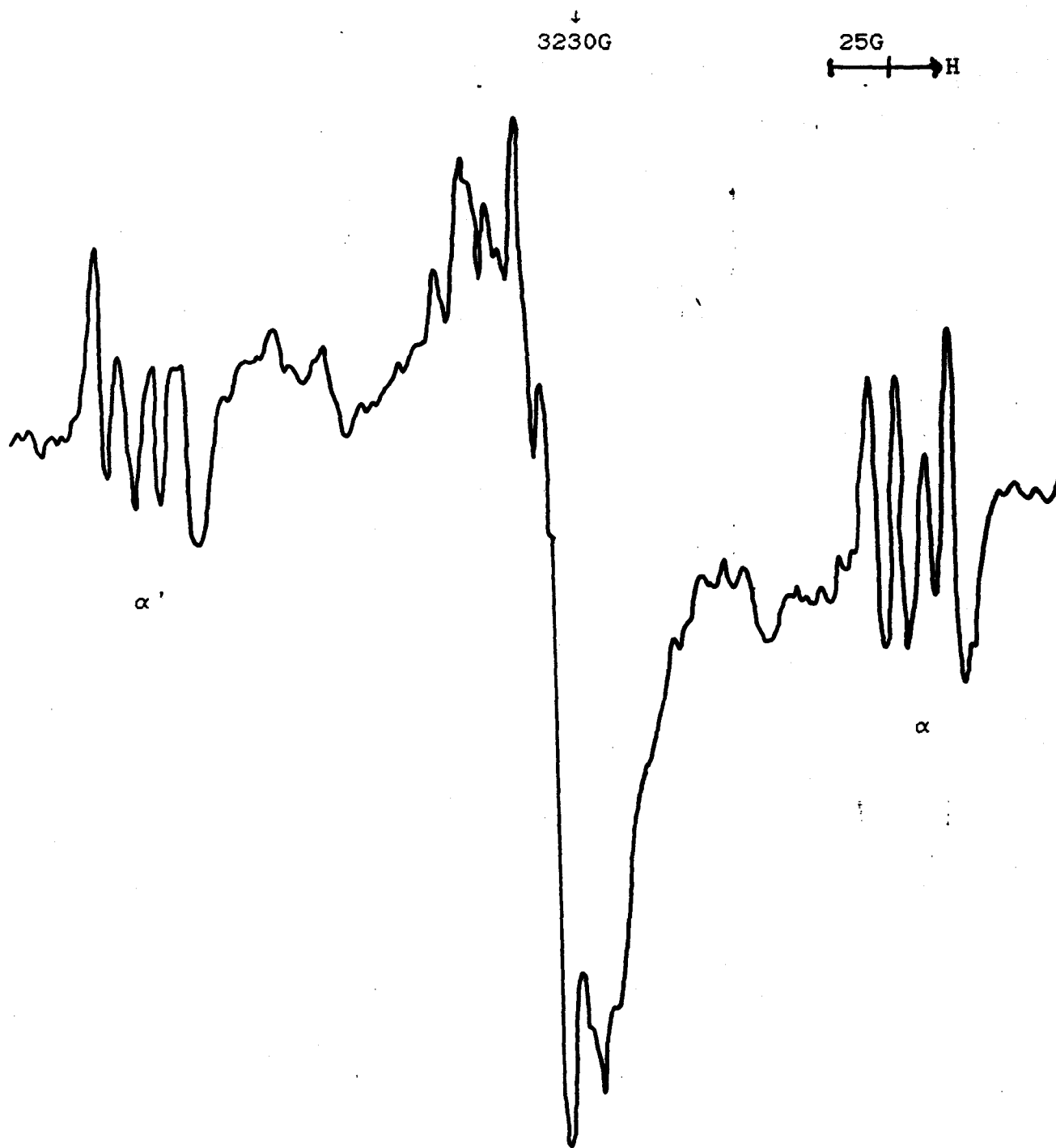
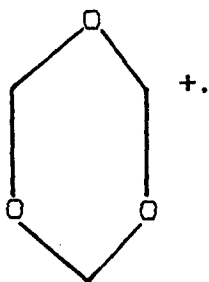


Figure 8(1): First-derivative X-band esr spectrum of formaldehyde in CFC1₂, after exposure to ⁶⁰Co γ-rays at 77K, showing features assigned to the s-trioxane radical cation, marked α, at 77K.

central region became no less interpretable but the α lines became clearer. As the sample warmed during the anneal, two of these lines remained stationary and two lines moved, but the splitting between each pair was unchanged, *fig. 8(11)*. Thus the four lines must actually be two doublets, with splittings of 20G and 23G, which overlap in the esr spectrum. This spectrum is similar to that obtained for s-trioxane, $\langle \text{e}^{\cdot} \text{-} \text{2} \rangle$ which is itself the trimer of formaldehyde. Thus the α features are assigned to the s-trioxane radical cation, *(XIX)*,



(XIX)

the SOMO being largely confined to one $-\text{O}-\text{CH}_2-\text{O}-$ unit. The trimerisation of formaldehyde probably occurred before it was added to the CFCl_3 , since the CFCl_3 solution was too dilute for trimerisation to be likely. The radical cation study of formaldehyde was undertaken in collaboration with Dr. C.J. Rhodes, who has continued the research, and has identified the parent radical cation.

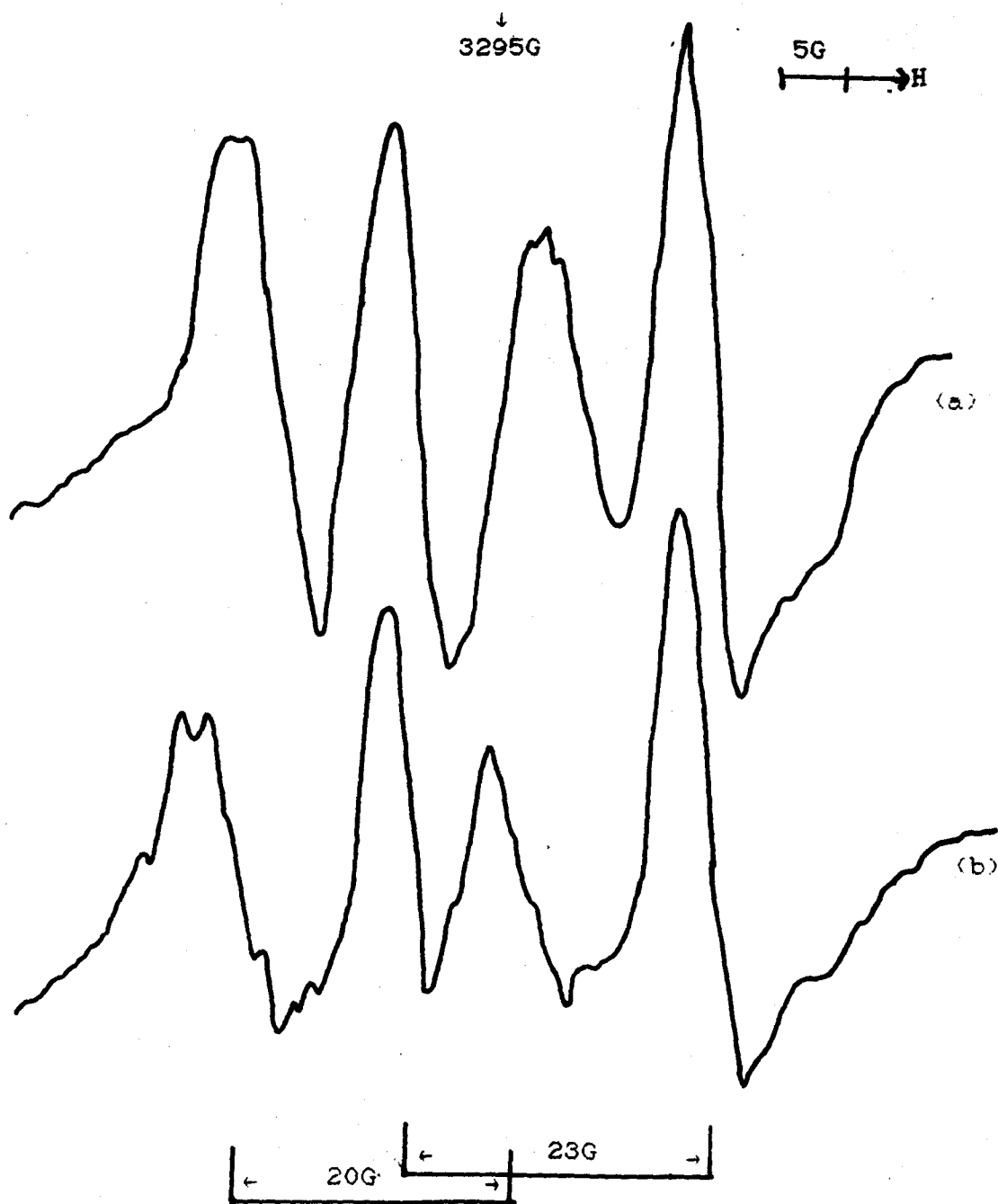
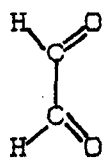
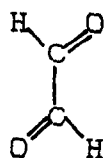


Figure 8(11): First-derivative X-band esr spectrum of formaldehyde in CFCl_2 , after exposure to ^{60}Co γ -rays at 77K, showing features assigned to the s-trioxane radical cation; (a) at 77K, (b) at ca. 140K. (low field set)

8.3 Aldehydic Dicarbonyls

Glyoxal

The spectrum at 77K, *fig. 8(iii)*, gave a large central triplet which is assigned to the parent radical cation. The spin is delocalised onto both carbonyl groups, giving two equivalent protons, the proton splitting being ca. 84G. This splitting is significantly larger than expected, since it is greater than half the value found for monocarbonyl compounds (ca. 68G). This enhancement is particularly surprising in view of the greater delocalisation of the positive charge on the glyoxal cation. The parent molecules have been shown to exist mainly in the *s-trans* conformation, (XX).⁽²²⁻⁴⁾



We might therefore expect that the radical cation would retain this geometry unless the *s-cis* conformation, (XXI), is stabilised by a bonding interaction between the two oxygen atoms. Hopefully calculations will be able to provide some insight into this problem and efforts are being made to this end.⁽²²⁾

Also observed in the 77K spectrum were widely spaced wing features, marked α , separated by 312G. These features

↓
3215G

20G
→H

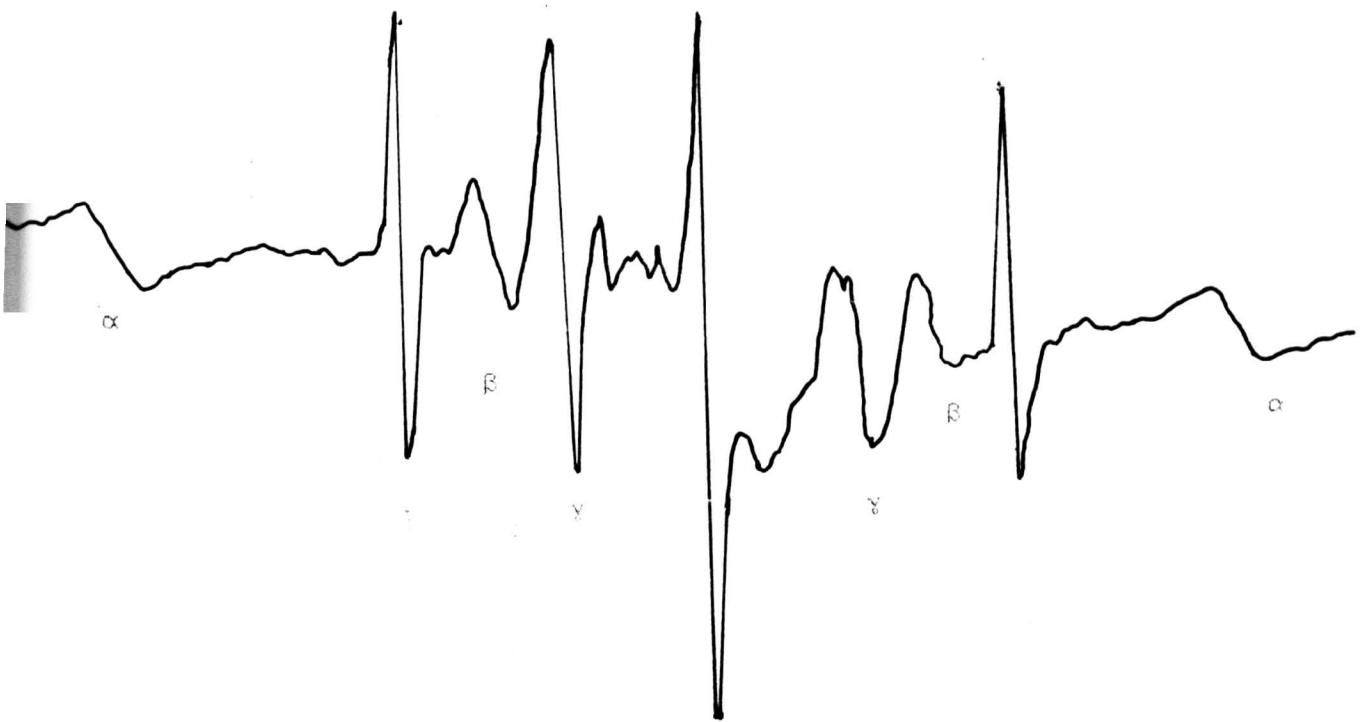
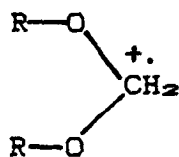


Figure 8(iii): First-derivative X-band esr spectrum of glyoxal in CFC_{13} , after exposure to ^{60}Co γ -rays at 77K, showing features assigned to the parent radical cation, at 77K. Other features marked α , β and γ are discussed in the text.

are assumed to be the $M_s = \pm 1$ lines of a triplet of 156G, with a g-value of 2.0068. On enlargement these α lines showed no further splitting, unlike formaldehyde, but the large hyperfine coupling constant implies that these α lines are probably due to an acetal type species, $\langle \bullet \rangle$ (XXII), derived from the parent molecule or cation.



(XXII)

R \neq CH₃

The doublet, marked β , was much weaker and anisotropic. The proton coupling constant and the anisotropic shape indicate that this doublet can be assigned to the radical HCO \cdot . $\langle \bullet \bullet \bullet \rangle$ The doublet, marked γ , was also asymmetric and is similar to that assigned to the methylglyoxal radical cation, see later. As yet the species giving rise to the γ doublet has not been identified.

So as to try to get a better understanding of the α species, a dilution study was undertaken. The glyoxal sample was diluted prior to irradiation, and the spectra recorded such that the intensity of the esr signal of the parent radical cation remained constant, thus a direct comparison of signal intensities was possible. It is postulated that if the γ species is formed by intermolecular reactions then dilution will reduce the possibility

of such reactions and thus the esr signal will decrease, relatively, on dilution. If the α species is formed by intramolecular reactions then dilution will not effect the relative intensity of its esr signal. Various dilutions were prepared and all were studied; it was noticed that as the dilution increased, the intensity of the esr signal due to the α species decreased relatively, *fig. 8(iv)*.

Therefore, it is postulated that the α species is formed by intermolecular reactions between parent molecules or radicals.

Methylglyoxal

The spectrum obtained at 77K, *fig. 8(v)*, showed an asymmetric doublet due to the parent radical cation. To facilitate the extraction of the g and A tensor components the spectrum was studied at Q-band frequencies. It is noteworthy that the isotropic proton coupling is almost identical with that for the glyoxal radical cation despite the change in symmetry.

The wing features, marked α , are separated by 303G, and they are assigned to the $M_1 = \pm 1$ lines of a triplet of ca. 152G, the g -value of 2.0064 agrees with this assignment. At 77K some structure was visible on the α lines, but interpretation was not possible, so the sample was warmed and, at ca. 140K, the structure became clearer, *fig. 8(vi)*. Each of the α lines is a binomial quartet with a splitting of 12.6G. If this splitting is due to a methyl

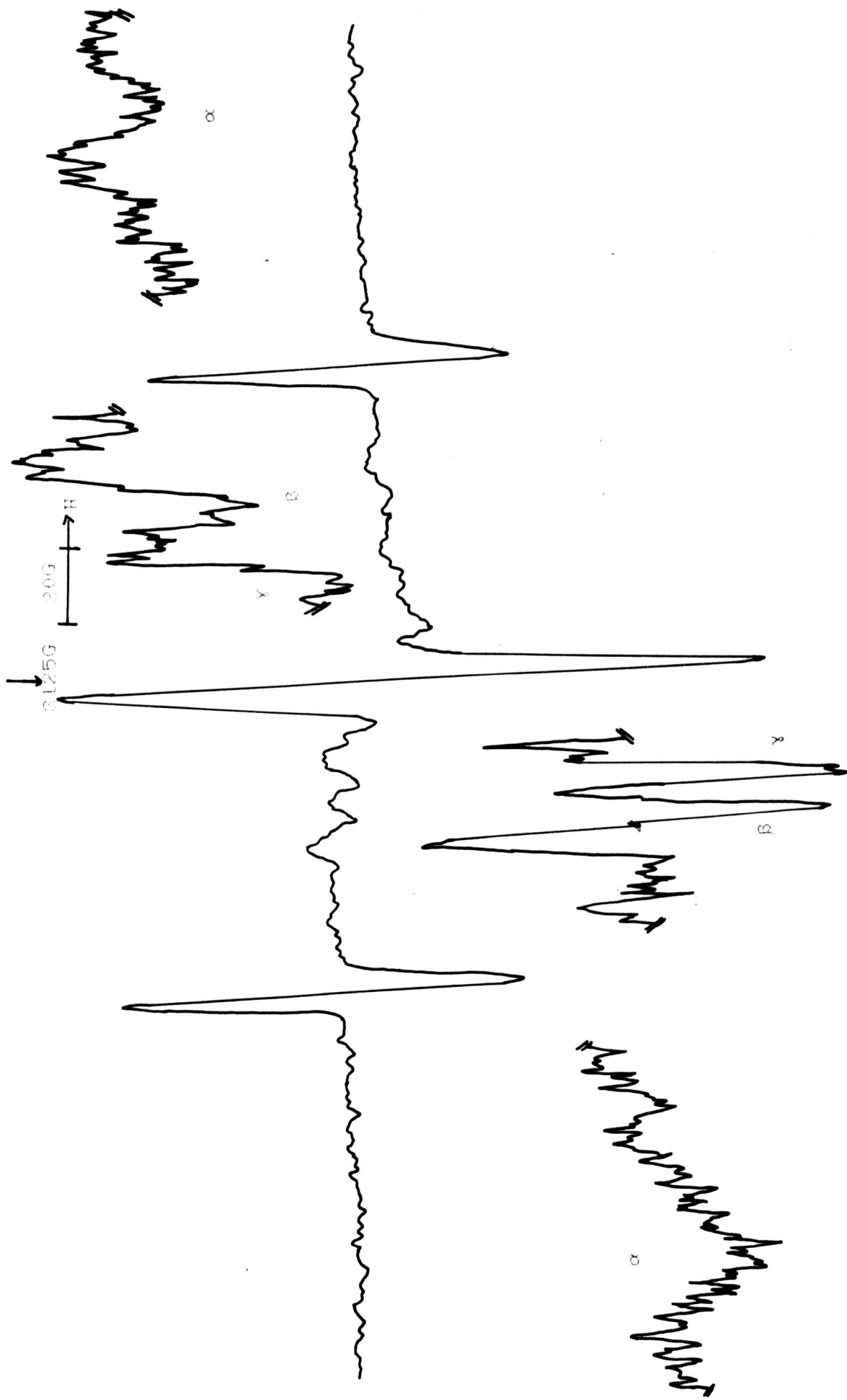


Figure 8(iv): First-derivative X-band esr spectrum of a four fold dilution of glyoxal in CFC1₂, after exposure to ⁶⁰Co γ -rays at 77K, showing features assigned to the parent radical cation, at 77K.

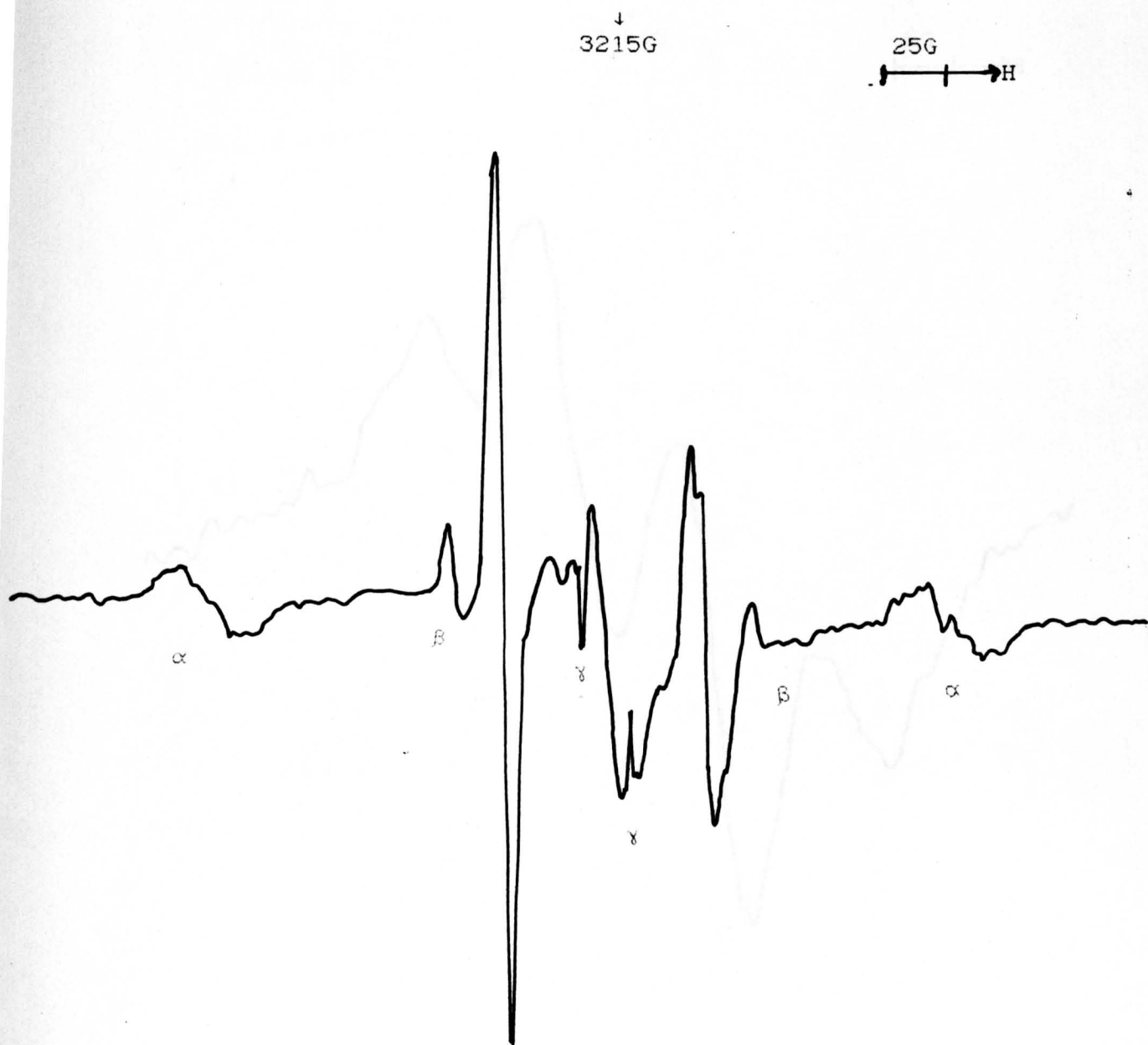


Figure 8(v): First-derivative X-band esr spectrum of methylglyoxal in CFC_{13} , after exposure to ^{60}Co γ -rays at 77K, showing features assigned to its parent radical cation, at 77K. Other features marked α , β and γ are discussed in the text.

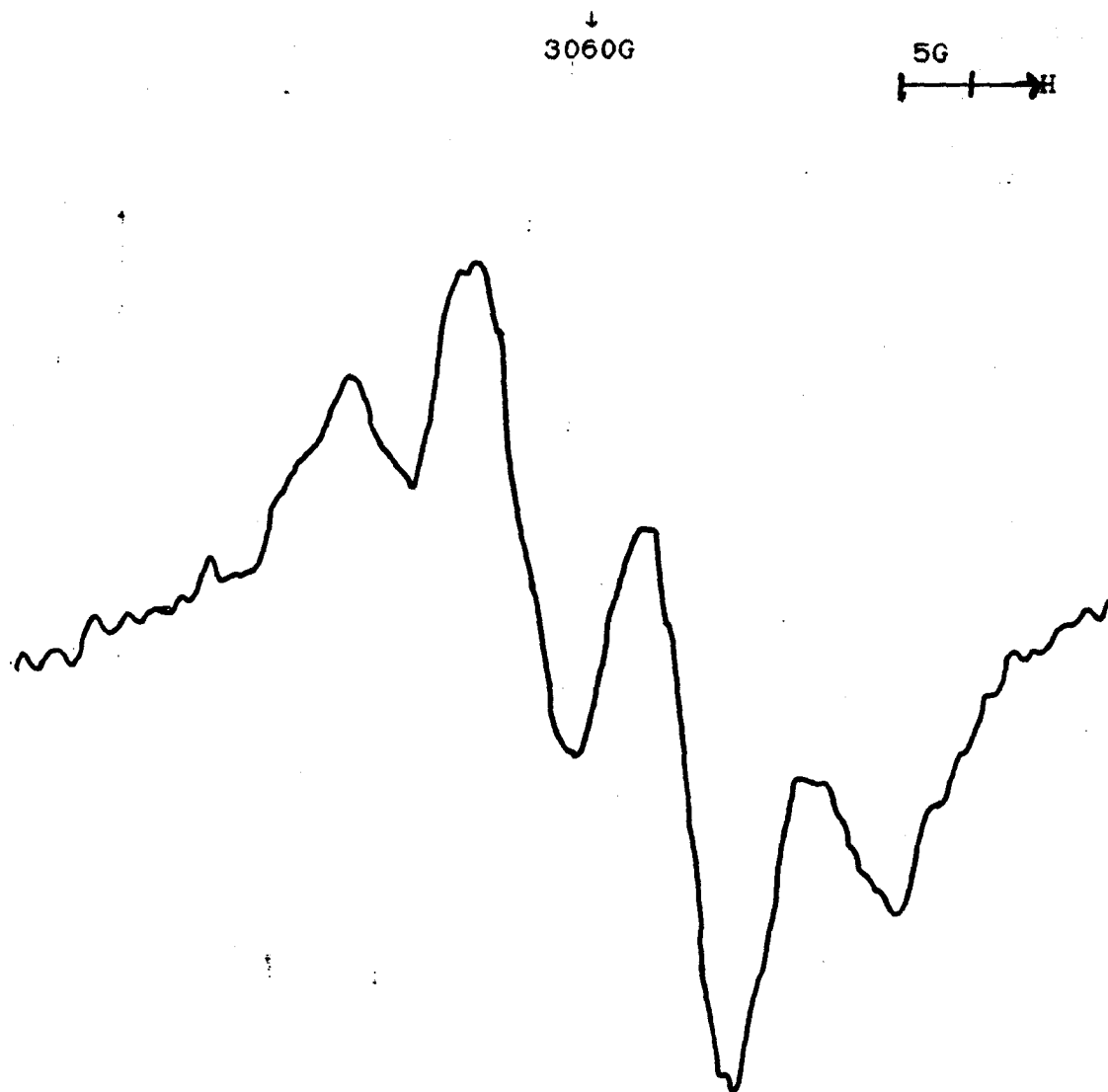
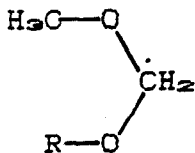


Figure 8(vi): First-derivative X-band esr spectrum of methylglyoxal in CFC_{12} , after exposure to ^{60}Co γ -rays at 77K, showing features assigned to an acetal type species, at ca. 140K.

group, the species giving rise to the α lines must be of the form depicted in (XXIII).

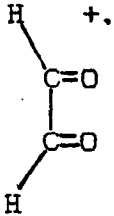
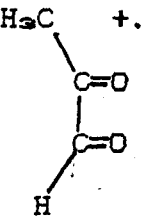


(XXIII)

The lines marked β are assigned to the radical HCO^\bullet , see earlier. The lines marked γ are assigned to the radical CH_2^\bullet . (87)

Table 8

Esr Parameters for Aldehydic Carbonyl Radical Cations.

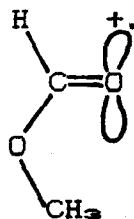
| Cation (in CFC1 ₃) | A(¹ H) (G) | | g-Values | |
|---|------------------------|-------|-----------------|--------|
|  | A _{iso} | 84.2 | g _{av} | 2.0029 |
|  | A _x | 81.0 | g _x | 2.0061 |
| | A _y | 82.0 | g _y | 2.0025 |
| | A _z | 86.25 | g _z | 1.9989 |
| | A _{iso} | 83.1 | g _{av} | 2.0025 |

Chapter 9

2 Derivatives of Carbonyl Compounds

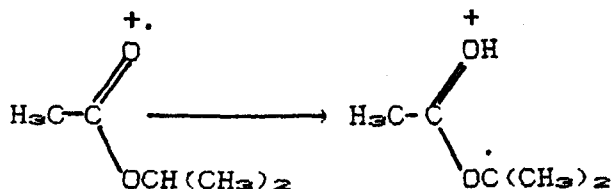
2.1 Introduction

The compounds dealt with in this chapter are of the form CH_3COX , where $\text{X} = \text{CO}_2\text{CH}_3$, OCOCH_3 , Cl , SCH_3 etc. Analogous to these compounds are the acetate esters, where $\text{X} = \text{OCH}_3$, OCH_2CH_3 etc. According to the results of photoelectron spectroscopy and theory⁽²²⁻²⁾ ester cations are expected to have the σ (non-bonding) structure, (XXIX), the SOMO being largely confined to the in-plane 2p orbital on the carbonyl oxygen.



(XXIX)

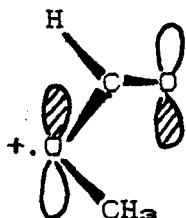
In all cases except for the primary product from methyl formate, this is not seen. Rearrangements, such as that depicted in (XXX), clearly occur for various higher esters.



(XXX)

A well defined example being the radical cation of

isopropyl acetate.⁽³⁰⁾ It was summarised by Rideout and Symons⁽⁷³⁾ that these rearranged complexes are derived from the σ -structure, (XXIX), rather than from the alternative π -structure, (XXXI).



(XXXI)

The absence of any large temperature effect implies that there is a major contribution from quantum mechanical tunnelling in this rearrangement.⁽³¹⁾ In summary, it seems that for these methyl esters, hydrogen-atom migration involves a rapid tunnelling which takes place readily for the σ -structured cation, even at 4K.

9.2 Hydroxyl Derivatives

Acetic anhydride

The spectrum obtained at 77K was a singlet with marked parallel and perpendicular features, *fig. 9(1)*. The magnitude of the deviation of the g -tensor from free spin gives g_{\parallel} and g_{\perp} , see *table 9*. As discussed in the introduction, the structure is probably σ and not π , but it is not rearranged. If the cation had been rearranged, then coupling to the α -protons would be present and this is not

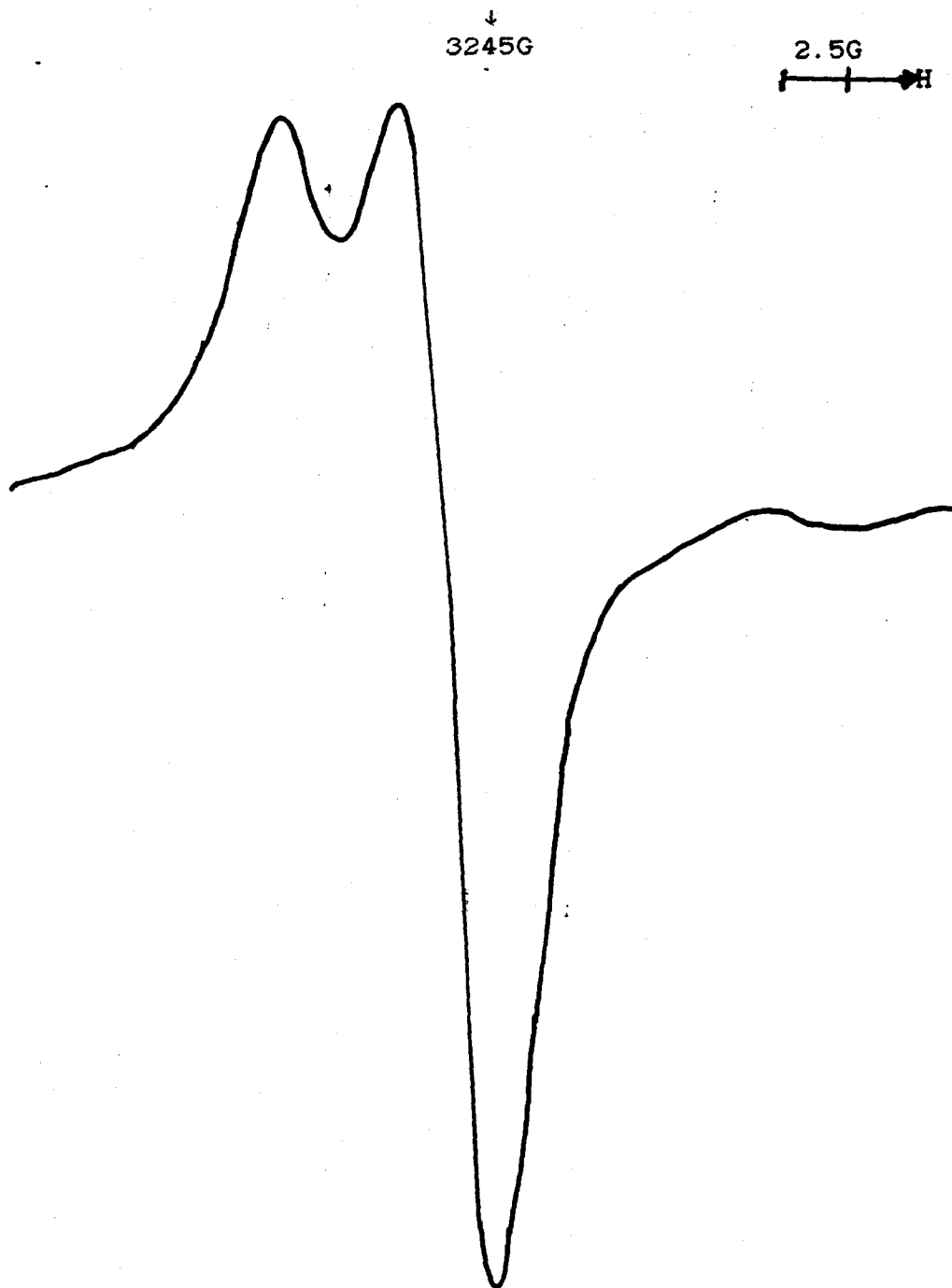


Figure 9(i): First-derivative X-band esr spectrum of acetic anhydride in CFCl_3 , after exposure to ^{60}Co γ -rays at 77K, showing features assigned to its radical cation, at 77K.

observed in the esr spectrum. It is possible that the cation could cyclise, as is seen with its hydrocarbon analogue, 2,4-pentanedione, chapter 6.3. However the absence of any colour, and thus the $\sigma \rightarrow \sigma^*$ transition, seems to argue against a cyclised structure.

The cyclic analogue of acetic anhydride, maleic anhydride, was proposed for study, but no results were obtained because of the insolubility of maleic anhydride in CFCl_3 .

Methyl pyruvate

The spectrum obtained was a singlet with marked g anisotropy, *fig. 9(ii)*. Again, here the structure of the cation is σ and not rearranged, as again no coupling to protons is seen.

Dimethyl oxalate

The spectrum obtained at 77K was a singlet with g -value variation, *fig. 9(iii)*. As with both the preceding compounds the structure is σ and not π , and the cation is not rearranged.

9.3 Halogenated Derivatives

Acetyl chloride

All that was detected at 77K was a low intensity singlet. After warming the sample to ca. 140K and then

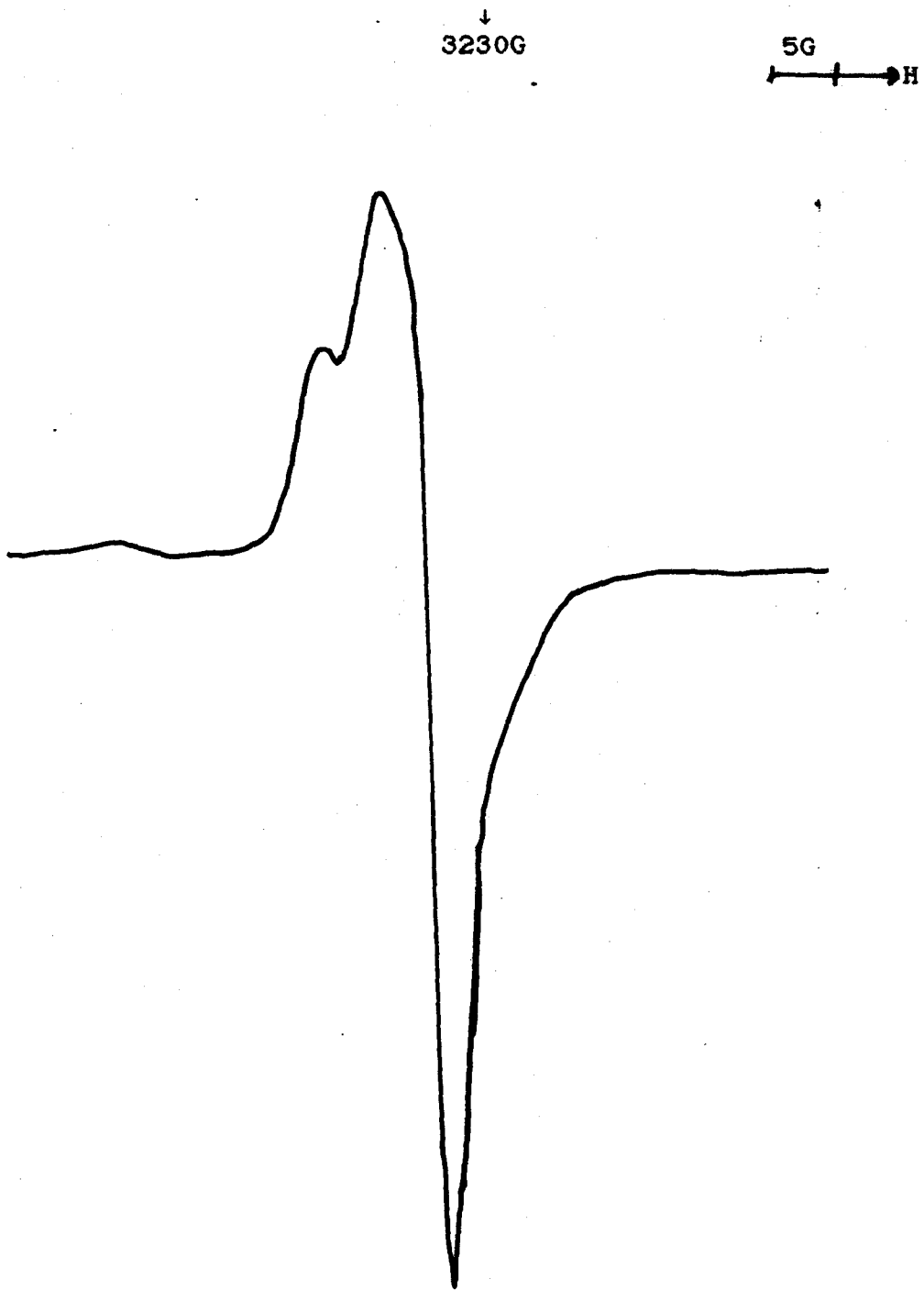
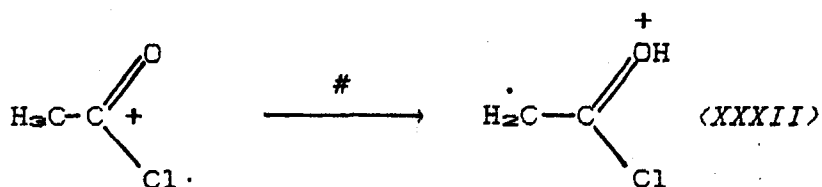


Figure 9(ii): First-derivative X-band esr spectrum of methyl pyruvate in CFCl_3 , after exposure to ^{60}Co γ -rays at 77K, showing features assigned to its radical cation, at 77K.

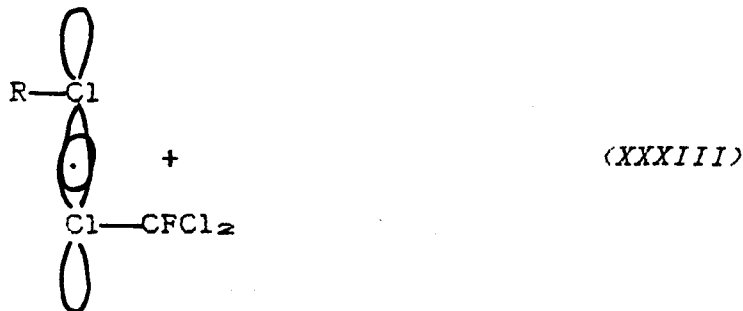


Figure 9(iii): First-derivative X-band esr spectrum of dimethyl oxalate in CFCl_3 , after exposure to ^{60}Co γ -rays at 77K, showing features assigned to its radical cation, at 77K.

recooling to 77K an intense triplet was observed, *fig. 9(iv)*. This triplet is a factor of ten more intense than the initial singlet and thus the triplet cannot be derived from breakdown products of the species which gives rise to the singlet. The post anneal triplet is assigned to the rearranged parent cation, (XXXII).



The triplet is assigned to the methylene protons. The parent cation was not detected at 77K though it must, clearly, have been present. Since no resolved quartet splitting was observed the spin density on chlorine must be surprisingly low. This result can be contrasted with that for chloroalkanes, $(\text{RCl})^{\cdot+}$. Here the parent cation is detected at 77K but the lone electron is shared with a chlorine atom of a solvent molecule via the formation of a σ -bond, (XXXIII). <92>



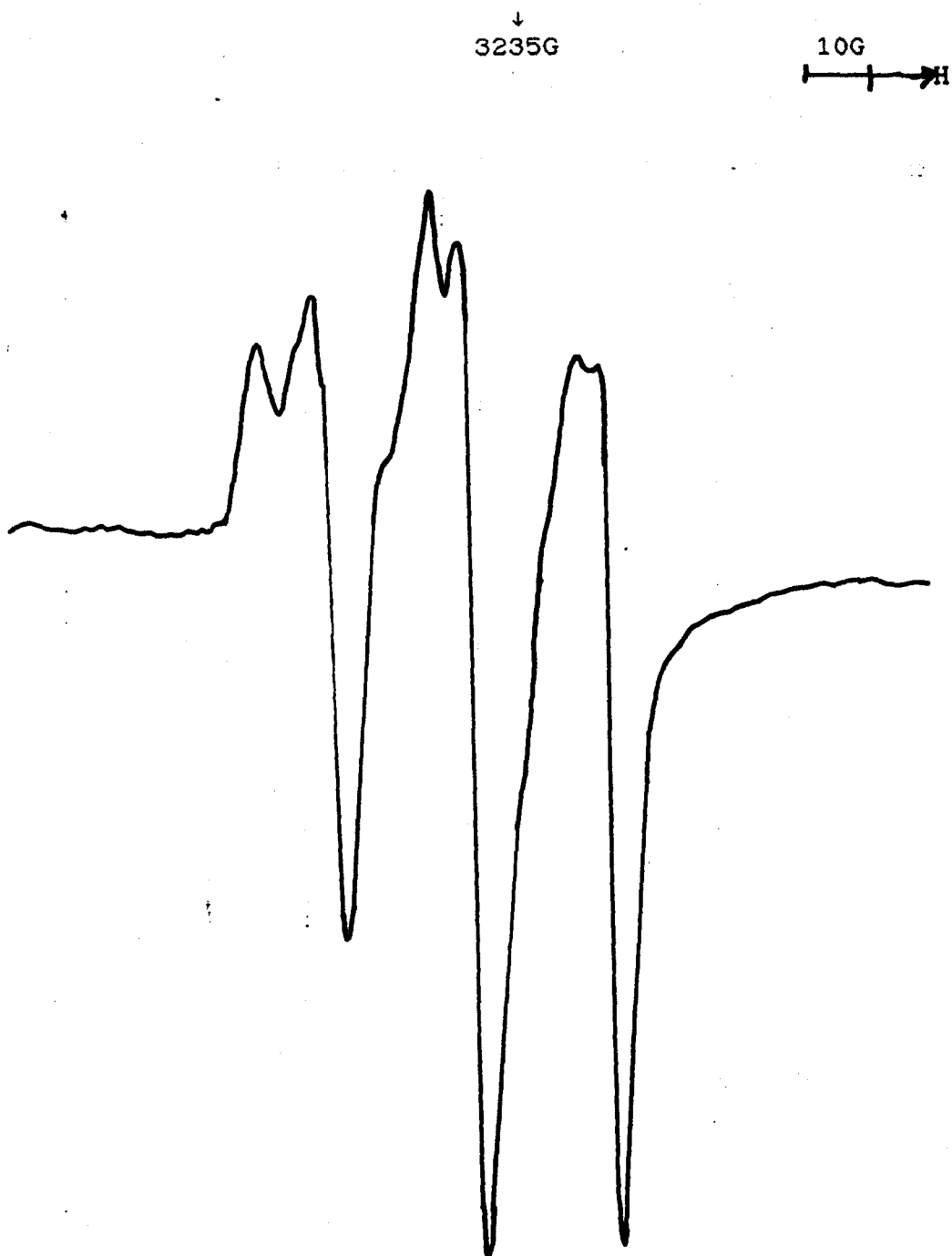
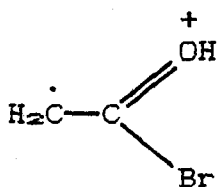


Figure 9(iv): First-derivative X-band esr spectrum of acetyl chloride in CFCl_2 , after exposure to ^{60}Co γ -rays at 77K, showing features assigned to its rearranged radical cation, at 77K.

Acetyl bromide

At 77K the spectrum obtained was very complex and uninterpretable; the spectrum taken during the anneal gave no further information. It is thought that these spectra are not due to the parent cation, but may be attributed to impurities, or the rearranged cation, (XXXIV), as was the case with acetyl chloride.



(XXXIV)

However, in this case, coupling to bromine must have complicated the spectrum so much that no clear resolution was obtained.

9.4 Nitrogen and Sulphur Derivatives

N-acetylimidazole

The spectrum observed at 77K was a distorted quintet, fig. 9(v). This quintet is assigned to the lone electron being shared between the two nitrogen atoms in the imidazole ring. If both nitrogen atoms are equivalent then a binomial quintet is expected, but if the two nitrogen atoms are inequivalent then the expected spectrum is a triplet of triplets. A distorted quintet is observed,

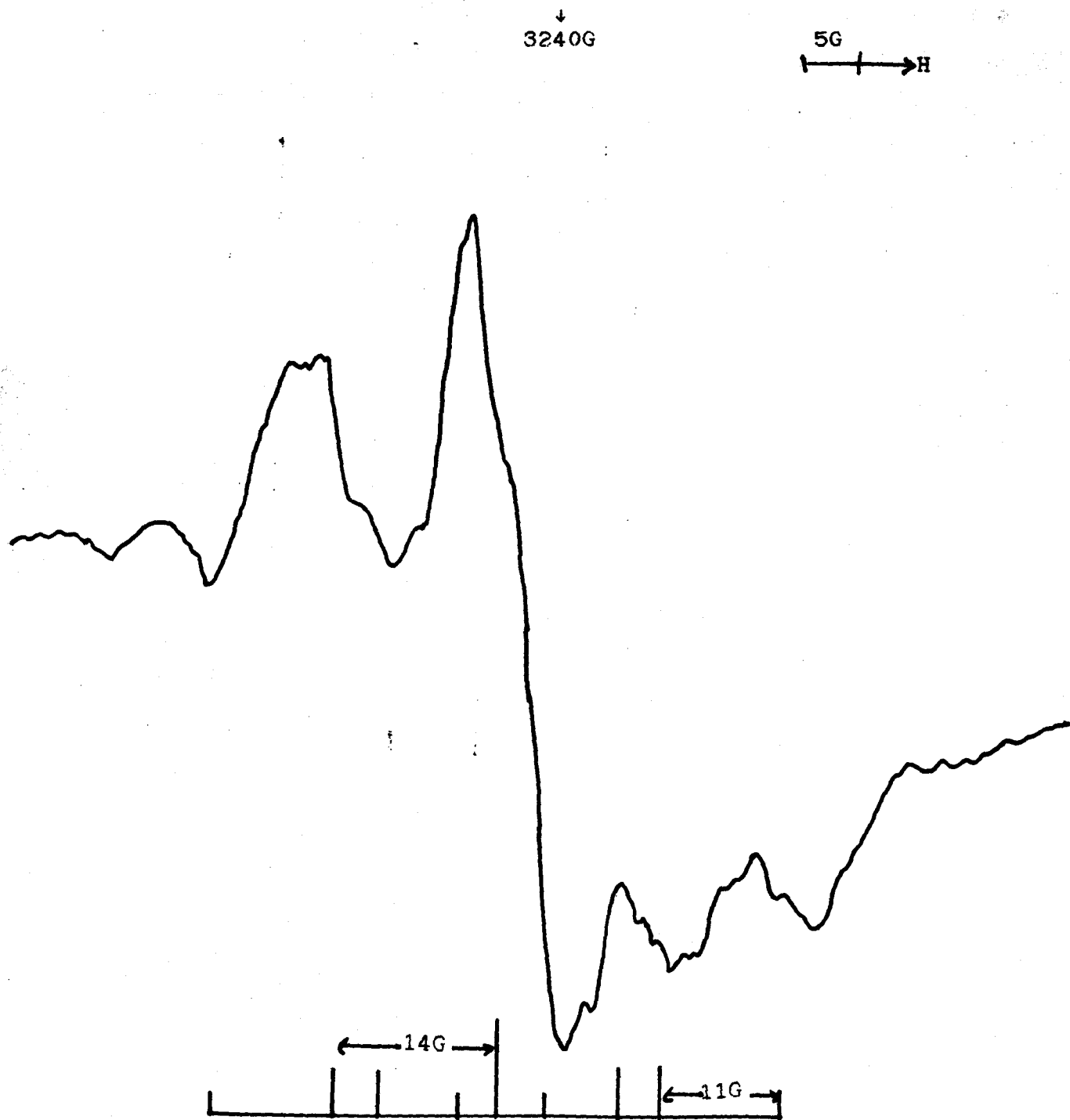


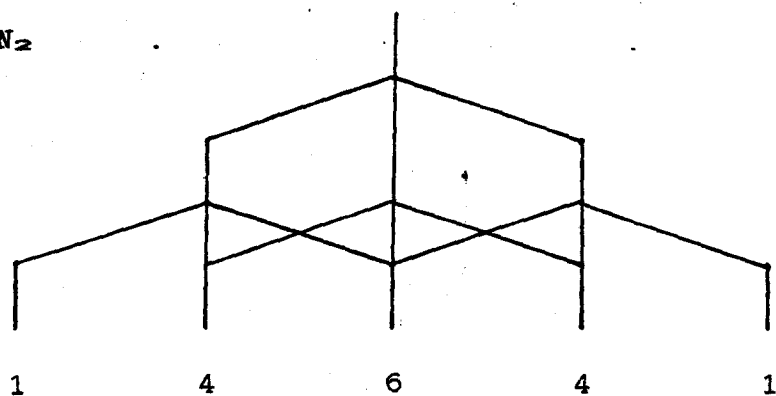
Figure 9(v): First-derivative X-band esr spectrum of N-acetylimidazole in CFCl_3 , after exposure to ^{60}Co γ -rays at 77K, showing features assigned to its radical cation, at 77K.

implying that the two nitrogen atoms are in similar but not identical environments, *fig. 9(vi)*. The spin is localised into the aromatic imidazole ring and thus no coupling to the methyl group is observed. The parallel ^{14}N couplings are 14G and 11G and the perpendicular coupling must be close to zero.

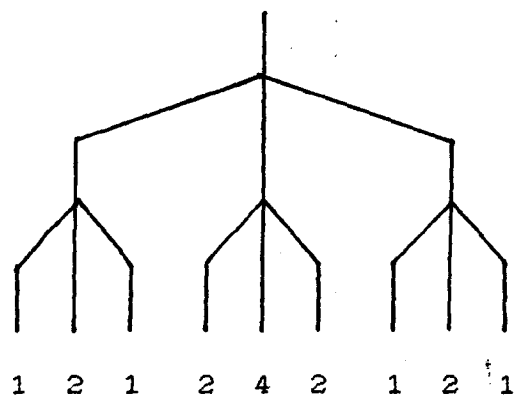
Methyl thioacetate

The spectrum obtained at 77K was complex, *fig. 9(vii)*. The signal is assigned to the parent radical cation with high spin density on sulphur. Interpretation is difficult since there are large positive g shifts giving rise to extra features that can readily be mistaken for poorly resolved hyperfine splittings. It is expected that the radical will be $\text{CH}_3\text{COS}^+\cdot\text{CH}_3$, by analogy with compounds such as $\text{CH}_3\text{CON}^+\cdot(\text{CH}_3)_2$,⁽³³⁾ is a π -delocalised system with spin density largely on sulphur. This can be compared with $(\text{CH}_3)_2\text{S}^+\cdot$; where coupling is observed to six protons, $A(^1\text{H}) = 21\text{G}$.⁽³⁴⁾ Hence coupling to the sulphur methyl protons is expected. In the 77K spectrum the total splitting, $\Sigma A = 126\text{G}$. There is a clear splitting of ca. 26G which can be assigned to the sulphur methyl protons (A_{Me}), together with an extra doublet splitting of ca. 6G which is assigned to one proton in the methyl group attached to the carbon atom (A_{H}), which is a favourable position. The extra splitting must then be assigned to g -value variation. From these figures the g shift, Δg , can be calculated.

$N_1 = N_2$



$N_1 \neq N_2$



$N_1 = N_2$

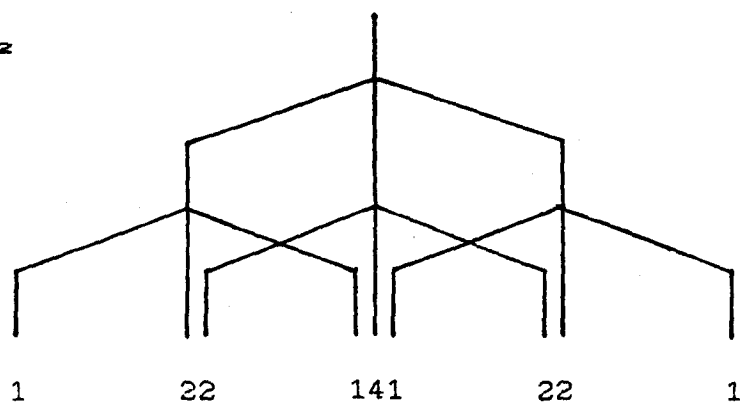


Figure 9(vi): Diagram showing arrangement of *esr* lines due to two nitrogen atoms.

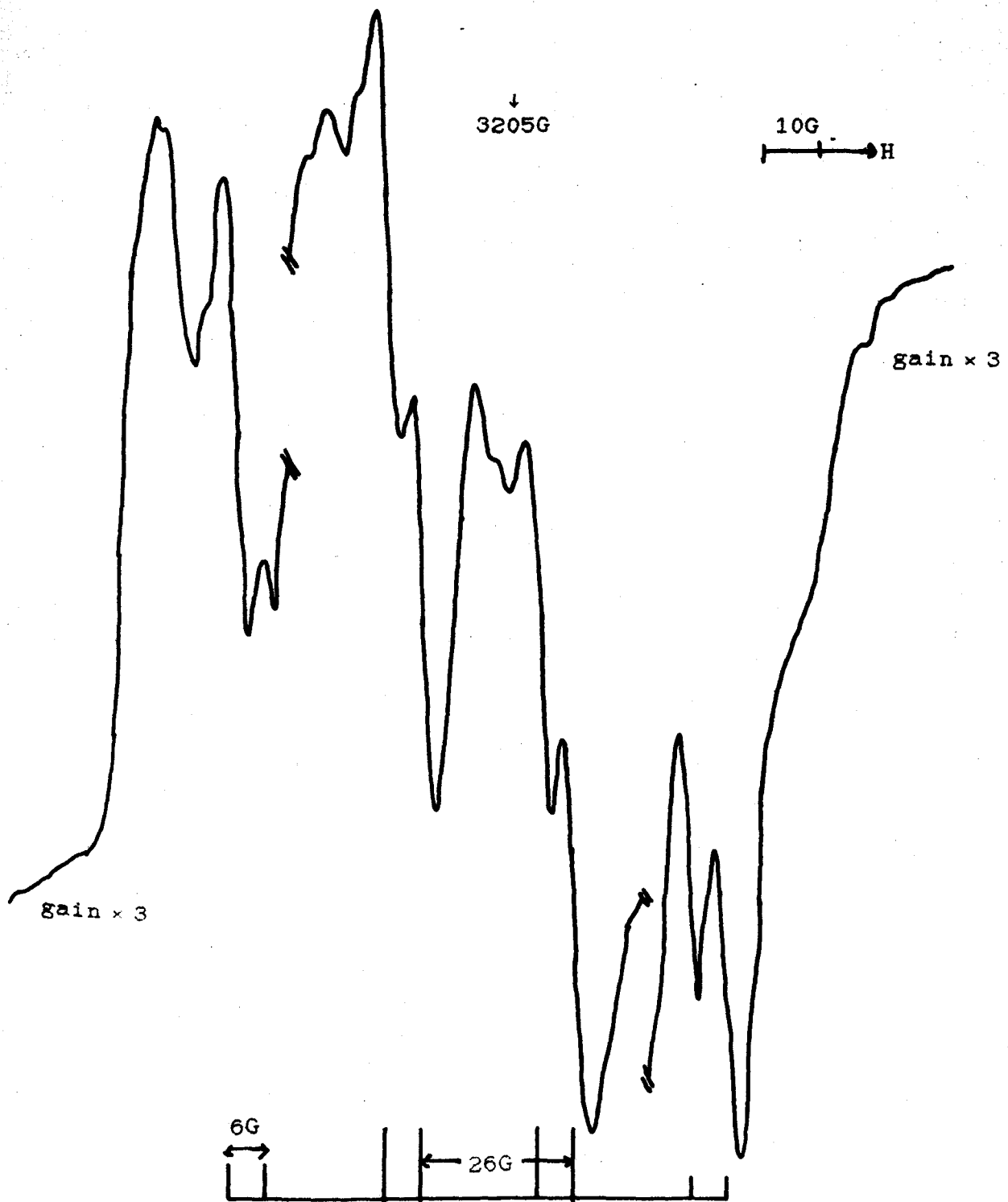


Figure 9(vii): First-derivative X-band esr spectrum of methyl thioacetate in CFCl_3 , after exposure to ^{60}Co γ -rays at 77K, showing features assigned to its radical cation, at 77K.

$$\Delta g = \Sigma A - (\Sigma A_{m\alpha}) - A_H$$

$$= 126 - (3 \times 26) - 6$$

$$\Delta g = 42G$$

This value of Δg agrees well with the observed spectrum.

Thus if $g_{min} \approx 2.002G$ then $g_{max} \approx 2.031G$; also there is no clear evidence for an intermediate g-tensor.

Table 2

Esr Parameters For Radical Cations of Carbonyl Compound Derivatives

| Cation (in CFC1 ₂) | T (K) | g-Values | |
|--|--------|-----------------|----------------|
| | | g | g _⊥ |
| $ \begin{array}{c} \text{H}_3\text{C} \quad + \\ \diagdown \quad / \\ \text{C}=\text{O} \\ \\ \text{O} \\ \\ \text{C}=\text{O} \\ / \quad \backslash \\ \text{H}_3\text{C} \end{array} $ | 77 | | |
| $ \begin{array}{c} \text{H}_3\text{CO} \quad + \\ \diagdown \quad / \\ \text{C}=\text{O} \\ \\ \text{C}=\text{O} \\ / \quad \backslash \\ \text{H}_3\text{C} \end{array} $ | 77 | 2.0073 | 2.0024 |
| $ \begin{array}{c} \text{H}_3\text{CO} \quad + \\ \diagdown \quad / \\ \text{C}=\text{O} \\ \\ \text{C}=\text{O} \\ / \quad \backslash \\ \text{H}_3\text{CO} \end{array} $ | 77 | 2.0089 | 2.0045 |
| $ \begin{array}{c} \text{H}_2\text{C} \quad + \\ \diagdown \quad / \\ \text{C}=\text{OH} \\ \\ \text{Cl} \end{array} $ | 77 (†) | 2.0079 | 2.0017 |
| $ \begin{array}{c} \text{H}_3\text{C} \quad + \\ \diagdown \quad / \\ \text{C}=\text{O} \\ / \quad \backslash \\ \text{H}_3\text{CS} \end{array} $ | 77 | 2.031 | 2.002 |

† sample warmed to ca. 140K then cooled to 77K.

References
to Part II

REFERENCES TO PART II

61. H.L. Retcofsky, J.M. Stark and R.A. Friedel; *Chem. Ind. London*, 1967, 31, 1327.
62. M.C.R. Symons and I.G. Smith; *J. Chem. Res. (S)*, 1979, 382.
63. T. Shida and W.H. Hamill; *J. Chem. Phys.*, 1966, 44, 2369
64. J. Doucet, P. Sauvageau and C. Sandorfy; *J. Chem. Phys.*, 1973, 58, 3708.
65. T. Cvitas, H. Güsten and L. Klasinc; *J. Chem. Phys.*, 1977, 67, 2687.
66. M. Iwasaki; *J. Chem. Phys.*, 1966, 45, 990.
67. M.C.R. Symons and P.J. Boon; *Chem. Phys. Lett.*, 1982, 89, 516.
68. D.N.R. Rao and M.C.R. Symons; *Tet. Lett.*, 1983, 24, 1293.
69. G.W. Eastland, D.N.R. Rao, J. Rideout, M.C.R. Symons and A. Hasegawa; *J. Chem. Res. (S)*, 1983, 258.
70. P.J. Boon, L. Harris, M.T. Olm, J.L. Wyatt and M.C.R. Symons; *Chem. Phys. Lett.*, 1984, 106, 408.
71. L.D. Snow and F. Williams; *J. Chem. Soc., Chem. Commun.*, 1983, 1090.
72. P.J. Boon, M.C.R. Symons, K. Ushida and T. Shida; *J. Chem. Soc. Perkin Trans. 2*, 1984, 1213.
73. J. Rideout and M.C.R. Symons; *J. Chem. Soc. Perkin Trans. 2*, 1986, 625.

74. J.H. Busch and J.R. de la Vega; *J. Amer. Chem. Soc.*, 1977, **99**(8), 2397.
75. J.R. de la Vega; *Acc. Chem. Res.*, 1982, **15**, 185.
76. T. Shida; Personal Communication.
77. G.A. Russell, G.R. Underwood, and D.C. Lini; *J. Amer. Chem. Soc.*, 1967, **89**(25), 6636.
78. D.N.R. Rao, G.W. Eastland and M.C.R. Symons; *J. Chem. Soc. Faraday Trans. 1*, 1985, **81**, 727.
79. M.C.R. Symons and L. Harris; *J. Chem. Res.*, 1982, 268.
80. L.B. Knight Jr. and J. Steadman; *J. Chem. Phys.*, 1984, **80**, 1018.
81. M.C.R. Symons and B.W. Wren; *J. Chem. Soc. Perkin Trans. 2*, 1984, 511.
82. L.D. Snow, J.T. Wang and F. Williams; *J. Amer. Chem. Soc.*, 1982, **104**, 2062.
83. C.E. Dyllick-Brenzinger and A. Bauder; *Chem. Phys.*, 1978, **30**, 147.
84. G.N. Currie and D.A. Ramsay; *Can. J. Phys.*, 1971, **49**, 317.
85. A. Hasegawa; personal communication.
86. J.A. Brivati, N. Keen and M.C.R. Symons; *J. Chem. Soc.*, 1962, 237.
87. M.C.R. Symons and I.G. Smith; *J. Chem. Soc. Faraday Trans 1*, 1985, **81**(4), 1095.

88. K. Kimura, S. Katsumata, Y. Achiba, T. Yamazaki and S. Iwata; "Handbook of He⁺ Photoelectron Spectra of Fundamental Molecules", 1972, Japan Sci. Soc. Press, vol. 94, p. 5592.
89. D.A. Sweigart and D.W. Turner; *J. Amer. Chem. Soc.*, 1972, 94(16), 5592.
90. D.N.R. Rao, J. Rideout and M.C.R. Symons; *J. Chem. Soc. Perkin Trans. 2*, 1984, 1221.
91. F. Williams and E.D. Sprague; *Acc. Chem. Res.*, 1982, 15, 408.
92. G.W. Eastland, S.P. Maj, M.C.R. Symons, A. Hasegawa, C. Glidewell, M. Hayashi and T. Wakabayashi; *J. Chem. Soc. Perkin Trans. 2*, 1984, 1439.
93. D.N.R. Rao and M.C.R. Symons; *Chem. Phys. Lett.*, 1982, 93(5), 4985.
94. D.N.R. Rao, M.C.R. Symons and B.W. Wren; *J. Chem. Soc. Perkin Trans. 2*, 1984, 1681.

The following published article is not available in the electronic version of this thesis due to copyright restrictions:

**Portwood, Lynn; Rhodes, Christopher J.; Symons, Martyn C. R., 'An E.S.R. Study of Glyoxal Radical Cations',
Journal of the Chemical Society, Chemical
Communications, 1986, 20, pp. 1535-1536. DOI:
[10.1039/C39860001535](https://doi.org/10.1039/C39860001535)**

The full version can be consulted at the University of Leicester Library.